

**The Effects of Altered Expression of *clueless* on Ageing and Neurodegeneration in
*Drosophila melanogaster***

by Allison L. Porter

A thesis

submitted to the School of Graduate Studies

in partial fulfillment of the requirements

for the degree of

Master of Science

Department of Biology

Memorial University of Newfoundland

July 2024

St. John's Newfoundland and Labrador

Abstract

Mitochondrial dysfunction is linked to the pathology of age-related and neurodegenerative disease, including Parkinson disease and amyotrophic lateral sclerosis. Preservation of mitochondrial function is determined by the interconnected processes governing mitochondrial homeostasis: fission, fusion, trafficking, mitophagy, and biogenesis. The *Drosophila melanogaster* protein Clueless and its mammalian homologue CLUH are cytoplasmic RNA-binding proteins essential for mitochondrial function that may influence all of these processes. Clueless and its homologues may act as master regulators of mitochondrial homeostasis to control these processes in response to environmental cues including stress-response signalling. The effects of altered expression of *clueless* in *Drosophila melanogaster* dopaminergic and motor neurons on ageing and neurodegeneration were examined through lifespan and climbing assays. In humans, dopaminergic neuron degeneration causes Parkinson disease, and motor neurons degeneration causes amyotrophic lateral sclerosis. Inhibited *clueless* expression in *Drosophila melanogaster* dopaminergic and motor neurons reduced early-life climbing ability, and inhibited *clueless* expression in motor neurons caused impaired lifespan and a more rapidly progressive loss of climbing ability with age. Inhibited expression of *clueless* in motor neurons therefore causes age-related disease in this model organism. RNAi-mediated *clueless* suppression in motor neurons is a promising novel model for investigation of the role of mitochondrial dysfunction in the pathology of amyotrophic lateral sclerosis.

General Summary

Mitochondrial dysfunction is linked to age-related and neurodegenerative disease in humans, including Parkinson disease and amyotrophic lateral sclerosis. Mitochondrial function is determined by interconnected processes that control mitochondrial replication, degradation, and positioning. The insect protein Clueless and its mammalian counterpart CLUH bind to mitochondria-related mRNA transcripts, and so may influence the function of mitochondria-related genes. Expression of the *clueless* gene was inhibited in disease-associated neurons of the fruit fly *Drosophila melanogaster*, and effect on longevity and climbing ability was assessed. Inhibited expression of the *clueless* gene in motor neurons, the loss of which is associated with amyotrophic lateral sclerosis in humans, caused impaired lifespan and a more rapidly progressive loss of climbing ability with age. Inhibited expression of *clueless* in motor neurons therefore causes age-related disease in this model organism. Suppressed *clueless* expression in motor neurons is a promising novel model for investigation of the role of mitochondrial dysfunction in amyotrophic lateral sclerosis.

Acknowledgments

I am grateful to my supervisor Dr. Brian E. Staveley for his guidance, advice, and support. I am also grateful to my supervisory committee members Dr. H. Dawn Marshall and Dr. Jennifer D. Slade. Thank you to Dr. David C. Schneider for statistical consults for climbing assay analyses. Thank you to Dr. Rachel T. Cox for providing *clu*^{d08713}/*CyO*; *UAS-clu/TM6C* and *clu*^{d08713}/*CyO*; *UAS-CLUH Drosophila melanogaster* lines. Other *Drosophila melanogaster* lines were obtained from the Vienna Drosophila Resource Center, and from the Bloomington Drosophila Stock Center (NIH P40OD018537). Funding for this research was provided by a Memorial University of Newfoundland School of Graduate Studies Fellowship, Memorial University of Newfoundland Department of Biology Teaching Assistantships, a Memorial University of Newfoundland Seed Fund, an Aging Research Centre-Newfoundland and Labrador Research Grant, and Natural Sciences and Engineering Research Council of Canada Discovery Grants.

Table of Contents

Abstract.....	ii
Acknowledgments.....	iii
Table of Contents.....	iv
List of Tables.....	ix
List of Figures.....	x
List of Abbreviations.....	xii
Chapter 1: Introduction.....	1
1.1 Mitochondria, Ageing, and Neurodegenerative Disease.....	1
1.2 The Model Organism <i>Drosophila melanogaster</i> and Neurodegenerative Disease.....	4
1.3 Parkinson Disease.....	8
1.4 Risk Factors for Parkinson Disease.....	9
1.5 Lewy Body Pathology in Parkinson Disease.....	10
1.6 <i>Drosophila melanogaster</i> as a Model for Parkinson Disease.....	11
1.7 Amyotrophic Lateral Sclerosis.....	12
1.8 Risk Factors for Amyotrophic Lateral Sclerosis.....	13
1.9 Amyotrophic Lateral Sclerosis and Frontotemporal Lobe Degeneration.....	15
1.10 <i>Drosophila melanogaster</i> as a Model for Amyotrophic Lateral Sclerosis..	16
1.11 Regulation of Mitochondrial Homeostasis.....	17
1.12 Mitochondrial Dynamism.....	18
1.13 Mitophagy.....	23

1.14 Mitophagy in <i>Drosophila melanogaster</i>	24
1.15 Mitochondrial Biogenesis.....	25
1.16 RNA-Processing in Regulation of Mitochondrial Biogenesis.....	27
1.17 Clueless.....	30
1.18 Clueless and Mitochondrial Localization.....	32
1.19 Clueless and Mitochondrial Dynamism.....	33
1.20 Clueless and Mitophagy.....	34
1.21 Clueless and Localized Translation at Mitochondria.....	35
1.22 Clueless as a Potential Master Regulator of Mitochondrial Homeostasis...	37
1.23 Clueless in Model Organisms.....	39
1.24 Research Goals.....	40
Chapter 2: Methods.....	42
2.1 <i>Drosophila melanogaster</i> Care and Maintenance.....	42
2.2 <i>Drosophila melanogaster</i> Lines and Crosses.....	42
2.3 Lifespan Assay.....	46
2.4 Climbing Assay.....	51
Chapter 3: Results.....	53
3.1 Inhibited Expression of clueless in Dopaminergic Neurons Reduces Climbing Ability but Does Not Affect Mean Lifespan.....	53
3.2 Inhibited Expression of clueless in Motor Neurons Decreases Mean Lifespan and Reduces Climbing Ability.....	53

3.3 Heterozygous clueless Mutants Expressing Ectopic clueless in Dopaminergic Neurons Have Reduced Climbing Ability But Not Mean Lifespan.....	58
3.4 Heterozygous clueless Mutants Expressing Ectopic clueless in Motor Neurons Have Reduced Mean Lifespan, and Heterozygous clueless Mutants Expressing Either Ectopic clueless or CLUH in Motor Neurons Have Reduced Climbing Ability.....	58
Chapter 4: Discussion.....	64
4.1 Altered <i>clueless</i> Expression in Dopaminergic Neurons Does Not Cause Age-Related Disease.....	64
4.2 Altered <i>clueless</i> Expression in Motor Neurons Causes Age-Related Disease.....	64
4.3 Inhibition of <i>clueless</i> Expression in Motor Neurons Replicates Features of ALS.....	65
4.4 Ectopic Expression of <i>clueless</i> and <i>CLUH</i> in Dopaminergic and Motor Neurons of Heterozygous <i>clu</i> ^{d08713} Mutants.....	66
4.5 Early-Life Impairment of Locomotor Function.....	
4.6 Transgene Expression.....	67
4.7 Clueless and Mitochondrial Function.....	70
4.8 Further Characterization of Clueless Function.....	72
4.9 Sex Considerations.....	73
4.10 Conclusion.....	74

Literature Cited.....	75
Appendix 1. Parameter estimates for modeled climbing ability across lifespan where expression of <i>clueless</i> in <i>Drosophila melanogaster</i> dopaminergic neurons is inhibited.	97
Appendix 2. Parameter estimates for modeled climbing ability across lifespan where expression of <i>clueless</i> in <i>Drosophila melanogaster</i> motor neurons is inhibited.....	98
Appendix 3. Parameter estimates for modeled climbing ability across lifespan where <i>clueless</i> or <i>CLUH</i> are ectopically expressed in <i>Drosophila melanogaster</i> dopaminergic neurons in heterozygous <i>clu</i> ^{d08713} mutants.....	99
Appendix 4. Parameter estimates for modeled climbing ability across lifespan where <i>clueless</i> or <i>CLUH</i> are ectopically expressed in <i>Drosophila melanogaster</i> motor neurons in heterozygous <i>clu</i> ^{d08713} mutants.....	100
Appendix 5. Bang Sensitivity Assay.....	101

List of Tables

Table 1.1 Genetic models of Parkinson disease and amyotrophic lateral sclerosis in <i>Drosophila melanogaster</i>	7
Table 2.1 <i>Drosophila melanogaster</i> lines used in experimental crosses.....	47
Table 2.2 Transgenic constructs expressed independently of <i>Gal4</i>	48
Table 2.3 <i>UAS</i> -associated transgenic constructs expressed under the control of <i>TH-Gal4</i> or <i>D42-Gal4</i>	49

List of Figures

Figure 1.1 Mitochondria facilitate aerobic respiration in eukaryotic cells.....	2
Figure 1.2 The <i>Drosophila melanogaster</i> life cycle.....	6
Figure 1.3 PINK1 acts as a sensor to detect mitochondrial damage, and PINK1Parkin signalling regulated mitochondrial fission and mitophagy.....	21
Figure 1.4 <i>Drosophila melanogaster</i> Clueless is an RNA-binding protein that may regulate mitochondrial homeostasis in response to stress signalling.....	38
Figure 2.1 Use of the UAS/GAL4 system to direct expression of <i>Escherichia coli</i> β -galactosidase (<i>lacZ</i>) in <i>Drosophila melanogaster</i> dopaminergic neurons.....	43
Figure 2.2 RNA interference (RNAi) is a conserved response to double-stranded RNA that can be exploited to inhibit expression of a target gene.....	44
Figure 2.3 Use of the UAS/Gal4 system to direct ectopic expression of <i>UAS-clu</i> and <i>UAS-CLUH</i> in <i>clu</i> ^{d08713} heterozygotes.....	45
Figure 3.1 Inhibited expression of <i>clueless</i> in dopaminergic neurons via RNAi does not significantly affect lifespan.....	54
Figure 3.2 Inhibited expression of <i>clueless</i> in dopaminergic neurons via RNAi reduces climbing ability across lifespan.....	55
Figure 3.3 Inhibited expression of <i>clueless</i> in motor neurons via RNAi reduces lifespan.....	56
Figure 3.4 Inhibited expression of <i>clueless</i> in motor neurons via RNAi reduces climbing ability across lifespan.....	57

Figure 3.5 Lifespan is not affected in heterozygous *clueless* mutants expressing ectopic *clueless* or *CLUH* in dopaminergic neurons..... 59

Figure 3.6 Climbing ability across lifespan is reduced in heterozygous *clueless* mutants expressing ectopic *clueless* but not *CLUH* in dopaminergic neurons..... 60

Figure 3.7 Heterozygous *clueless* mutants expressing ectopic *clueless* but not *CLUH* in motor neurons have reduced lifespan..... 61

Figure 3.8 Climbing ability across lifespan is reduced in heterozygous *clueless* mutants expressing ectopic *clueless* or *CLUH* in motor neurons..... 63

List of Abbreviations

°C – degree Celsius

AAA+ – adenosine triphosphatase associated with diverse cellular activities

ALS – amyotrophic lateral sclerosis

αPS2 – α position-specific antigen 2

ATP – adenosine triphosphate

ATPase – adenosine triphosphatase

Bcl-2 – B cell lymphoma 2

BDSC – Bloomington Drosophila Stock Center

C-terminus – carboxyl-terminus

C9orf72 – chromosome 9 open reading frame gene

C9orf72 – chromosome 9 open reading frame 72

CI – confidence intervals

clu – *Drosophila melanogaster* *clueless* gene

Clu domain – clustered mitochondria domain

cluA – *clustered mitochondria* gene

cluA – clustered mitochondria

CLUH – *clustered mitochondria homologue* gene

CLUH – clustered mitochondria homologue

cm – centimetres

CO₂ – carbon dioxide

D. discoideum – *Dictyostelium discoideum*

D. melanogaster – *Drosophila melanogaster*

D42-Gal4 – P{GawB}D42

DA – dopaminergic

Drp1 – dynamin related protein 1 gene

DRP1 – dynamin related protein 1

DNA – deoxyribonucleic acid

FTLD – frontotemporal lobe degeneration

FUS – fused in sarcoma gene

FUS – fused in sarcoma

G3BP – Ras-GAP SH3 domain binding protein

Gal4 – Saccharomyces cerevisiae galactose responsive regulatory protein 4 gene

Gal4 – *Saccharomyces cerevisiae* galactose responsive regulatory protein 4

GTPase – guanosine triphosphatase

InR – insulin like receptor

lacZ – Escherichia coli β-galactosidase

LC – low-complexity

LC3 – microtubule-associated protein 1A/1B-light chain 3

LRRK2 – leucine rich repeat kinase 2 gene

Marf – mitochondrial assembly regulatory factor gene

Marf – mitochondrial assembly regulatory factor

Mff – mitochondrial fission factor

MFN2 – mitofusin 2

Mid49 – mitochondrial dynamic protein of 49 kDa

Miro – mitochondrial Rho

mL – millilitres

MPTP – 1-methyl-4-phenyl-1, 2, 3, 6-tetrahydropyridine

mRNA – messenger ribonucleic acid

mRNP – messenger ribonucleoproteins

mTOR – mammalian target of rapamycin

N – sample size

N-terminus – amino terminus

Normal Q-Q – normal quantile-quantile

Opa1 – *optic atrophy 1* gene

OPA1 – optic atrophy 1

p62 – *ubiquitin binding protein p62* gene

p62 – ubiquitin binding protein p62

PARIS – Parkin interacting substrate

PD – Parkinson disease

PGC-1 – peroxisome proliferator-activated receptor- γ coactivator 1

Pink1 – *PTEN -induced kinase 1* gene

PINK1 – PTEN -induced kinase 1

RNA – ribonucleic acid

RNAi – ribonucleic acid interference

RpL7a –ribosomal protein L7a

SNCA – *α -synuclein* gene

SOD1 – *superoxide dismutase 1* gene

SOD1 – superoxide dismutase 1

SOD2 – superoxide dismutase 2 gene

SOD2 – superoxide dismutase 2

TARDBP – TAR DNA-binding protein gene

TDP-43 – TAR DNA binding protein 43

TBPH – TAR DNA-binding protein homologue gene

TER94 – transitional endoplasmic reticulum 94 gene

TFAM – mitochondrial transcription factor A

TH – tyrosine hydroxylase gene

Tom20 – translocase of outer membrane 20

TOR – target of rapamycin

TPR – tetrcopeptide repeat

UAS –upstream activation sequence gene

UAS –upstream activation sequence

VCP – valosin containing protein gene

VCP – valosin containing protein

VDRC – Vienna Drosophila Resource Center

Chapter 1: Introduction

1.1 Mitochondria, Ageing, and Neurodegenerative Disease

Age-related and neurodegenerative disease in humans is linked with mitochondrial dysfunction, including Parkinson disease (PD) and amyotrophic lateral sclerosis (ALS) (B. Wang *et al.*, 2016; Carri *et al.*, 2017). Mitochondrial function is essential for ongoing cellular health and survival (Figure 1.1), as these organelles are the primary source of both energy in the form of ATP and damaging free radical species (Aryal and Lee, 2019). Mitochondria are essential for calcium buffering and apoptosis regulation, and provide an environment for biochemical reactions within the cell including fatty acid beta-oxidation and heme, steroid, and nucleotide biosynthesis (Sen and Cox, 2017). Impaired mitochondrial respiration rate is associated with ageing and age-related disease including PD, Alzheimer disease, and diabetes (Horan, *et al.*, 2012). Longevity and the efficacy of mechanisms for maintaining mitochondrial function are linked, and declines in mitochondrial function with age have been observed in humans and model organisms; these include oxidative damage, metabolic impairment, and impaired calcium buffering (Markaki and Tavernarakis, 2020; Fu *et al.*, 2018). These studies suggest that enhanced mitochondrial homeostasis could result in prevention of neurodegenerative disease and extension of human life.

Neurons have especially high energy demands, with cells in the human brain consuming 20% and 25% of the body's oxygen and glucose supplies, respectively, although the brain accounts for only 2% of body mass (Lee *et al.*, 2018). This intensive energy demand necessitates efficient oxidative phosphorylation, and results in more rapid free radical species generation by reactions of the mitochondrial electron transport chain.

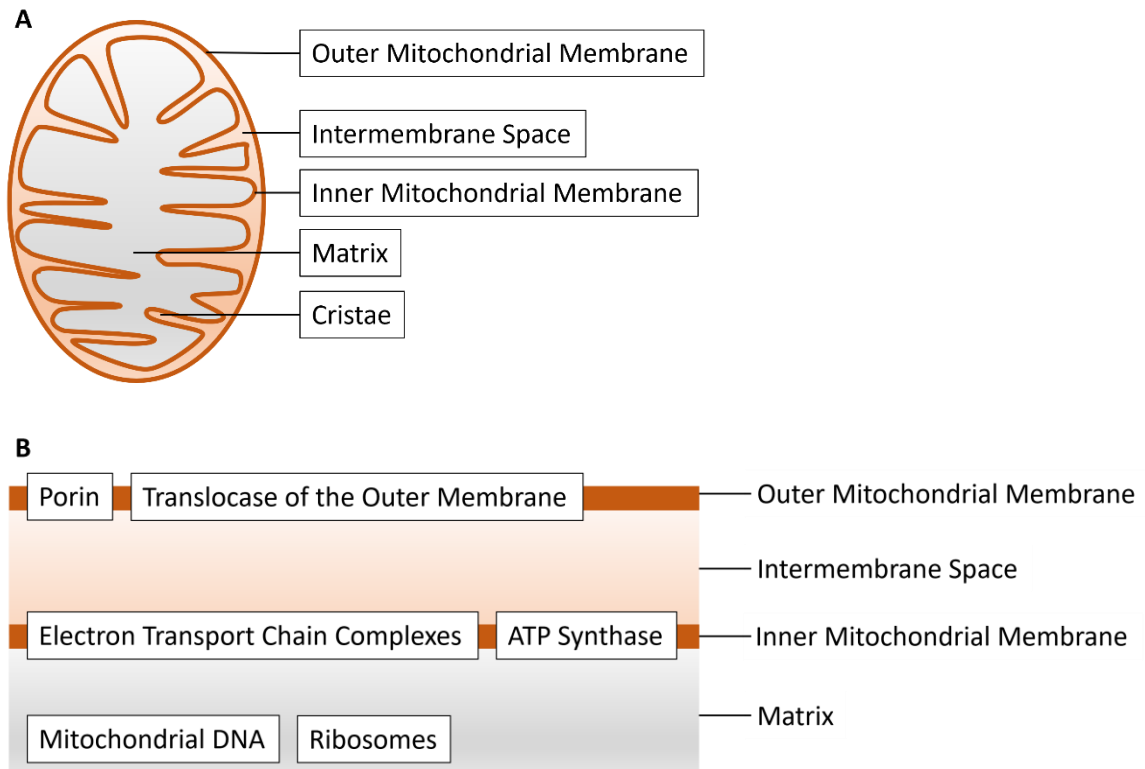


Figure 1.1 Mitochondria facilitate aerobic respiration in eukaryotic cells. A) Mitochondria are semi-autonomous organelles that continuously join and divide within the cell. Mitochondria have outer and inner membranes, separating the intermembrane space from the interior matrix. The inner mitochondrial membrane folds in on itself to form cristae, increasing its surface area. B) The double-membraned structure of mitochondria allows for the formation of an electrochemical proton gradient across the inner membrane. Electron transport chain complexes I, III, and IV cause protons to be pumped from the mitochondrial matrix into the intermembrane space. Protons are translocated back into the matrix via ATP synthase, which uses the energy from the proton gradient to synthesize ATP. Reviewed in Giacomello *et al.*, 2020. This figure was prepared using Microsoft PowerPoint for Microsoft 365 version 2406.

Reactive oxygen species (ROS) are highly reactive and therefore transitory (Alfadda and Sallam, 2012). This nature gives functionality in a wide array of signalling pathways (Winterbourn, 2008). Damage by ROS accumulates when ROS generation surpasses cellular ability to prevent and repair biomolecule oxidization (Garza-Lombó *et al.*, 2020). Defences include enzymatic antioxidants such as catalase and the superoxide dismutases, radical scavenging antioxidants like ascorbate and glutathione, and quality control mechanisms responsible for the selective degradation of mitochondria with compromised inner membrane potential (Winterbourn, 2008; Ge *et al.*, 2020). As the high energy requirements of neurons results in the production of elevated reactive oxygen species (Coyle and Puttfarcken, 1993), the function of these defences are of critical importance for the prevention of neurodegeneration.

Neurons are post-mitotic cells that must survive throughout the lifespan of an organism, and the cumulative loss of these populations of cells in humans causes progressive age-related neurodegenerative disease (Markaki and Tavernarakis, 2020). In such neurodegenerative diseases, neurons are most commonly lost through apoptosis, which is regulated by mitochondria (Cacciatore *et al.*, 2012). Severe damage to mitochondria can cause apoptotic signals including cytochrome c to be released from the mitochondrial intermembrane space into the cytosol to induce apoptotic cell death (Ma *et al.*, 2020). Specific neurodegenerative diseases are defined by the specific loss of certain neuronal cell populations such as dopaminergic neuron loss in PD, and motor neuron in ALS (Cacciatore *et al.*, 2012). Though the etiology of neurodegenerative diseases are heterogenous, examining causes of heritable forms of these diseases elucidates mechanisms of disease progression (Rodolfo *et al.*, 2018). Mutations linked to heightened

disease risk affect diverse pathways; including those directly associated with mitochondrial function (Fu *et al.*, 2018). These include ALS-associated mutations to the autophagy receptor *ubiquitin binding protein (p62)* causing impaired autophagy, a process by which components in the cytosol are degraded within lysosomes; and mutations to PD associated *parkin*, important for mitophagy, the mitochondria-specific form of autophagy (Fu *et al.*, 2018; Rodolfo *et al.*, 2018). Often, neurodegenerative disease is associated with the toxic aggregation of misfolded proteins, usually in the same population of neurons that experiences catastrophic losses. Expression of self-aggregating mutant proteins in model organisms can replicate features of neurodegenerative disease (Feany and Bender, 2000; McGurk *et al.*, 2015). Neurodegenerative diseases have diverse cognitive and physical symptoms which progress as the molecular basis of disease progresses, and may differ even among individuals that share a common genetic disease cause (Rodolfo *et al.*, 2018; Corti *et al.*, 2011; Kim *et al.*, 2013).

1.2 The Model Organism *Drosophila melanogaster* and Neurodegenerative Disease

A detailed understanding of the etiology of neurodegenerative diseases may lead to development of effective treatments. As it would be unsafe, unethical, and expensive to perform many of the experiments necessary to generate such an understanding directly on humans, alternative approaches must be taken (Jennings, 2011). Goals in model organism research include the generation of hypotheses related to the underlying mechanisms of human disease, and development of knowledge that may lead to methods of treatment and prevention of these diseases in humans whose efficacy may then be validated through clinical trial (Partridge and Gems, 2007). The *D. melanogaster* model organism is ideal for use in the study of neurodegenerative disease because these are easy and inexpensive

to culture, and have short lifespans well-suited to the study of age-related disease (Linford *et al.*, 2013). The *D. melanogaster* life cycle is illustrated in Figure 1.2. Considerable resources for research involving this model organism have been developed, including a vast knowledge of the *D. melanogaster* genome and methods for performing and assaying genetic experiments (Adams *et al.*, 2000; Brand and Perrimon, 1993; Dietzl *et al.*, 2007; Linford *et al.*, 2013; Todd and Staveley, 2004). Though humans and *D. melanogaster* are long-diverged, molecular mechanisms that determine cell function and disease are highly conserved such that approximately 70% of genes associated with neurodegenerative disease identified in humans are considered to have homologues in *D. melanogaster* (Lenz *et al.*, 2013). Like humans, *D. melanogaster* have complex central and peripheral nervous systems that consist of neurons and glia, and that use many common neurotransmitters (Sen and Cox, 2017; Lenz *et al.*, 2013; Yamamoto and Seto, 2014). Wild-type *D. melanogaster* experience age-related neurodegeneration (Sunderhaus and Kretschmar, 2016). Mitochondria are virtually identical between both our species with mitochondrial DNA encoding the same protein products, with the same remaining products required for mitochondrial function encoded within the nucleus (Sen and Cox, 2017). Humans and *D. melanogaster* similarly have decreased mitochondrial aerobic respiration efficiency with age, typically accompanied by increased mitochondrial turnover (Green *et al.*, 2011; Ferguson *et al.*, 2005 ; Markaki and Tavernarakis, 2020). Thus, *D. melanogaster* can be used to examine the role of conserved mechanisms for the regulation of mitochondrial homeostasis in neurodegeneration and ageing. Genetic models of Parkinson disease and amyotrophic lateral sclerosis are summarized in Table 1.1.

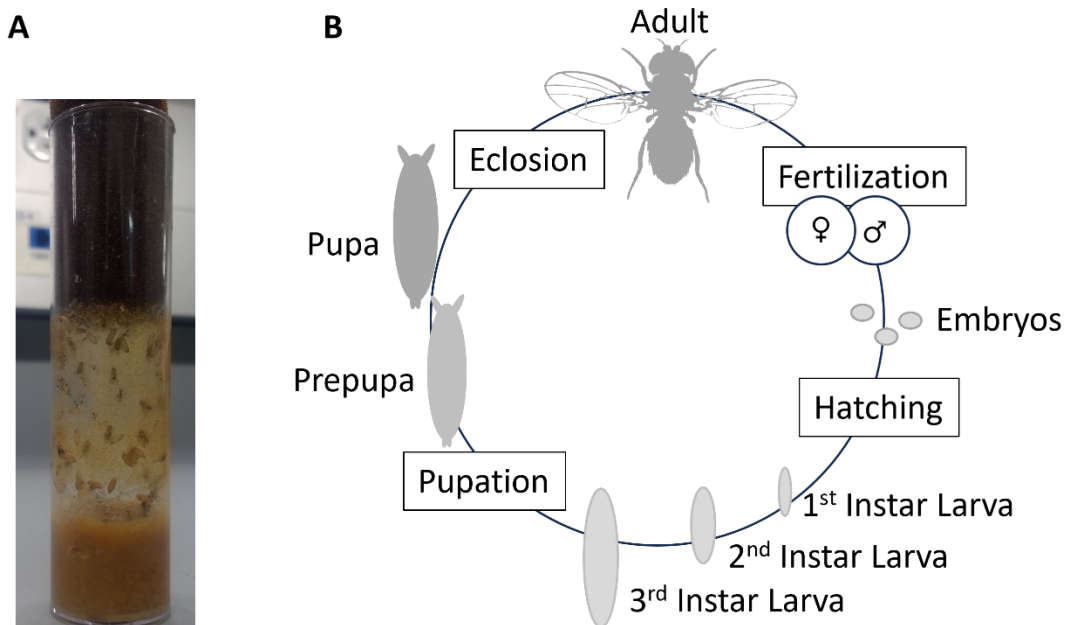


Figure 1.2 The *Drosophila melanogaster* life cycle. A) Experimental *Drosophila melanogaster* are cultured in plastic vials stopped with sponges containing ~5 mL of standard media. This photograph was taken on November 10, 2022. B) At an experimental temperature of 25°C, *Drosophila melanogaster* reach sexual maturity approximately 10 days following fertilization. Mature females store sperm after mating for up to two weeks. Fertilization occurs upon deposit of eggs into the media. Larvae hatch from the egg after one day and remain in the media through four days of larval development. Larvae progress through three larval stages (first, second, and third instar), separated by molting events. Third instar larvae climb out of the medium and adhere to the side of the vial to pupate. Adult structures form during metamorphosis, which takes approximately five days. Adults eclose from pupal cases and then reach sexual maturity within eight to twelve hours. This figure was prepared using Microsoft PowerPoint for Microsoft 365 version 2406. Adult organism artwork was modified from image created by Hegna (2012; Public Domain Mark 1.0).

Table 1.1 Genetic models of Parkinson disease and amyotrophic lateral sclerosis in *Drosophila melanogaster*. Expression of the proteins detailed was used to model neurodegenerative disease.

Disease Model	Protein Expressed	Reference
Parkinson disease	α -synuclein	Feany and Bender, 2000
Parkinson disease	Parkin (loss of function)	Greene <i>et al.</i> , 2003
Parkinson disease	LRRK2	Liu <i>et al.</i> , 2008
Parkinson disease	PINK1 (loss of function)	Clark <i>et al.</i> , 2006
Amyotrophic lateral sclerosis	GGGGCC repeat (C9orf72)	Xu <i>et al.</i> , 2013
Amyotrophic lateral sclerosis	TDP-43	Ritson <i>et al.</i> , 2010
Amyotrophic lateral sclerosis	SOD1	Elia <i>et al.</i> , 1999
Amyotrophic lateral sclerosis	FUS	Chen <i>et al.</i> , 2011

1.3 Parkinson Disease

Parkinson disease (PD) is one of the most common human neurodegenerative diseases, with a 1.5% lifetime risk of developing PD (Pringsheim *et al.*, 2014; Aryal and Lee, 2019). Symptoms commonly begin as very mild in nature and become more severe as pathology of the disease progresses, such that often PD is not diagnosed until several years following the initial symptom presentation (Lees *et al.*, 2009). Early symptoms include disturbed sleep, impaired dexterity, stiffness, fatigue, and loss of smell. Severe locomotor dysfunction in the later stages of the disease impairs quality of life by causing loss of independent mobility, difficulty in communication through speech and facial expressions, incontinence, constipation, loss of ability to chew and swallow, and dementia. Locomotor dysfunction caused by PD increases risk of falling and choking, and increases vulnerability to respiratory disease including pneumonia: the leading cause of death of PD patients. Though PD increases vulnerability to these risk factors, PD diagnosis is not usually associated with drastic reduction in life expectancy. PD pathology is heterogeneous, and individuals with the disease may experience symptoms earlier or later relative to one another, or not at all (Corti *et al.*, 2011). The “core triad” of PD symptoms are resting tremor, increased rigidity at rest, and bradykinesia (Ge *et al.*, 2020; Lees *et al.*, 2009). Definitive evidence of bradykinesia, or slowness of movement, is required for diagnosis (Abeliovich and Gitler, 2016). Though diverse symptoms are associated with PD progression, ultimately these are caused by the progressive loss of dopaminergic (DA) neurons of the *substantia nigra pars compacta* (Aryal and Lee, 2019). Dopamine is involved in coordinating movement and in reward, learning, and memory (Yamamoto and Seto, 2014). Impaired dopamine production causes many of the

symptoms associated with PD, and dopamine replacement therapies including supplementation of the dopamine precursor levodopa relieve symptoms in the early stages of the disease (Yamamoto and Seto, 2014; Abeliovich and Gitler, 2016).

1.4 Risk Factors for Parkinson Disease

Age is the greatest known risk factor for PD development, acting in combination with other genetic and environmental causes (Lees *et al.*, 2009). Symptoms of PD begin in adulthood and frequency of diagnoses increase with age, such that 90% of those diagnosed are over the age of 45 years. Environmental risk factors may include exposure to oxidative stress-inducing toxins such as the synthetic opioid 1-methyl-4-phenyl-1, 2, 3, 6-tetrahydropyridine (MPTP) and the pesticide rotenone, and exposure to viruses such as influenza (Aryal and Lee, 2019; Huang *et al.*, 2022; Corti *et al.*, 2011). While specific causes of PD are unknown in most cases, 10% may be attributed to single-gene mutations in known PD-causing genes (Aryal and Lee, 2019; Ge *et al.*, 2020). Genome-wide association studies reveal more than 200 genes that influence PD pathology (Funayama *et al.*, 2022). There are 24 genes whose mutation is known to cause PD including α -synuclein (*SNCA*), leucine rich repeat kinase 2 (*LRRK2*), *PTEN*-induced kinase 1 (*Pink1*), and *parkin* (Funayama *et al.*, 2022; Aryal and Lee, 2019). While the majority of PD cases are considered sporadic, the disease is believed to be inherited in more than 5% of affected individuals (B. Wang *et al.*, 2016). Genes believed to be responsible for heritable forms of PD seem to have a role in many of the sporadic forms (Corti *et al.*, 2011). For example, *LRRK2* mutations contribute to over 10% of familial PD and mutations in this gene are the most common known genetic cause of sporadic PD, with more than 50 different *LRRK2* mutations identified in PD patients (B. Wang *et al.*, 2016;

Aryal and Lee, 2019). Mitochondrial dysfunction including impaired respiration is associated with both sporadic and heritable forms of PD (Corti *et al.*, 2011; Horan, *et al.*, 2012). Evidence of mitochondrial complex I dysfunction has consistently been identified in post-mortem analysis of the *substantia nigra pars compacta* of PD patients (Ge *et al.*, 2020).

1.5 Lewy Body Pathology in Parkinson Disease

Lewy bodies are toxic cytoplasmic inclusion structures primarily composed of aggregated α -synuclein, and are widely distributed in neurons throughout the brains of PD patients with *SNCA* mutations (B. Wang *et al.*, 2016; Abeliovich and Gitler, 2016; Lees *et al.*, 2009). *SNCA* encodes the primary Lewy body component α -synuclein, and mutations in this gene can cause PD (Aryal and Lee, 2019). A mitochondrial targeting signal is located near the N-terminus of the α -synuclein and causes it to associate with mitochondrial membranes (Aryal and Lee, 2019). Accumulation of α -synuclein aggregates in the inner membrane can lead to impaired complex I function, and α -synuclein aggregates in the outer membrane can induce mitochondrial fragmentation by inhibiting fusion (Aryal and Lee, 2019; Zhu *et al.*, 2018). Aggregates of α -synuclein in mitochondrial membranes can disrupt membrane potential through the activation of mitochondrial permeability transition pore through interaction with inner and outer membrane transport proteins to initiate degradation of these organelles (B. Wang *et al.*, 2016). Mutations in other PD-associated genes cause Lewy body formation, including autophagy related-*LRRK2* (Lees *et al.*, 2009; B. Wang *et al.*, 2016). Postmortem analysis of patients who die with mild symptoms shows that Lewy bodies are mainly concentrated in the lower regions of the brainstem including the *substantia nigra pars compacta*, but

where patients had severe symptoms these inclusions are found more widely and in forebrain regions (Abeliovich and Gitler, 2016). This reveals a pattern of progression associated with severity of the disease. Lewy bodies are also be found in approximately 10% of those aged 60 or above who die without known neurological disease (Lees *et al.*, 2009). Postmortem analysis reveals reduced immunoreactivity to the dopaminergic-neuron specific enzyme tyrosine hydroxylase (TH) in these cases, similar to that found in analysis of postmortem PD patients but to a lesser degree (Dickson *et al.*, 2008). It is possible that these cases represent pre-clinical stages of PD progression, highlighting the importance of developing treatment for this quality-of-life impacting disease as medical advancement continues to extend human lifespan.

1.6 *Drosophila melanogaster* as a Model for Parkinson Disease

Genetic methods of modeling PD in *D. melanogaster* cause progressive loss of DA neurons *in vivo* (Aryal and Lee, 2019). *D. melanogaster* have approximately 130 DA neurons, of approximately 100 000 total neurons, which are located in clusters within the central nervous system and projected throughout most of the brain (Yamamoto and Seto, 2014; Hartenstein *et al.*, 2016). DA neurons in humans are located in clusters, of which the PD-associated *substantia nigra pars compacta* is just one (Fu *et al.*, 2018). Dopamine regulates locomotor activity in *D. melanogaster* as well as sleep, learning, and memory (Hartenstein *et al.*, 2016). Pan-neuronal expression of α -synuclein constructs in a *D. melanogaster* model of PD causes the formation of α -synuclein-containing inclusions in the brain, specific loss of DA neurons beginning in adulthood, and progressive locomotor dysfunction as determined by the premature loss of climbing ability with age (Feany and Bender, 2000). Thus, *D. melanogaster* may be used in experimental examination of the

genetic mechanisms that regulate the protection of DA neurons from age-related cellular stress.

1.7 Amyotrophic Lateral Sclerosis

Amyotrophic lateral sclerosis (ALS) is a rapidly progressive adult-onset paralytic human disease that is usually fatal within two to five years of symptom presentation (Rodolfo *et al.*, 2018; Masrori and Van Damme, 2020). ALS is characterized by the degeneration of both the upper and lower motor neurons of the brainstem and spinal cord, and the upper motor neurons of the motor cortex (Fu *et al.*, 2018). Motor neurons are responsible for controlling and enabling movement, with the loss of these neurons resulting in weakness and muscle wasting beginning at a focal point and spreading throughout the body as the disease progresses (Abdul Wahid *et al.*, 2019; Masrori and Van Damme, 2020). Motor neuron loss is preceded by loss of neuromuscular connections and retraction of axons (Masrori and Van Damme, 2020). Symptom onset usually occurs at distal muscles of the limbs. Following onset, weakness and muscle wasting spreads to adjacent regions and throughout the motor system. Axial muscles are typically affected late in the progression of the disease, causing postural problems. Cumulative loss of locomotor function in ALS necessitates reliance on increased supports as the disease progresses, including nutritional and respiratory support at the latest stages of the disease. Finally, respiratory muscle failure results in death. Nearly 70% of ALS patients report pain at some point in their disease progression including muscle cramping as movement becomes more difficult and headaches as respiration is impaired (Zarei *et al.*, 2015; Foster and Salajegheh, 2019).

ALS progression rate is variable, with 50% of patients dying within 30 months of symptom onset, but as many as 10% surviving for more than a decade (Ingre *et al.*, 2015). Presently, there is very little that can be done to slow progression of ALS following diagnosis (Masrori and Van Damme, 2020). Drugs used in the treatment of ALS include riluzole and edaravone (Masrori and Van Damme, 2020). Riluzole is a glutamine antagonist that was found in clinical trial to extend mean patient lifespan by three to six months (Masrori and Van Damme, 2020). Edaravone is a free radical scavenger that was found in clinical trial to slow the decline in locomotor ability in some patients. Management of symptoms to ease discomfort, however, continues to be the primary clinical approach to ALS management. Effective treatment to protect against motor neuron loss would preserve life and alleviate human suffering. It is essential that we understand the factors that influence the progression of ALS to aid in the diagnosis, treatment, and prevention of this disease.

1.8 Risk Factors for Amyotrophic Lateral Sclerosis

Age is the greatest ALS risk factor, with 95% of cases occurring in those greater than 30 years of age (Zarei *et al.*, 2015). Mean age of onset is between 58 and 63 years for those with no family history, and between 40 and 60 years for those with affected close relatives (Masrori and Van Damme, 2020). Greater age at time of symptom onset is associated with more rapid disease progression. Environmental risk factors may include ingestion seeds from the cycad *Cycas micronesica*, which contain the neurotoxin β -methylamino-L-alanin, and populations that consume these have increased incidence of Parkinsonism and dementia (Zarei *et al.*, 2015; Ingre *et al.*, 2015). Treatment of *D. melanogaster* with this toxin replicates features of neurodegenerative disease including

impaired lifespan and locomotor function, and impaired learning and memory (Zhou *et al.*, 2010). Approximately 15% of ALS cases can be attributed to single-gene mutations in known ALS-causing genes (Masrori and Van Damme, 2020); including *chromosome 9 open reading frame 72 (C9orf72)*, *TAR DNA-binding protein (TARDBP)*, *fused in sarcoma (FUS)*, *superoxide dismutase 1 (SOD1)*, and *valosin containing protein (VCP)*.

Mutations in the but TAR DNA binding protein 43 (TDP-43)-encoding protein *TARDBP* are responsible for fewer than 5% of ALS cases, but TDP-43 aggregates are present in more than 95% of post-mortem ALS brain tissue examined (Masrori and Van Damme, 2020). TDP-43 is a RNA- and DNA- binding protein with roles in transcription, splicing, and stress granule formation (Masrori and Van Damme, 2020). Aggregated TDP-43 localizes primarily to the cytoplasm which impairs the ability of this protein to perform its DNA-binding functions within the nucleus, and aggregated TDP-43 has impaired cytoplasmic RNA-processing function. Mutated TDP-43 accumulates in the cytoplasm after being cleaved and phosphorylated, but in other cases protein aggregation may be due to dysregulated autophagy (Ingre *et al.*, 2015; Carri *et al.*, 2017). *C9orf72* and *VCP*, for example, both have roles in autophagy pathways, and mutations in these ALS-associated genes cause TDP-43 aggregation (Masrori and Van Damme, 2020; Buchan *et al.*, 2013). Other protein aggregates may be found in the motor neurons of ALS patients, including SOD1 aggregates as a result of *SOD1* mutations, and FUS as a result of *FUS* mutations. Aggregated SOD1 may interact with the autophagy and apoptosis-regulating protein B cell lymphoma 2 (Bcl-2), disrupting function of these pathways (Zarei *et al.*, 2015; Ma *et al.*, 2020). In the spinal cords of ALS patients, mutant SOD1 aggregates accumulate within the mitochondrial matrix and on the outer membrane, where

interactions may alter the structure of mitochondrial proteins and cause impaired ATP production and mitochondrial transport (Zarei *et al.*, 2015; Liu *et al.*, 2004). Aggregated proteins within the cytoplasm may induce subsequent aggregation of normal forms of these proteins (Buchan *et al.*, 2013). Thus cytoplasmic protein aggregation may play an important role in the progression of ALS.

1.9 Amyotrophic Lateral Sclerosis and Frontotemporal Lobe Degeneration

The most common genetic cause of ALS is the repeat expansion of the hexanucleotide GGGGCC from within a noncoding region of the *C9orf72* gene (Masrori and Van Damme, 2020). These mutations are responsible for 30 to 50% of inherited ALS, and approximately 7% of sporadic cases. *C9orf72* mutations are a common cause of frontotemporal lobe degeneration (FTLD) and multiple sclerosis (Masrori and Van Damme, 2020; Ingre *et al.*, 2015). Up to 15% of ALS patients meet the diagnostic criteria for FTLD, a progressive dementia defined by degeneration of the frontal and anterior temporal lobes (Masrori and Van Damme, 2020). Behavioural and cognitive symptoms that might be attributed to changes in these regions are present in 25 to 40% of ALS cases. Up to 15% of FTLD patients likewise meet the diagnostic criteria for ALS, with up to one in three showing signs of motor neuron dysfunction (Azuma *et al.*, 2014). ALS patients may have greater than 1000 *C9orf72* hexanucleotide repeats, whereas healthy individuals usually have less than 30 (Ingre *et al.*, 2015). Patients with *C9orf72* hexanucleotide expansions show accumulations of dipeptide repeat proteins translated from expansions, which are neurotoxic (Bolus *et al.*, 2020). Normal function of the *C9orf72* protein may be disrupted, including its role in autophagy (Ingre *et al.*, 2015). Furthermore, cytoplasmic TDP-43 aggregates are found in motor neurons in

approximately half of FTLN patient tissue analyzed (McGurk *et al.*, 2015; Ingre *et al.*, 2015). Thus, ALS and FTLN have been described as a “continuous clinical spectrum” (Nguyen *et al.*, 2019). *C9orf72* mutations in particular are associated with cognitive and behavioural symptoms in ALS patients (Masrori and Van Damme, 2020). ALS and FTLN share other common underlying molecular mechanisms such that many ALS-linked genes including *C9orf72*, *FUS*, *TARDBP*, and *VCP* are associated with FTLN (Nguyen *et al.*, 2019; Kimonis *et al.*, 2008). The relationship of ALS and FTLN including common genetic causes illustrates that common molecular mechanisms may underlie the progression of neurodegenerative diseases.

1.10 *Drosophila melanogaster* as a Model for Amyotrophic Lateral Sclerosis

The *D. melanogaster* neuromuscular system is simple compared to humans, however the basic structural components that enable locomotor function are conserved (Lloyd and Taylor, 2010). Like humans, the *D. melanogaster* neuromuscular system is composed of motor neurons whose axons connect to muscle cells through complex neuromuscular junctions and sensory neurons. The molecular mechanisms enabling operation of these components are highly conserved and altering function of these these has reproduced central features of human neuromuscular disease, including ALS (Lloyd and Taylor, 2010; McGurk *et al.*, 2015). For example, expression of human TDP-43 in *D. melanogaster* motor neurons causes neurodegenerative disease as determined by premature loss of climbing ability with age and reduced lifespan (McGurk *et al.*, 2015). Expression of mutated human TDP-43 that is disrupted in its RNA-binding ability, however, does not recreate these phenotypes. Inhibited expression of the *D. melanogaster* *TARDBP* homologue *TBPH* causes similar impairments to locomotor function and

lifespan. Together these data suggest that it is the dysregulation of TDP-43 function in RNA metabolism and gene expression, rather than toxic effects of aggregates, that lead to motor neuron degeneration in ALS.

1.11 Regulation of Mitochondrial Homeostasis

Mitochondria form a dynamic network that responds to the needs of the cell through regulation of the interconnected processes determining morphology, distribution, fission, fusion, degradation, and biogenesis (Dorn and Kitsis, 2014; Chen and Chan, 2009). The nuclear genome encodes all but 13 of the protein subunits required to form mitochondrial electron transport chain complexes, necessitating replication of, and transcription from, the mitochondrial genome (Sen and Cox, 2017). Mitochondria have therefore retained their ability to proliferate through fission and to exchange DNA and other components through fusion (Dorn, 2019). Proliferation of mitochondria enables their distribution as required within the cell via trafficking along the microtubules, and mitochondrial trafficking conversely enables fusion by bringing mitochondria in proximity to one another. Fission and fusion are important determinants of mitochondrial morphology, affecting function, while trafficking itself is morphology-dependent (Ravanelli *et al.*, 2020; Chen and Chan, 2009). For example, impaired trafficking of enlarged mitochondria to distal regions of axons and dendrites may cause their retraction and lead to loss of neuronal function (Zhu *et al.*, 2018). Damage to mitochondrial respiratory complexes results in less efficient oxidative respiration, producing greater amounts of damaging ROS (Cacciatore *et al.*, 2012). Damage to mitochondria caused by ROS can also trigger the release of cytochrome c and other pro-death factors into the cytosol, initiating apoptosis (Ma *et al.*, 2020). In a network of content-exchanging toxin-

producing mitochondria it is important that mitochondrial damage be controlled, as failure to do so endangers the entire intracellular population as well as the cell itself (Dorn and Kitsis, 2014). Fission enables the segregation of mitochondrial damage and produces small morphology appropriate for degradation by mitophagy. Fission and mitophagy can effectively preserve mitochondrial function only where an abundant supply of healthy mitochondria are maintained through fusion and biogenesis (Ge et al., 2020; Dorn and Kitsis, 2014). Thus mitochondrial homeostasis depends on the precise and responsive function of these conserved and interdependent processes.

1.12 Mitochondrial Dynamism

Mitochondrial dynamism refers to the processes of fission, fusion, and trafficking (Dorn, 2019). Dynamism is primarily mediated by the GTPases including optic atrophy 1 (OPA1), dynamin related protein 1 (DRP1), and mitofusin 1 and mitofusin 2 in mammals or the single mitofusin mitochondrial assembly regulatory factor (Marf) in most *D. melanogaster* cells (Dorn, 2019). Fission and fusion occur continuously, resulting in an intracellular mitochondrial population nearly homogenous in content (Ravanelli *et al.*, 2020; Chan, 2007). Mitochondria do not retain individual identities upon fusion: they merge membranes, matrices, and have continuity of function (Chan, 2007; Dorn, 2019). Fusion has a protective role in mitochondrial function as the merging of individuals enables mitochondrial DNA repair, protein complementation, and can provide greater access to metabolites that may have been lacking (Chen and Chan, 2009). Enhanced fusion produces elongated mitochondria that may be more efficient in ATP production and that are resistant to engulfment, which is required for mitophagy (Zhu *et al.*, 2018; Zemirli *et al.*, 2018). Exposure to mild stress conditions including nutrient deprivation

and exposure to some toxins cause hyperfusion (Ge et al., 2020). Enhanced fission produces smaller mitochondria which are more efficiently trafficked via microtubules (Chen and Chan, 2009). Asymmetric fission acts to segregate damaged components by selectively incorporating undamaged components into one daughter organelle, resulting in one healthy mitochondrion and one that is severely impaired and will quickly be degraded by mitophagy (Dorn and Kitsis, 2014). Conditions of severe stress such as prolonged nutrient deprivation and oxidative stress cause enhanced fission which enables mitophagy, limits respiration and thus free radical production, and promotes apoptosis in the absence of mitophagy (Zemirli *et al.*, 2018; Hung *et al.*, 2018; Chen and Chan, 2009; Garza-Lombó *et al.*, 2020). Thus regulation of fission and fusion play an important role in regulation of the cellular mitochondrial network, including in stress response processes.

Mitochondrial trafficking is intimately connected to fusion and fission. Not only are the function of these processes interdependent; they also share molecular mechanisms (Dorn, 2019). In animal cells, mitochondrial motility mostly occurs via trafficking along the microtubules (Chen and Chan, 2009). Mitochondrial trafficking is regulated by mitofusins localized to the outer membrane (Dorn, 2019). These mitofusins can bind to Miro proteins and tether mitochondrial Miro-Milton-kinesin-dynein complexes that facilitate attachment to, and movement along, microtubules. Distribution of mitochondria is of particular concern in polarized cells and those with complex morphology, including neurons (Chen and Chan, 2009; Zhu *et al.*, 2018). Neurons have high energy needs at distal axons and dendrites, necessitating the trafficking of mitochondria far from the cell body (Zhu *et al.*, 2018). Dysfunction in mitochondrial dynamics causes the accumulation of mitochondria with abnormal morphology, which has been linked to cellular damage

(Zhu *et al.*, 2018). Impaired processes determining mitochondrial dynamics cause neuronal dysfunction and neurodegeneration.

Genes linked to neurodegenerative disease that interact with dynamism genes and processes include PD-associated *Pink1* and *parkin*, and ALS-associated *VCP* (Fu *et al.*, 2018). Abnormalities in mitochondrial morphology have been observed in *Pink1* and *parkin* mutant *D. melanogaster*, which could in part be due to their interaction with dynamism genes as well as their role in mitophagy (Corti *et al.*, 2011). PINK1 phosphorylation and Parkin ubiquitinylation promote degradation of outer membrane proteins including mitofusins, suppressing fusion and thus favouring smaller mitochondria which can be engulfed to form phagophores prior to maturation to autophagosomes (Hung *et al.*, 2018; Rodolfo *et al.*, 2018; Ravanelli *et al.*, 2020; Zhu *et al.*, 2018; Imai, 2020; Markaki and Tavernakis, 2020; Garza-Lombó *et al.*, 2020). *VCP*, which binds to the mitochondrial outer membrane following Parkin ubiquitinylation of outer membrane proteins, is required for PINK1-Parkin-associated degradation of mitofusins (Kim *et al.*, 2013). Suppression of fusion may be protective through inhibition of the spread of damaged components and toxic molecules throughout the mitochondrial network (Bhandari *et al.*, 2014). PINK1 promotes fission through recruitment of DRP1 to the outer membrane (Ge *et al.*, 2020). On the other hand, activated Parkin at mitochondria ubiquitinylates DRP1 and promotes its degradation, suppressing fission (B. Wang *et al.*, 2016). The relationship between PINK1-Parkin signalling, fission, and mitophagy is illustrated in Figure 1.3. Phenotypes associated with *D. melanogaster Pink1* and *parkin* mutants including climbing impairments and muscle degeneration can be ameliorated through the misexpression of dynamism proteins (Chen and Chan, 2009). Specifically,

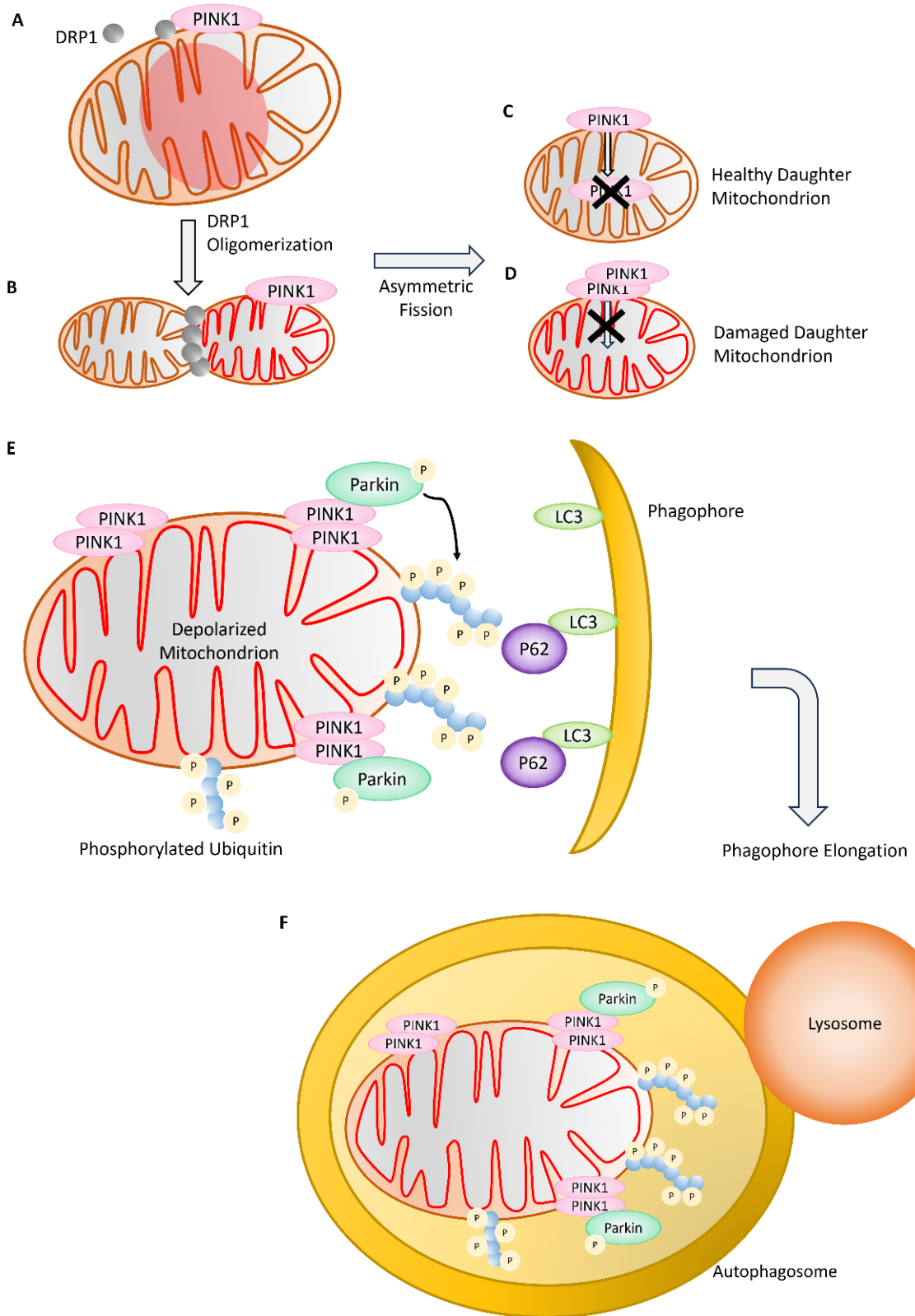


Figure 1.3 PINK1 acts as a sensor to detect mitochondrial damage, and PINK1-Parkin signalling regulate mitochondrial fission and mitophagy. A) Outer membrane proteins, including accumulated PINK1 on damaged mitochondria, recruit the fission protein DRP1 to the mitochondrial surface. PINK1 phosphorylation and subsequent ubiquitylation by activated Parkin also promotes degradation of mitofusins, suppressing fusion. B) Fission is induced by DRP1 at the mitochondrial surface, which oligomerizes to form spiral filaments that constrict the mitochondrion and cause it to separate into two daughter mitochondria. Asymmetric fission acts to segregate damaged components into one daughter cell. C) One healthy mitochondrion is produced as a result of asymmetric fission. PINK1 is targeted to healthy mitochondria but does not accumulate, as it is instead imported and degraded within the mitochondrial matrix. D) A mitochondrion with damaged components may undergo a loss of inner membrane potential (depolarization), triggering PINK1-Parkin-mediated mitophagy. This causes PINK1 to accumulate on the mitochondrial surface and dimerize. E) Homodimerized PINK1 undergoes autophosphorylation, and activated PINK1 phosphorylates ubiquitin chains present at the mitochondrial surface. PINK1 phosphorylation activates Parkin, which then ubiquitinylates mitochondrial proteins including translocase of the outer membrane. Autophagy receptors including p62 have ubiquitin-binding domains as well as microtubule-associated protein 1A/1B-light chain 3 (LC3)-interacting regions. LC3 domains facilitate binding of autophagy receptors to phagophores, which enable engulfment of ubiquitin-marked mitochondria to form autophagosomes. F) Autophagosomes fuse with lysosomes for proteolytic degradation of damaged mitochondria. This figure was prepared using Microsoft PowerPoint for Microsoft 365 version 2406.

promotion of fission over fusion has this rescuing effect; whether through *Drp1* overexpression or inhibited expression of *Marf* or *Opal*. Mitofusins likewise are involved in PINK1-Parkin mitophagy signalling (Dorn, 2019). In mammals, mitofusin 2 mediates the recruitment of Parkin to damaged mitochondria (Zhu *et al.*, 2018). When *MFN2*, encoding mitofusin 2, is suppressed in mouse neurons and cardiomyocytes, Parkin-mediated mitophagy is impaired and cells show an accumulation of morphologically abnormal mitochondria. Thus dysregulation of dynamism processes may be a common consequence of mutations that impact neurodegenerative disease-associated genes.

1.13 Mitophagy

Mitophagy is a specialized form of autophagy that functions to identify damaged mitochondria and target them for lysosomal degradation (Ravanelli *et al.*, 2020; Dorn and Kitsis, 2014). Autophagy occurs at basal levels in healthy conditions in almost all cell types (Garza-Lombó *et al.*, 2020). Basal mitophagy is widespread, though rates under ideal conditions are apparently low as evidenced by the observation that some stable isotope-labeled mitochondrial proteins in *D. melanogaster* have half-lives of greater than 30 days (Ge *et al.*, 2020; Vincow *et al.*, 2013). Mitophagy can be induced by oxidative stress, and mitophagy rates are age-dependent (Garza-Lombó *et al.*, 2020; Ge *et al.*, 2020). Levels of mitophagy have been reported to increase with age in wild-type *D. melanogaster*, but decrease with age in mice (Ge *et al.*, 2020). As mitochondria are continuously joining and dividing, mitochondrial quality control mechanisms including mitophagy must rapidly respond to prevent stress-induced mitochondrial damage from spreading throughout the cellular network (Harper *et al.*, 2018). Stress-induced mitophagy usually has a pro-cell survival effect; preventing the release of pro-apoptotic

factors from damaged mitochondria (Garza-Lombó *et al.*, 2020; Lee *et al.*, 2020).

Mitophagy works alongside other mitochondrial quality control processes such as the ubiquitin-proteasome system, which functions to remove ubiquitinated mitochondrial proteins, and some proteins including VCP have roles in both process (Ge *et al.*, 2020; Yeo and Yu, 2016). Mutations in mitophagy-regulating genes that are associated with neurodegenerative disease include *VCP* and *p62* which are associated with ALS, and *Pink1* and *Parkin* which are associated with early-onset forms of PD (Carri *et al.*, 2017; B. Wang *et al.*, 2016). Deficiency of *parkin* may be associated with other forms of PD as the Parkin protein can be sequestered into Lewy bodies, and impaired PINK1-Parkin signalling is also associated with ALS and other neurodegenerative disease (Ge *et al.*, 2020; Quinn *et al.*, 2020). Investigation of the proteins that regulate mitophagy may be informative in elucidating the role of this key process in the progression of neurodegenerative disease.

1.14 Mitophagy in *Drosophila melanogaster*

Mutant *Pink1* and *parkin* *D. melanogaster* have locomotor defects, decreased lifespan, and specific degeneration of DA neurons; indicating that these mutants may be useful in PD modelling to enhance understanding of mechanisms of this disease (Aryal and Lee, 2019). In *D. melanogaster* aged to four weeks, mitophagy occurs at approximately 10 times the rate as that of *D. melanogaster* aged to one week (Cornelissen *et al.*, 2018). This age-dependent mitophagy increase was not observed in *D. melanogaster* inhibited in *Pink1* and *parkin* expression. Further, they found that mitophagy occurring at low levels in one-week-aged *D. melanogaster* was not affected by *Pink1* or *parkin* inhibition. This finding is consistent with no differences found in the

mitophagy levels of *Pink1*- and *parkin*- null *D. melanogaster* compared to control at one to three days of age (Lee *et al.*, 2018). Parkin-independent alternative mitochondrial quality control mechanisms including the ubiquitin-proteasome may compensate for loss of *Pink1* and *parkin* in young individuals (Markaki and Tavernarakis, 2020; Livnat-Levanon and Glickman, 2011). Proteasomal activity declines with age in *D. melanogaster*, emphasizing the role of Parkin-mediated mitophagy in age-related disease such as PD (Livnat-Levanon and Glickman, 2011). Interestingly, *parkin* null mutants at two to three days of age do show locomotor defects as evaluated through climbing and flight assays (Greene *et al.*, 2003). This suggests that loss of Parkin may have mitophagy-independent roles in young *D. melanogaster*. VCP is an AAA+ ATPase with roles in autophagosome maturation and initiation, and autophagy is impaired in ALS and FTLD patients with *VCP* mutations (Yeo and Yu, 2016). VCP is highly conserved, and is encoded in *D. melanogaster* by *TER94* (Yeo and Yu, 2016; Carri *et al.*, 2017). *TER94* overexpression rescues phenotypes associated with *Pink1* deficiency in *D. melanogaster*, including locomotor defects, but not those associated with Parkin deficiency (Kim *et al.*, 2013). *TER94*-null *D. melanogaster* mutants typically do not survive pupation, and those that do die shortly after eclosion. RNAi-mediated *TER94* inhibition in *D. melanogaster* motor and dopaminergic neurons can cause a reduction in lifespan (Hurley and Staveley, 2020). Thus *D. melanogaster* models have played a role in elucidating the function of PINK1, Parkin, and VCP in mitophagy.

1.15 Mitochondrial Biogenesis

Replicative fission and the longevity of mitochondrial networks are enabled by mitochondrial biogenesis: the synthesis of mitochondrial-encoded proteins, and the

synthesis and import of nuclear-encoded proteins and components (Popov, 2020; Dorn and Kitsis, 2014). The majority of mitochondrial proteins are encoded in the nucleus, and their expression is largely controlled by the peroxisome proliferator-activated receptor- γ coactivator 1 (PGC-1) family of transcription factors (Ravanelli *et al.*, 2020; Ge *et al.*, 2020). Most nuclear-encoded mitochondrial proteins are imported following translation through translocase of the outer membrane complexes embedded within the outer membrane (Eliyahu *et al.*, 2010). PGC-1 transcription factors regulate the expression of mitochondria-encoded genes, including through control of the mitochondrial transcription factor A (Popov, 2020; Markaki and Tavernarakis, 2020). PGC-1 α is a master regulator of mitochondrial biogenesis that controls the activity of multiple other biogenesis-associated transcription factors (Palikaras *et al.*, 2015). PGC-1 α is, in turn, regulated by Parkin interacting substrate (PARIS); a ubiquitinylation target of activated Parkin (Palikaras *et al.*, 2015; Markaki and Tavernarakis, 2020). PGC-1 α is upregulated upon degradation of ubiquitinated PARIS, thus coordinating biogenesis with mitophagy (Ge *et al.*, 2020). Sequestration of PINK1 to Lewy bodies in PD brain tissue is associated with elevated levels of PARIS and downregulated PGC-1 α ; linking dysregulation of mitochondrial biogenesis with PD (Ge *et al.*, 2020; Popov, 2020). High insulin levels cause increased mitochondrial protein synthesis through regulation of PGC-1 α , whereas low levels of insulin signalling induce mitophagy (Palikaras *et al.*, 2015; Ruegsegger *et al.*, 2018). These findings demonstrate that biogenesis is coordinated with other processes to control mitochondrial homeostasis.

1.16 RNA-Processing in Regulation of Mitochondrial Biogenesis

Many identified ALS-causing genes are involved in RNA-processing, and RNA-processing defects may contribute to mitochondrial dysfunction (Carri *et al.*, 2017). Regulation of mitochondrial biogenesis necessitates control of mitochondrial gene transcription and processing of these transcripts (Palikaras *et al.*, 2015). Cytoplasmic mRNA processing is an important means by which to control gene expression, including regulation of mRNA stability, translation, and localization (Buchan and Parker, 2009). Localization of nuclear-encoded mitochondrial mRNAs often occurs prior to translation (Eliyahu *et al.*, 2010). Translation of nuclear-encoded mitochondrial mRNAs in proximity to mitochondria by local ribosomes and translation factors is more energy-efficient than transportation of mitochondria-bound proteins, and enables rapid translation at mitochondria in response to intracellular signals. Pre-translational localization can occur as the result of mRNA interaction with RNA-binding proteins, which inhibits translation while bound and facilitates translocation towards mitochondria (Lesnik *et al.*, 2015). An alternative mechanism of mRNA localization is co-translational protein targeting and import: a mechanism that is most well-understood in relation to endoplasmic reticulum-associated proteins, but which has been reported to occur at the mitochondria (Nyathi *et al.*, 2013; Lesnik *et al.*, 2015). By this mechanism, ribosome-bound mRNAs complex with a signal recognition particle following the translation of a short signal sequence, and are then targeted to signal recognition particle receptors (Nyathi *et al.*, 2013). Once targeted to a receptor the protein can be translocated through the membrane pore as translation continues, where protein folding is completed following translocation. Co-translational import thus couples protein synthesis with localization

(Lesnik *et al.*, 2015). Modulation of biogenesis through regulation of localized translation at mitochondria may be a point where cells can exert a rapidly responsive control of mitochondrial homeostasis.

mRNAs are associated with RNA-binding proteins in messenger ribonucleoprotein (mRNP) complexes throughout their life cycles: determining mRNA stability, degradation, translation, and localization (Erickson and Lykke-Andersen, 2011). Non-translating mRNPs in the cytoplasm can assemble to form mRNP granules, which rapidly form and disperse in response to cues from the cellular environment (Erickson and Lykke-Andersen, 2011; Tian *et al.*, 2020). mRNP granules have distinct functions depending on location and composition, though different types of mRNP granules interact and frequently exchange components (Tian *et al.*, 2020; Bowden and Dormann, 2016). Two well-described types of mRNP granules are processing bodies and stress granules, both of which form in response to stressors such as nutrient deprivation. Processing body formation is not stress-dependent, however their formation is upregulated in response to stress (Ivanov *et al.*, 2019; Erickson and Lykke-Andersen, 2011; Buchan and Parker, 2009). Processing bodies associate with components that act to repress translation and initiate mRNA decay, though mRNA degradation does not occur within these mRNP granules (Ivanov *et al.*, 2019). Stress granules form on impaired initiation of translation including in conditions of stress caused by nutrient deprivation, oxidative stress, and heat (Buchan and Parker, 2009; Buchan *et al.*, 2013). Stress granules form where translation is repressed through overexpression of RNA-binding proteins, and are related to pathological accumulations associated with neurodegenerative disease including ALS and FTLN (Buchan and Parker, 2009; McGurk *et al.*, 2015; Buchan *et al.*, 2013). Stress

granules associate with translation initiation components and disassemble during stress recovery (Buchan and Parker, 2009). They may function in translation repression, mRNA stabilization, and translation initiation complex assembly. mRNP granules act as specialized compartments which enables acute post-transcriptional mRNA regulation in response to cellular cues, and different types have distinct functions.

Stress granule dysregulation is genetically associated with ALS and FTLD through *TARDBP*, *FUS*, *C9orf72*, and *VCP* (Bowden and Dormann, 2016; Buchan *et al.*, 2013). mRNP granules form due to weak interactions between low-complexity (LC) domains which causes self-aggregation of translationally inactive mRNPs (Bowden and Dormann, 2016). TDP-43 and FUS contain LC domains and localize to stress granules under conditions of stress, and mutations affecting *TARDBP* and *FUS* LC domains cause ALS and FTLD (Bowden and Dormann, 2016; McGurk *et al.*, 2015). TDP-43 and FUS aggregates found in postmortem analysis of ALS and FTLD patients contain stress granule marker proteins (Bowden and Dormann, 2016). Impaired stress granule formation in *C9orf72* mutants on the other hand reduces stress granule function and causes increased cell death on stress. Stress granules are autophagy targets, and granule clearance is inhibited where autophagy is suppressed including in *VCP* mutants (Nguyen *et al.*, 2019; Buchan *et al.*, 2013). Therefore, mutations that impair autophagy can impair mRNA regulation via their effects on mRNP granule processing. Together, these indicate that altered function of mRNP complexes may result in impaired post-transcriptional mRNA regulation to influence the progression of neurodegenerative disease. Considering the importance of mitochondrial homeostasis in neurodegeneration and ageing, the function of RNA-binding proteins that influence mitochondrial biogenesis through

regulation of mitochondria-associated mRNAs may be vitally important in the pathology of age-related disease.

1.17 Clueless

The *clueless* gene in *Drosophila melanogaster* encodes a ubiquitously expressed RNA-binding protein that is essential for mitochondrial function and organism survival (Bastian *et al.*, 2021; Cox and Spradling, 2009). The Clueless protein consists of 1448 amino acids and has multiple domains, including highly conserved Clu and tetraco-peptide repeat (TPR) domains. The role of the Clu domain is unknown but it seems to be essential for protein function and is highly conserved (Yang *et al.*, 2022; Sen and Cox, 2016; Cox and Spradling, 2009). While Clueless and its mammalian homologue CLUH share 53% amino acid identity, these proteins share 85% amino acid identity in the Clu domain (Cox and Spradling, 2009). This domain is located towards the N-terminus of the protein in eukaryotic model organisms including *D. melanogaster*, mammals, and *Dictyostelium discoideum* (Sen and Cox, 2016). The well-conserved TPR domain, located towards the C-terminus, facilitates RNA-binding in Clueless and CLUH and is essential for protein function (Yang *et al.*, 2022; Sen and Cox, 2016; Hémono *et al.*, 2022). The RNA-binding function of TPR domains in Clueless and its homologues is somewhat atypical, as these have a more well-established role in facilitating protein-protein interactions (Schatton and Rugarli, 2018). The TPR domain may facilitate protein-protein interactions in Clueless and its homologues in addition to a role in RNA-binding, as mammalian CLUH was found to interact with itself in an RNA-independent but TPR-dependent manner (Hémono *et al.*, 2022). The *D. melanogaster* Clueless protein interacts with itself and with other proteins including translocase of outer membrane 20 (Tom20), PINK1, and DRP1 (Sen

and Cox, 2016; Sen *et al.*, 2015; Yang *et al.*, 2022). The ability of Clueless and its homologues to bind with mRNAs and other mitochondria-associated proteins may facilitate a role in regulation of mitochondrial homeostasis.

Though closely associated with mitochondrial function, Clueless is exclusively located within the cytoplasm (Cox and Spradling, 2009; Gao *et al.*, 2014). Clueless and its homologues, potentially along with bound mRNAs, are often found in large mitochondria-associated particles (Cox and Spradling, 2009; Yang *et al.*, 2022; Gao *et al.*, 2014). The peripheral association of the Clueless protein with the mitochondria may be enabled by the capacity of this protein to bind to mitochondrial outer membrane proteins including Porin, Tom20, and PINK1 (Sen *et al.*, 2015). *D. melanogaster* Clueless particles are mobile, and their mobility is determined by microtubules, as they move at speeds consistent with transport by microtubules and movement is disrupted on destabilization of the network (Sheard *et al.*, 2020). Clueless particles do not co-localize with processing bodies, and the behaviour of Clueless particles is unlike that of stress granules in that they form under healthy conditions and disaggregate in response to stressors including nutrient deprivation and oxidative stress (Sheard *et al.*, 2020). *Parkin* and *SOD2* mutants have no apparent Clueless particles, potentially due to increased stress conditions in these mutants (Sen *et al.*, 2013; Sheard *et al.*, 2020). In contrast, CLUH localizes to particles in mouse liver cells which become larger following starvation of the animal or following nutrient deprivation in cell culture (Pla-Martín *et al.*, 2020). CLUH granules are distinct from processing bodies and stress granules, but can contain stress granule components including Ras-GAP SH3 domain binding proteins (G3BPs). The

distribution and localization of Clueless and its homologues are responsive to cellular stress conditions and may act as an indicator of mitochondrial function.

1.18 Clueless and Mitochondrial Localization

The *clueless* gene and its orthologues have been described in many eukaryotes including plants, fungi, insects, and mammals (Logan *et al.*, 2003; Fields *et al.*, 1998; Cox and Spradling, 2009; Gao *et al.*, 2014). In all examined organisms, *clueless* orthologue mutants show phenotypes of mitochondrial clustering proximal to the nucleus (Schatton and Rugarli, 2018). The mitochondrial clustering phenotype in *D. melanogaster* *clueless* mutant cells is alleviated upon transfection with mammalian *CLUH*, indicating that the mechanisms by which Clueless and its homologues control mitochondrial localization are conserved between our species (Sen *et al.*, 2015). Clustered mitochondria have been described as discrete in *clueless* and *CLUH* mutants (Cox and Spradling, 2009; Gao *et al.*, 2014). Clueless binds with both PINK1 and Parkin, and these proteins may interact to control mitochondrial positioning (Cox and Spradling, 2009; Sen *et al.*, 2015). Mitochondria do not cluster in *D. melanogaster* *clueless* heterozygotes that have one functional copy of the allele, or in *parkin* heterozygotes, but *clueless* and *parkin* double heterozygotes do have clustered mitochondria (Cox and Spradling, 2009). A similar interaction was observed in *clueless* and *Pink1* double heterozygotes (Sen *et al.*, 2015). This suggests that these proteins may interact to control mitochondrial positioning. This could in part be due to the interaction of the PINK1 and Parkin proteins with dynamism proteins including mitofusins and DRP1 (Corti *et al.*, 2011; Kim *et al.*, 2013; Zemirli *et al.*, 2018). Overexpression of *parkin* in *clueless* mutant *D. melanogaster* cell culture rescues the mitochondrial clustering phenotype, but overexpression of *Pink1* in these cells

does not, suggesting that Clueless functions downstream of PINK1 but upstream of Parkin to determine mitochondrial positioning (Sen *et al.*, 2015). Therefore, Clueless and its homologues interact with mitophagy-associated proteins to control mitochondrial localization.

1.19 Clueless and Mitochondrial Dynamism

Expression of *clueless-RNAi* in *D. melanogaster* muscles and *CLUH* suppression in cultured human cells causes a morphology of elongated mitochondria: a common result of fusion being favoured over fission in the intracellular mitochondrial network (Yang *et al.*, 2022). Elongated mitochondria could in part be a consequence of the defects that cause mitochondrial mislocalization, as increased proximity results increases opportunity for fusion (Dorn, 2019). Alternatively, increased size of mitochondria results in impaired trafficking, so the phenotype of mitochondrial mislocalization could be caused by either increased fusion or decreased fission. The *clueless* gene interacts with mitochondrial dynamism-associated genes *Marf*, *Drp1*, and *TER94* (Z. Wang *et al.*, 2016; Yang *et al.*, 2022). The *clueless*-encoded protein Clueless binds to VCP *in vivo* (Z. Wang *et al.*, 2016). VCP facilitates the proteasomal degradation of Marf, and proteasomal Marf degradation was reduced upon *clueless* suppression. Overexpression of *Drp1* causes a partial rescue of phenotypes associated with *clueless* inhibition. Changes in Marf levels were not observed in response to *clueless* inhibition or overexpression and a rescue of phenotypes associated with *clueless* inhibition upon inhibited *Marf* expression was not found (Yang *et al.*, 2022). This study did find that *Drp1* overexpression rescues phenotypes associated with the inhibition of *clueless* in *D. melanogaster*, with mean survival extended from three to seven days post-eclosion. Similarly, a rescue of

phenotypes associated with *CLUH* inhibition in cultured human cells on *Drp1* overexpression was observed. It was further found that *CLUH* binds mRNAs encoding the mammalian DRP1 receptors mitochondrial fission factor (Mff) and mitochondrial dynamic protein of 49 kDa (Mid49), and that translation of these proteins is reduced on *CLUH* inhibition. Clueless and its homologues as negative regulators of mitofusins via interaction with VCP, or as positive regulators of fission via interaction with DRP1 receptor transcripts, is consistent with phenotypes observed on loss of these proteins including mitochondrial clustering proximal to the nucleus, mitochondrial elongation, and decreased mitophagy.

1.20 Clueless and Mitophagy

Mitochondria in *clueless* mutants show morphological abnormalities consistent with mitochondrial oxidative damage including disrupted cristae organization (Cox and Spradling, 2009; Z. Wang et al., 2016). ATP levels are reduced in *clueless*-null mutant adults, with ATP levels dropping each day following eclosion (Sen and Cox, 2016; Sen et al., 2013). Mutant *clueless* larvae have normal levels of ATP, highlighting the importance of Clueless for oxidative phosphorylation by mitochondria, as ATP defects in *clueless* mutants occur upon the switch from reliance on cytosolic glycolysis. (Sen et al., 2013). Increased mitochondrial damage upon inhibition of *clueless* expression in *D. melanogaster* may in part be explained by failure to remove damaged organelles through mitophagy. Clueless suppression *in vivo* causes autophagy markers including p62 to accumulate near mitochondria, though those mitochondria are not engulfed into autophagosomes and degraded (Z. Wang et al., 2016). Accumulation of p62 and decreased mitochondrial turnover were observed in the livers of *CLUH*-deficient mice

(Pla-Martín *et al.*, 2020). Mitophagy defects may in part be due to increased mitochondrial size, as enhanced fission by either *Drp1* overexpression or *Marf* suppression resulted decreased p62 accumulation near mitochondria in a *clueless*-inhibited background (Z. Wang *et al.*, 2016). RNAi-mediated *clueless* inhibition causes loss of mitochondrial inner membrane potential, and in *clueless* mutants Parkin localizes to mitochondria (Sen *et al.*, 2015). This demonstrates that the interaction of PINK1 with Parkin is not Clueless-dependent, and suggests that Clueless acts upstream of PINK1 and Parkin in mitophagy. High levels of *clueless* overexpression in *D. melanogaster* muscles rescue muscle degeneration associated with loss of both *Pink1* and *Parkin*, suggesting Clueless may act downstream of PINK1 and Parkin if Clueless, PINK1, and Parkin act exclusively in the same pathway (Yang *et al.*, 2022). Together, these indicate that Clueless may act in parallel to PINK1 and Parkin function to regulate mitochondrial homeostasis.

1.21 Clueless and Localized Translation at Mitochondria

Clueless interacts with ribosomal subunits and eukaryotic initiation factor components and specifically binds with the ribosomal subunit RpL7a at the mitochondria and not elsewhere in the cytoplasm, suggesting a role in localized translation at the mitochondria (Sen and Cox, 2016). Cytosolic chaperones and protein-import complex components were not identified in a CLUH proximity analysis, so although CLUH could be involved in the localized translation of mitochondrial proteins in mammals, a direct involvement in the co-translational import of proteins into the mitochondria is not apparent (Hémono *et al.*, 2022). Clueless and its homologues bind to mRNAs, and CLUH specifically binds to mRNAs for nuclear-encoded mitochondrial proteins (Sen and Cox,

2016; Vardi-Okun and Arava, 2019; Gao *et al.*, 2014). Target mRNAs of CLUH include those associated with proteins involved with oxidative phosphorylation, β -oxidation, amino acid catabolism, and mitochondrial quality control (Schatton and Rugarli, 2018). The association of Clueless and its homologues with mRNAs encoding proteins essential for mitochondrial function, as well as with translation components and outer membrane proteins, suggests an essential role in coordinating mitochondrial biogenesis.

Proximity labelling analysis identified mitochondrial proteins enriched near mammalian CLUH in the cytosol, most of which had mitochondrial targeting sequences (Hémono *et al.*, 2022). These proteins, found near the mitochondrial surface, accumulate in the mitochondria. All examined mitochondrial proteins found to be proximal to CLUH have CLUH-binding mRNA transcripts, and proximity of these proteins is dependent on active translation. Analysis of steady-state protein levels in *D. melanogaster* shows that *clueless* suppression causes the upregulation of proteins involved in stress response, vesicle transport, and cytoskeletal organization (Sen and Cox, 2022). Upregulation of proteins involved in stress response occurred upon the loss of PINK1 and SOD2 activities, however, so this could simply be a common response to increases in mitochondrial damage. Proteins downregulated upon *clueless* suppression include those involved in mitochondrial translation and respiratory chain components. Upon examination of six respiratory chain proteins discovered to be less abundant in *clueless* mutants, it was found that transcript levels for the mRNAs encoding these proteins was not altered as compared to a control transcript. This is consistent with involvement of *clueless* in post-transcriptional regulation of the translation of mitochondrial proteins in *D. melanogaster*. Together, these data indicate a role for Clueless and its homologues in

the regulation of mitochondrial biogenesis via control of localized translation of nuclear-encoded mitochondrial proteins.

1.22 Clueless as a Potential Master Regulator of Mitochondrial Homeostasis

Clueless and its homologues may act as master regulators of mitochondrial homeostasis through regulation of nuclear-encoded mitochondrial mRNA transcripts in the cytosol (Schatton and Rugarli, 2018). In mammals, CLUH is the only known RNA-binding protein that specifically binds multiple nuclear-encoded mRNA transcripts encoding mitochondrial proteins. *clueless* ortholog function is required for mitochondrial localization, biogenesis, turnover, and ultimately for cell and organism survival. Furthermore, Clueless and its homologues may coordinate intracellular responses to stress including stress-responsive regulation of mitochondria (Figure 1.4). Clueless particles disaggregate rapidly on response to stress, and if mRNA regulation is tied to the accumulation of Clueless in particles, this may represent flexible and responsive regulation of mitochondria in response to intracellular signals (Sheard *et al.*, 2020; Pla-Martin *et al.*, 2020). *CLUH* mutations have not been linked to mitochondrial dysfunction in humans, possibly because the expression of this gene is necessary for life. Analysis of genetic variation in 141 426 human genomes found only 10 *CLUH* loss of function variants, only 17% of what would be expected by chance, indicating likely intolerance of loss of function (Karczewski *et al.*, 2020). Microdeletions on chromosome 17 affecting *CLUH* and nearby genes have been observed, demonstrating that human heterozygotes expressing only one copy of *CLUH* are viable (Landrum *et al.*, 2018). However, as deletions in a neighbouring gene cause a dominant neurodevelopmental disorder that is usually fatal in early childhood, the effects of *CLUH* suppression in the ageing human

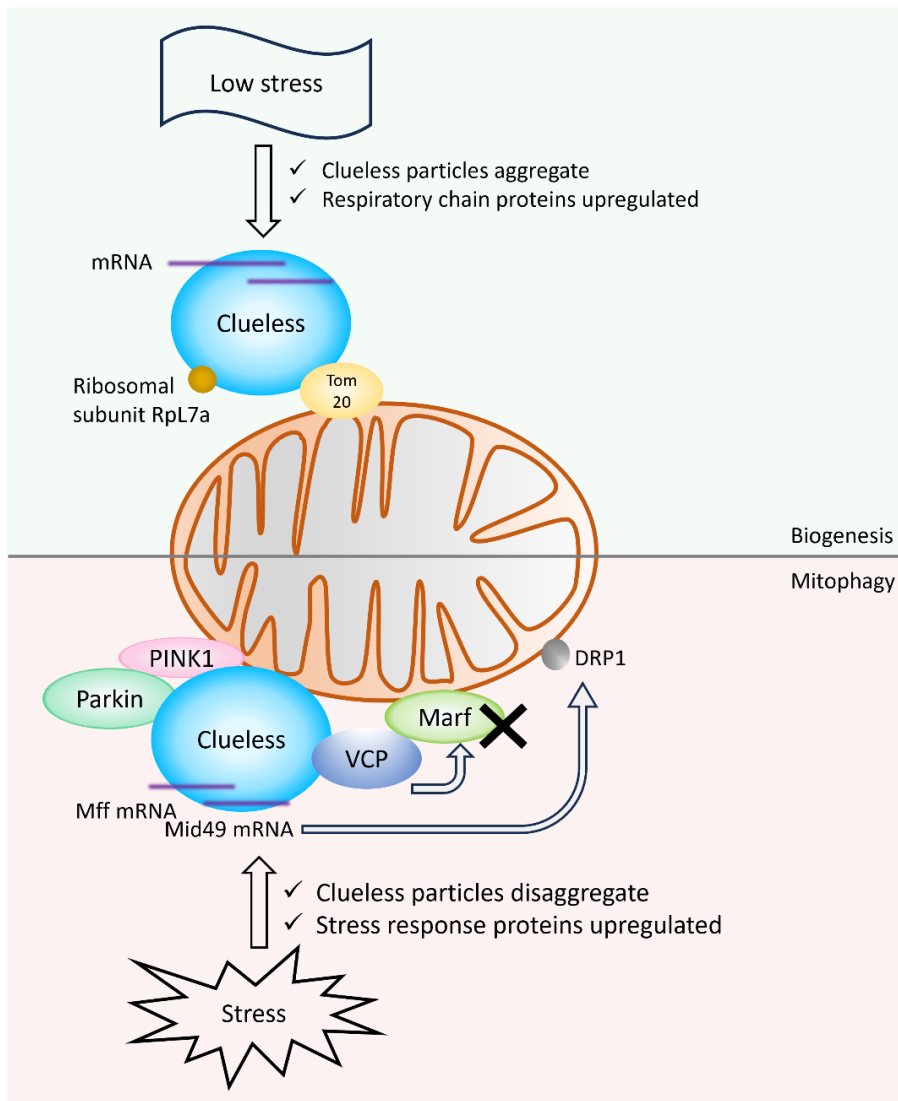


Figure 1.4 *Drosophila melanogaster* Clueless is an RNA-binding protein that may regulate mitochondrial homeostasis in response to stress signalling. Clueless is cytoplasmic, but localizes to mitochondria due to interaction with outer membrane proteins including Tom20 and PINK1. At the mitochondrial surface, Clueless binds with the ribosomal subunit RpL7a and may regulate localized translation. In low-stress conditions, Clueless forms particles and upregulates respiratory chain proteins. In stress conditions such as starvation, Clueless particles disaggregate and proteins associated with stress response including mitochondrial quality control are upregulated. Clueless interacts with VCP to promote Marf degradation, suppressing fusion. Clueless binds to mRNAs encoding the DRP1 receptors Mid49 and Mff, and positively regulates fission. Clueless promotes mitophagy through these interactions with dynamism proteins, as well as through interactions with the mitophagy proteins PINK1 and Parkin. This figure was prepared using Microsoft PowerPoint for Microsoft 365 version 2406.

body have not been observed (Chen and Chein, 2010; Mochida, 2009). CLUH might be important for human health, but the impacts of altered expression have not been characterized. Investigation of *clueless* in the model organism *D. melanogaster* could help to elucidate the function of *clueless* orthologues including mammalian *CLUH* in ageing and neurodegeneration.

1.23 Clueless in Model Organisms

Phenotypes of mitochondrial dysfunction on *clueless* orthologue suppression correspond to phenotypes of impaired health and longevity in model organisms. Where *D. melanogaster clueless* mutant homozygotes express the amorphic *clu*^{d08713} allele adults are small, sterile, uncoordinated, and do not survive more than three to seven days following eclosion (Cox and Spradling, 2009). Developmental viability is impaired, with only 40% of *clueless* mutant individuals successfully eclosing as compared to control. *Clueless* mutants have an abnormal wing posture phenotype similar to *Pink1* and *Parkin* mutants, and overexpression of *clueless* as well as ectopic expression of human *CLUH* rescues this phenotype in *Pink1* mutant *D. melanogaster* (Sen *et al.*, 2015). Many phenotypes associated with *Pink1* and *Parkin* mutants are reproduced in *clueless* mutants, though *clueless* depletion is more severe with an adult life expectancy of days rather than weeks (Sen *et al.*, 2013). Developmental viability is unaffected in *clueless* mutants at the larval stage, though mitochondria are mislocalized in developing neuroblasts and Clueless is highly expressed in these cells in wild-type individuals. Abnormal wing posture in adults is indicative of muscle degeneration and climbing ability degrades quickly, with adults unable to climb within one to two days following eclosion (Sen *et al.*, 2015). These locomotor defects in *clueless* mutants likely cannot be attributed solely to muscle

degeneration, however, as larval mobility is impaired upon RNAi-mediated directed inhibition of *clueless* expression in either muscles or neurons (Z. Wang et al., 2016). *CLUH* suppression in mice causes similar phenotypes: pups are underweight and die within hours of birth, when mammals undergo a shift from glycolysis to oxidative phosphorylation in several tissues (Schatton *et al.*, 2017; Schatton and Rugarli, 2018). Thus *clueless* orthologue suppression causes phenotypes of impaired health and longevity in mammalian and *D. melanogaster* models.

1.24 Research Goals

The *Drosophila melanogaster* model organism provides an opportunity to evaluate the complex genetic interactions that contribute to highly conserved biological functions including mitochondrial dynamics and function. Conserved function of Clueless and its homologues, and the processes with which they are associated, allows for experimental evaluation of the role of *clueless* in ageing and neurodegenerative disease. These investigations may yield insight into mechanisms underlying these processes in humans. Previous research in the Staveley laboratory at Memorial University of Newfoundland has examined the effects of altered expression of mitochondria-associated genes in *D. melanogaster*, including *parkin*, *Pink1*, and *TER94*, on whole-organism health and longevity (Haywood and Staveley, 2004; Todd and Staveley, 2012; Hurley and Staveley, 2020). These interact with *clueless*; and mutations *parkin* and *Pink1* are associated with PD, and mutations in *VCP* are associated with ALS. I examine the effects of altered *clueless* expression in DA neurons, whose degeneration is associated with PD; and motor neurons, whose degeneration is associated with ALS. Though subcellular phenotypes associated with *clueless* suppression in *D. melanogaster* have been well-

characterized, impacts of altered *clueless* expression in DA neurons and motor neurons on whole-organism health and longevity have not previously been examined. The objective of this research is to investigate the role of *clueless* in *D. melanogaster* by altering expression of this gene and assessing the effects on longevity and age-related locomotor function, in order to gain insight into the role of Clueless in the regulation of mitochondrial homeostasis and in protection from age-related neurodegenerative disease. If regulation of mitochondrial homeostasis by Clueless activity in *D. melanogaster* has a protective effect against age-related neurodegeneration, then a) *clueless* suppression in dopaminergic neurons should cause age-related disease comparable to PD, and b) suppression in motor neurons should cause age-related disease comparable to ALS.

Chapter 2: Methods

2.1 *Drosophila melanogaster* Care and Maintenance

Drosophila melanogaster were cultured in plastic vials stopped with sponges containing ~5 mL of standard media. Media was prepared in batches with 65 g of cornmeal, 10 g of yeast, 5.5 g of agar, 1 L of water, 50 mL of molasses, 2.5 mL propionic acid, and 5 mL of 10% methylparaben solution in ethanol. Media was refrigerated prior to use at 4 to 6°C. Stocks were maintained at a room temperature of ~22°C. Experimental crosses and assays were conducted using moisture-containing incubators kept at 23 to 25°C. All stocks and experimental *D. melanogaster* were maintained in a daily light/dark cycle via exposure to ambient external lighting. CO₂ anaesthetization was used to facilitate examination under a dissecting scope for the purposes of conducting experimental crosses and isolating critical-class progeny for assays. Experimental *D. melanogaster* were placed on fresh media on collection, with no more than 20 individuals per vial.

2.2 *Drosophila melanogaster* Lines and Crosses

The UAS/Gal4 system was used to direct the expression of *UAS*-associated transgenes in *Drosophila melanogaster* dopaminergic and motor neurons (Brand and Perrimon, 1993). A *UAS*-associated *lacZ* transgene was expressed was expressed in these tissues (Figure 2.1) in to control for the effects *Gal4* expression (Slade and Staveley, 2015). Expression of *clueless* was inhibited via expression of *UAS*-associated *clueless-RNAi* transgenes (Figure 2.2). The UAS/Gal4 system was used to direct ectopic expression of *UAS-clu* and *UAS-CLUH* in in DA neurons and motor neurons of *clu*^{d08713} heterozygotes (Figure 2.3). Virgin females from *Gal4* lines were crossed to males from

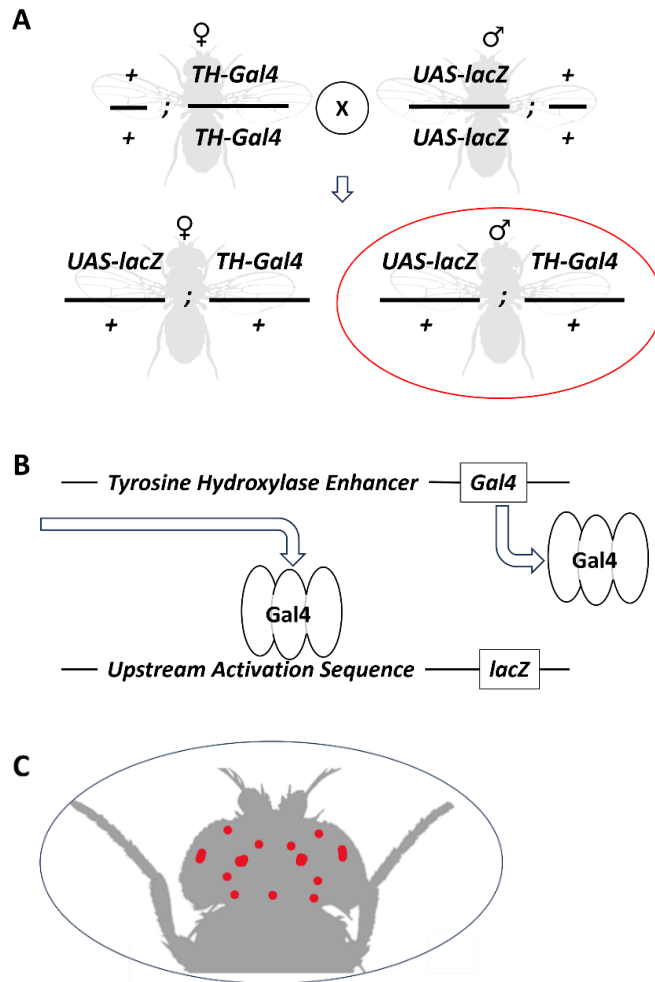


Figure 2.1 Use of the UAS/GAL4 system to direct expression of *Escherichia coli* β -galactosidase (*lacZ*) in *Drosophila melanogaster* dopaminergic neurons. A) Virgin females from a line containing a *tyrosine hydroxylase* (*TH*) enhancer-associated *Gal4* transgene inserted on Chromosome 3 are crossed to males from a line containing an *upstream activation sequence* (*UAS*)-associated *lacZ* transgene inserted on Chromosome 2. Progeny are heterozygotes containing both inserts, and male progeny were used to control for the affects of *Gal4* expression in dopaminergic neurons. + is used to denote wild-type chromosomes. B) Transcription of the *Saccharomyces cerevisiae* *Gal4* transcription factor is controlled by the *TH* enhancer. In tissue where the *Gal4* transcription factor is expressed, it binds to the *UAS* and facilitates transcription of transgenic *lacZ*. C) The pattern of *TH* expression is specific to all dopaminergic neurons and results in the specific expression of transgenic *lacZ* in these dopaminergic neurons. In the adult nervous system of *D. melanogaster*, transgenic *lacZ* is expressed in thirteen distinct dopaminergic neuron clusters (Friggi-Grelin *et al.*, 2003). This figure was prepared using Microsoft PowerPoint for Microsoft 365 version 2406. Organism silhouette was modified from an image created by Hegna (2012; Public Domain Mark 1.0).

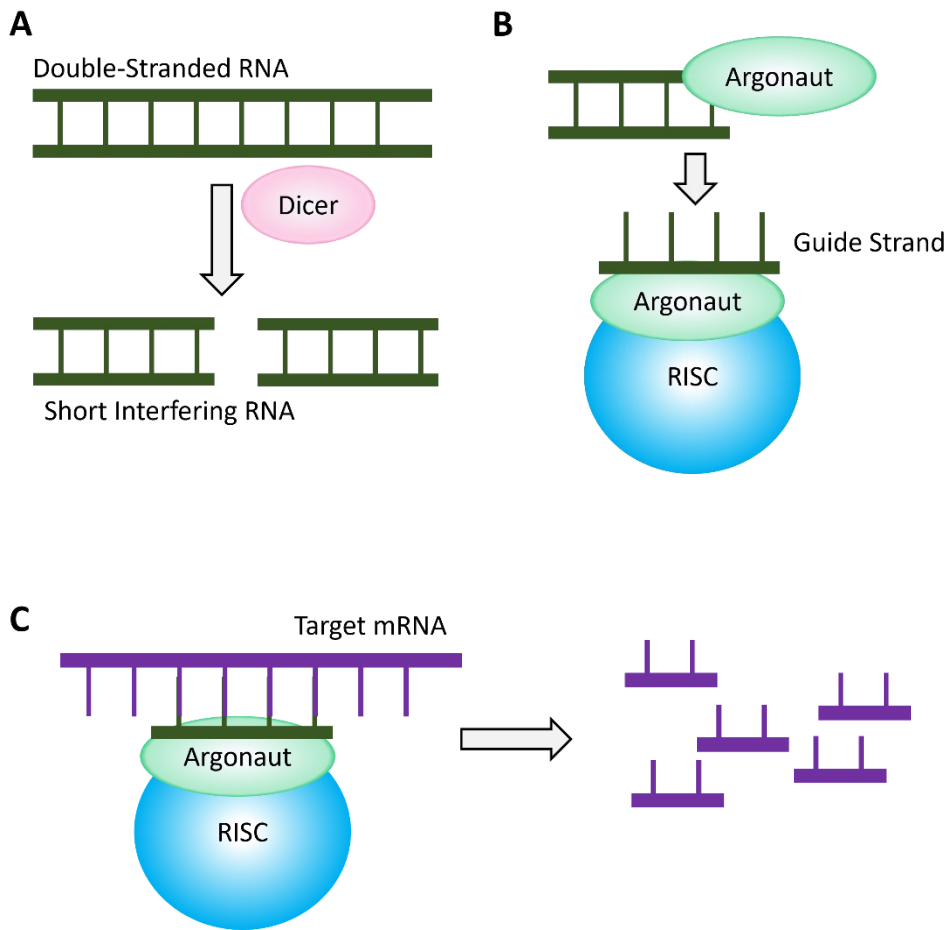


Figure 2.2 RNA interference (RNAi) is a conserved response to double-stranded RNA that can be exploited to inhibit expression of a target gene. A) Transcription of an *RNAi* transgene produces long double-stranded RNA with repeated-inverted fragment sequences corresponding to the messenger RNA (mRNA) of a target gene. In the cytoplasm, the enzyme Dicer cleaves long double-stranded RNA to produce double-stranded short-interfering RNA approximately 21-23 nucleotides in length. B) Short-interfering RNA associates with an Argonaut-family protein, which recruits other proteins to form a RNAi-induced silencing complex (RISC). C) The RISC causes degradation of the sense strand of the double-stranded RNA, leaving a single strand that acts as a “guide strand”. The guide strand will be complementary to a section of the mRNA for a target gene. This complementarity facilitates the binding of the guide strand to a section of the target mRNA for degradation by a RISC-associated nuclease. Reviewed in Zhu and Palli, 2020. This figure was prepared using Microsoft PowerPoint for Microsoft 365 version 2406.

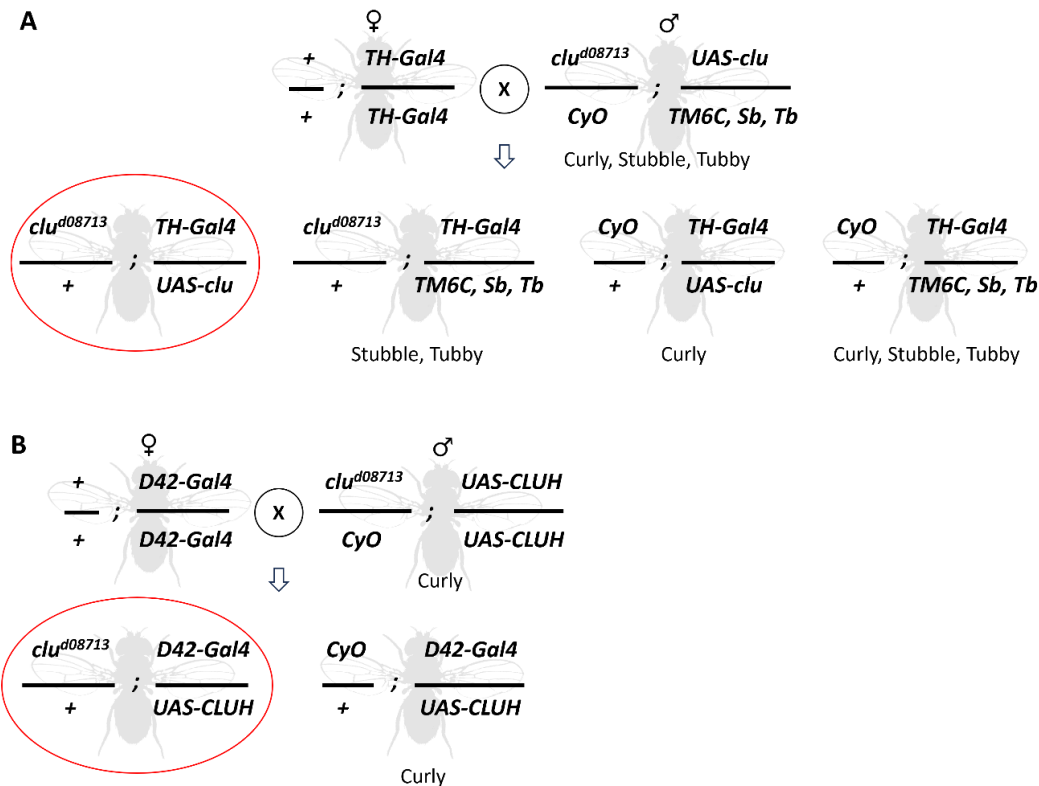


Figure 2.3 Use of the UAS/Gal4 system to direct ectopic expression of *UAS-clu* and *UAS-CLUH* in *clu*^{d08713} heterozygotes. A) *clu*^{d08713}/*CyO*; *UAS-clu*/*TM6C* individuals are double-heterozygotes which have the mutant *clueless* allele *clu*^{d08713} on one copy of the second chromosome and the balancer chromosome *CyO*, which carries a dominant marker causing curly wings in adult, on the other. Also heterozygous on the third chromosome, they have both a *UAS-clu* transgene and the balancer chromosome *TM6C*, which carries the dominant markers *Stubble* and *Tubby*. *Stubble* causes shortened mechanosensory bristles detectable in adults, and *Tubby* causes a reduction in body length most easily detected in pupae. *clu*^{d08713}/*CyO*; *UAS-clu*/*TM6C* males were crossed to *TH-Gal4* virgin females. Genotypes of progeny can be inferred through the use of dominant markers. Male progeny of this cross with no phenotypes associated with the dominant markers were selected for assessment. Their genotypes were inferred to *clu*^{d08713}/*clu*⁺; *TH-Gal4*; *UAS-clu*. B) *clu*^{d08713}/*CyO*; *UAS-CLUH* individuals are second-chromosome heterozygotes, which have the mutant *clueless* allele *clu*^{d08713} on one copy of the second chromosome and the balancer chromosome *CyO* on the other. These are third-chromosome *UAS-CLUH* homozygotes. *clu*^{d08713}/*CyO*; *UAS-CLUH* males were crossed to *D42-Gal4* virgin females. Genotypes of progeny were inferred through the use of the dominant markers, where the genotype of progeny without curly wings was inferred as *clu*^{d08713}/*clu*⁺; *D42-Gal4*; *UAS-CLUH*. This figure was prepared using Microsoft PowerPoint for Microsoft 365 version 2406. Organism silhouette was modified from an image created by Hegna (2012; Public Domain Mark 1.0).

UAS lines, and parental adults were allowed to lay eggs in media before being removed to produce critical-class progeny. Only critical-class male progeny expressing the *UAS*-associated transgene were collected and assayed. Experimental *D. melanogaster* were collected daily. The *TH-Gal4* (Friggi-Grelin *et al.*, 2003), *D42-Gal4* (Yeh *et al.*, 1995), and *UAS-lacZ* lines (Brand and Perrimon, 1993) were obtained from the Bloomington Drosophila Stock Center. *UAS-cluRNAi* lines were obtained from the Vienna Drosophila Resource Center. *clu^{d08713}/CyO*; *UAS-clu/TM6C* and *clu^{d08713}/CyO*; *UAS-CLUH* lines were generously provided by Dr. Rachel T. Cox of the Uniformed Services University, F. Edward Hébert School of Medicine in Bethesda, Maryland, USA (Cox and Spradling, 2009; Sen and Cox, 2015). See Table 2.1 for a list of *D. melanogaster* lines used.

Transgenic constructs are further described in Tables 2.2 and 2.3.

2.3 Lifespan Assay

Approximately 400 individuals of each experimental *D. melanogaster* genotype were collected and vials were labeled. Experimental *D. melanogaster* were transferred to fresh media every four days throughout the duration of the assay. Survival was scored every two days, where individuals that did not move upon agitation were considered deceased. Any individuals that were lost or were injured on handling were excluded from analyses. Mean lifespan of experimental genotypes were compared to mean lifespan of controls assayed concurrently. Results are reported as effect sizes with 95% confidence intervals (Wasserstein and Lazar, 2016; Wasserstein and Lazar, 2016; Nakagawa and Cuthill, 2007). All lifespan analysis calculations were performed using OASIS 2 (Han *et al.*, 2016).

Table 2.1 *Drosophila melanogaster* lines used in experimental crosses. Genotypes used are given. The genomic location of the transgenics are given as construct location. Lines obtained from the Bloomington Drosophila Stock Center are labeled with stock centre IDs with the prefix BDSC. Lines obtained from the Vienna Drosophila Resource Center are labeled with stock centre IDs with the prefix VDRC. Where no stock centre ID is given, lines were generated and gifted by Dr. Rachel Cox of the Uniformed Services University, F. Edward Hébert School of Medicine in Bethesda, Maryland, USA. Constructs of interest are further described in Tables 2.2 and 2.3.

Genotype	Stock Centre ID	Construct Location	Constructs of Interest
<i>D42-Gal4</i>	BDSC_8816	3	<i>D42-Gal4</i>
<i>TH-Gal4</i>	BDSC_8848	3	<i>TH-Gal4</i>
<i>clu^{d08713}/CyO;UAS-clu/TM6C</i>	-	2, 3	<i>clu^{d08713}</i> and <i>UAS-clu</i>
<i>UAS-cluRNAi^{KK108024}</i>	VDRC_100709	2	<i>UAS-cluRNAi^{KK108024}</i>
<i>UAS-cluRNAi^{V42136}</i>	VDRC_42136	2	<i>UAS-cluRNAi^{V42136}</i>
<i>UAS-cluRNAi^{V42138}</i>	VDRC_42138	2	<i>UAS-cluRNAi^{V42138}</i>
<i>clu^{d08713}/CyO;UAS-CLUH</i>	-	2, 3	<i>clu^{d08713}</i> and <i>UAS-CLUH</i>
<i>UAS-lacZ</i>	BDSC_1776	2	<i>UAS-lacZ</i>

Table 2.2 Transgenic constructs expressed independently of *Gal4*. Location of *Gal4* insertions of mutant alleles are given as chromosome of location. *D42-Gal4* was generated as described by Friggi-Grelin et al., 2003. *Tyrosine hydroxylase-Gal4* (*TH-Gal4*) was generated as described by Yeh et al., 1995. The *clueless* mutant allele *clu^{d08713}* was generated as described by Thibault et al., 2004. P-element-mediated transformation is illustrated in Figure 2.4.

Transgenic Construct	Method of Generation	Expression Pattern	Chromosome of Location	Validation
<i>D42-Gal4</i>	P-element-mediated transformation of an enhancer-associated <i>Gal4</i>	Motor neurons	3	Immunofluorescence of expression of UAS- <i>GFP</i> (Yeh et al., 1995)
<i>TH-Gal4</i>	P-element-mediated transformation of an enhancer-associated <i>Gal4</i>	Dopaminergic neurons	3	Immunofluorescence on expression of UAS- <i>GFP</i> (Friggi-Grelin et al., 2003)
<i>clu^{d08713}</i>	P-element-mediated insertion of FRT sites to facilitate FLP-FRT based deletion (Parks et al., 2004)	Ubiquitous	2	Western blot (anti-Clueless antibody): homozygotes lack detectable 160 kD Clueless protein (Cox and Spradling, 2009)

Table 2.3 UAS-associated transgenic constructs expressed under the control of *TH-Gal4* or *D42-Gal4*. UAS-associated transgenic inserts are expressed in tissue dependent on the presence of Gal4. *UAS-clu* and *UAS-CLUH* were generated as described by Sen and Cox, 2015. *UAS-cluRNAi^{KK108024}*, *UAS-cluRNAi^{V42136}*, and *UAS-cluRNAi^{V42138}* were generated as described by Dietzl *et al.*, 2007. *UAS-lacZ* was generated as described by Brand and Perrimon, 1993. *clueless* is abbreviated to *clu*, RNA interference is abbreviated to RNAi, and *Escherichia coli* β -galactosidase is abbreviated to *lacZ*. P-element-mediated transformation is illustrated in Figure 2.4.

Transgenic Construct	Insertion Method	Insertion Chromosome	Validation
<i>UAS-clu</i>	P-element-mediated transformation of a <i>UAS</i> -associated transgene	3	Western blot (anti-Clueless antibody) on expression under the control of da-Gal4 in a <i>clu^{d08713}</i> background (Sen and Cox, 2015)
<i>UAS-cluRNAi^{KK108024}</i>	ϕ C31-based integration of a <i>UAS</i> -associated RNAi transgene (Bischof <i>et al.</i> , 2007)	2	Sanger sequencing to determine presence of construct (Dietzl <i>et al.</i> , 2007)
<i>UAS-cluRNAi^{V42136}</i>	P-element-mediated transformation of a <i>UAS</i> -associated RNAi transgene	2	Restriction digest and PCR to determine presence of fragment of expected construct length (Dietzl <i>et al.</i> , 2007)
<i>UAS-cluRNAi^{V42138}</i>	P-element-mediated transformation of a <i>UAS</i> -associated RNAi transgene	2	Restriction digest and PCR to determine presence of fragment of expected construct length (Dietzl <i>et al.</i> , 2007)
<i>UAS-CLUH</i>	P-element-mediated transformation of a <i>UAS</i> -associated RNAi transgene	3	Western blot (anti-CLUH antibody) on expression under the control of da-Gal4 in a <i>clu^{d08713}</i> background (Sen and Cox, 2015)
<i>UAS-lacZ</i>	P-element-mediated transformation of a <i>UAS</i> -associated RNAi transgene	2	Expressed under the control of various Gal4 lines, staining for anti- β -galactosidase antibodies (Brand and Perrimon, 1993)

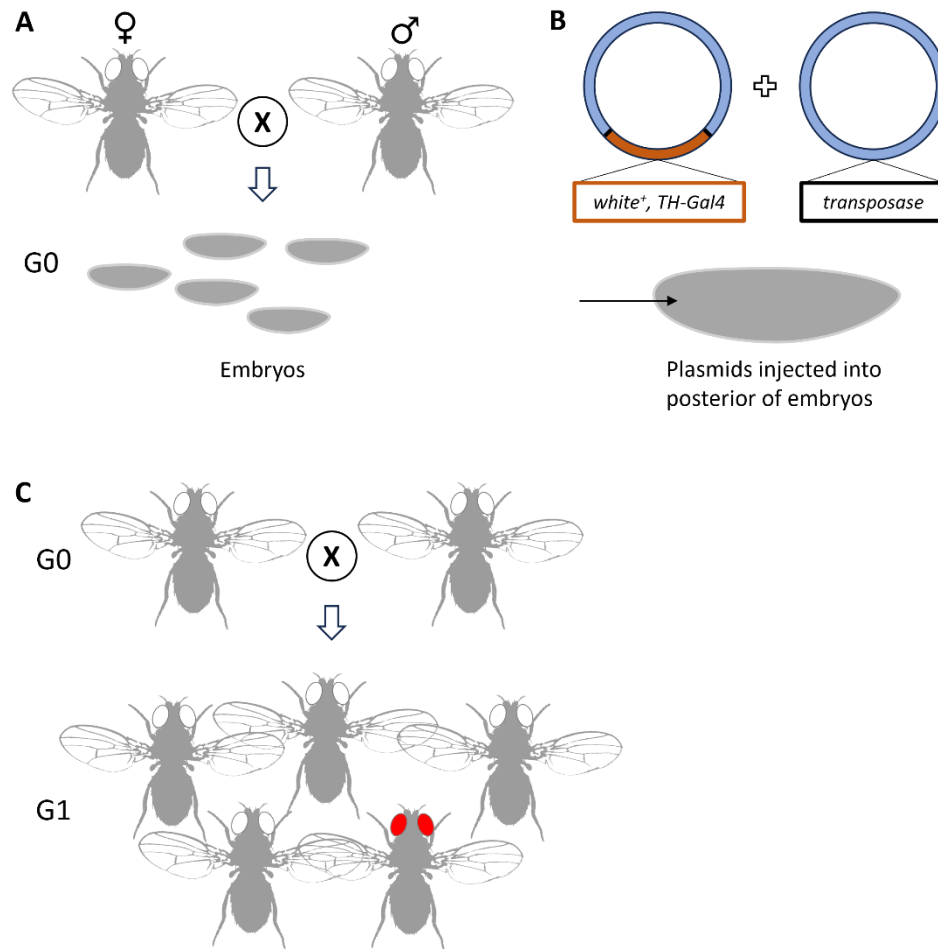


Figure 2.4 Generation of *TH-Gal4 Drosophila melanogaster* by P-element-mediated germ-line transformation (Friggi-Grelin *et al.*, 2003). A) P-element-mediated germ-line transformation was performed by standard techniques (Rubin and Spradling, 1982). *Drosophila melanogaster* homozygous for a recessive *white* mutant (w^{118}) causing a mutant phenotype of white eyes were allowed to mate and lay eggs. B) A P-element transposon was constructed to contain a wild-type *white* allele (w^{+mC}) and a *Saccharomyces cerevisiae Gal4* transcription factor sequence fused to a regulatory *Drosophila melanogaster tyrosine hydroxylase (TH)* regulatory region. This construct, along with the *transposase*-containing plasmid $\pi 25.7wc$ (Karess and Rubin, 1984), were injected into the posterior region of w^{118} embryos, from which germ cells develop. The enzyme transposase facilitates insertion of the P-element into chromosomes of the host cells. C) As these embryos develop, P-element insertion is limited to germ cells. In the second generation, the dominant red-eyed phenotype shows the integration of the P-element containing w^{+mC} and *TH-Gal4* into chromosomes of the somatic cells. This figure was prepared using Microsoft PowerPoint for Microsoft 365 version 2406. Organism silhouette was modified from an image created by Hegna (2012; Public Domain Mark 1.0).

2.4 Climbing Assay

Approximately 200 individuals of each experimental *D. melanogaster* genotype were collected and labeled. Experimental *D. melanogaster* were transferred to fresh media every three to four days throughout the duration of the assay, including between 30 minutes and one day prior to measurement of climbing ability. Climbing ability was assessed within the first two weeks following eclosion and every week thereafter until fewer than 10 total individuals of each genotype remained. Any individuals that were lost or injured on handling were excluded from analyses. Climbing ability was assessed during daylight hours only, and experimental *D. melanogaster* were allowed at least 20 minutes to acclimate to room temperature of ~22°C prior to measurement. The *D. melanogaster* negative geotaxis response was exploited to assess climbing ability (Iliadi *et al.*, 2016). The ability of experimental *D. melanogaster* to climb up a sponge-stoppered glass tube 30 cm length and 1.5 cm in diameter was scored. The climbing apparatus was divided into sections one through five, with section one encompassing the areas within 2 cm from the bottom sponge, section two encompassing the next 2 cm, section three encompassing the next 2 cm, section four encompassing the next 2 cm, and section five encompassing the remaining area. Experimental *D. melanogaster* were tapped into the tube via a plastic funnel, allowed at least 30 seconds to acclimate, then firmly knocked down to the bottom by repeat vertical tapping of the tube upon a soft surface. Climbing ability was scored as section reached 10 seconds after tapping was ceased. This procedure was followed twice for each group of experimental *D. melanogaster* measured, with only the second time being scored. Experimental *D. melanogaster* were measured in groups of up to 20 individuals, until all individuals of each genotype were scored.

Climbing indices for each genotype at each day measured were calculated as per Todd and Staveley (Todd and Staveley, 2004). Climbing indices were calculated as $\text{Climbing Index} = \Sigma(nm) / N$, where n is the number of individuals scored at each section, m is the numbered section associated with height climbed, and N is the total number of individuals for a genotype scored at that day. All climbing index calculations were performed using Microsoft Excel version 2301. Climbing indices were fit to curves according to the model $\text{Climbing Index} = 5 - (Ce^{Kt})$, where C is the y-intercept, e is the mathematical constant e , K is the slope of the fitted curve, and t is age in days. Curve fitting was done according to this model as described by Todd and Staveley except that indices were weighted by number of individuals measured at each point as age-related mortality resulted in fewer individuals measured as the assay progressed. Diagnostic plots were visually analyzed to confirm that the assumptions of the nonlinear regression were satisfied. Residual versus fitted, normal Q-Q, scale location, and residual versus leverage plots were used to assess for normality, heteroscedasticity, and for the presence of outliers. Climbing ability across lifespan of experimental genotypes were compared to climbing ability of controls assayed concurrently. Fitted curves were compared within 95% confidence intervals to determine differences in climbing ability across lifespan. The estimated slope parameter representing change in climbing ability across lifespan was compared. All curve fitting and parameter estimates were performed using R version 4.2.2.

Chapter 3: Results

3.1 Inhibited Expression of *clueless* in Dopaminergic Neurons Reduces Climbing Ability but Does Not Affect Mean Lifespan

Expression of *UAS-cluRNAi^{KK108024}*, *UAS-cluRNAi^{V42136}*, and *UAS-cluRNAi^{V42138}* under the control of *TH-Gal4* causes slightly altered mean lifespan compared to *UAS-lacZ* controls, however 95% confidence intervals overlap around the means (Figure 3.1). Expression of *UAS-cluRNAi^{KK108024}*, *UAS-cluRNAi^{V42136}*, and *UAS-cluRNAi^{V42138}* under the control of *TH-Gal4* causes reduces climbing ability across lifespan (Figure 3.2). Inhibited *clueless* expression in DA neurons causes impaired initial climbing ability, and climbing indices do not overlap within 95% confidence intervals across much of the climbing assay.

3.2 Inhibited Expression of *clueless* in Motor Neurons Decreases Mean Lifespan and Reduces Climbing Ability

Expression of *UAS-cluRNAi^{KK108024}*, *UAS-cluRNAi^{V42136}*, and *UAS-cluRNAi^{V42138}* under the control of *D42-Gal4* decrease mean lifespan compared to *UAS-lacZ* controls, and 95% confidence intervals do not overlap around the means (Figure 3.3). Mean lifespan is similarly decreased on expression of each *clueless-RNAi* transgene, with decreases of 17-22%. Expression of *UAS-cluRNAi^{KK108024}*, *UAS-cluRNAi^{V42136}*, and *UAS-cluRNAi^{V42138}* under the control of *D42-Gal4* causes reduces climbing ability across lifespan (Figure 3.4). Expression of *cluRNAi^{KK10802}* causes severely impaired initial climbing ability and climbing indices do not overlap within 95% confidence intervals across much of the climbing assay. These individuals show some climbing ability which does not significantly decline across lifespan. Expression of *UAS-cluRNAi^{V42136}* does not

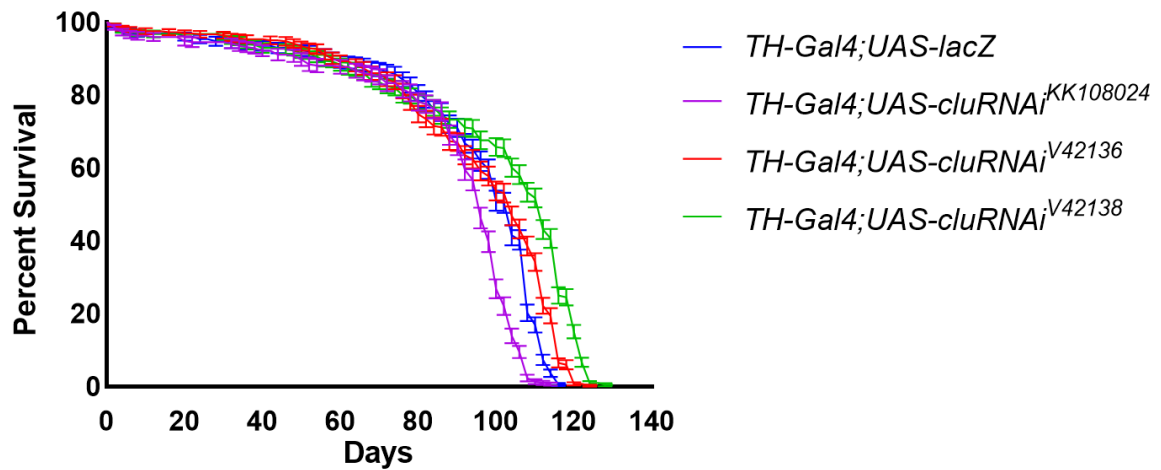


Figure 3.1 Inhibited expression of *clueless* in dopaminergic neurons via RNAi does not significantly affect lifespan. Mean lifespans differ by 7% or less, and 95% confidence intervals overlap around the means where *UAS-cluRNAi*^{KK108024}, *UAS-cluRNAi*^{V42136}, and *UAS-cluRNAi*^{V42138} are expressed under the control of *TH-Gal4* and compared to *UAS-lacZ* controls. *TH-Gal4;UAS-lacZ* controls have a mean survival of 93 days (95% CI: 90-96 days, N=325). *TH-Gal4;UAS-cluRNAi*^{KK108024} individuals have a mean lifespan of 88 days (95% CI: 85-90 days, N=294), while *TH-Gal4;UAS-cluRNAi*^{V42136} individuals have a mean lifespan of 95 days (95% CI: 92-97 days, N=365), and *TH-Gal4;UAS-cluRNAi*^{V42138} individuals have a mean lifespan of 97 days (95% CI: 90-96 days, N=371). Results of lifespan assay are depicted as percent survival with error bars representing standard error of the mean. This figure was prepared using Prism version 10.1.2.

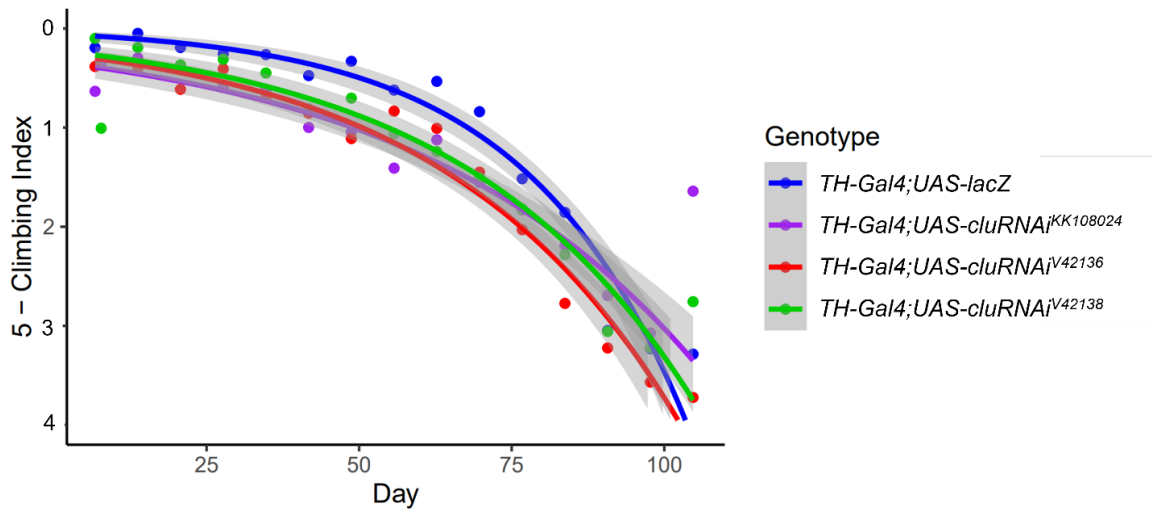


Figure 3.2 Inhibited expression of *clueless* in dopaminergic neurons via RNAi reduces climbing ability across lifespan. Climbing ability declines less rapidly on the expression of *UAS-cluRNAi^{KK108024}*, *UAS-cluRNAi^{V42136}*, and *UAS-cluRNAi^{V42138}* under the control of *TH-Gal4*, however impaired initial climbing ability compared to *UAS-lacZ* controls results in climbing indices that do not overlap within 95% confidence intervals across much of the climbing assay. Climbing ability for *TH-Gal4;UAS-lacZ* controls declines at an estimated rate of 3.8% per day, while climbing ability for *TH-Gal4;UAS-cluRNAi^{KK108024}* individuals declines at an estimated rate of 2.1% per day, climbing ability for *TH-Gal4;UAS-cluRNAi^{V42136}* individuals declines at an estimated rate of 2.6% per day, and climbing ability for *TH-Gal4;UAS-cluRNAi^{V42138}* individuals also declines at an estimated rate of 2.6% per day. Climbing indices were calculated as per Todd and Staveley (Todd and Staveley, 2004), with curves calculated according to the model $5\text{-Climbing Index} = Ce^{Kt}$ and weighted according to number of individuals measured at each time point. Shaded regions indicate 95% confidence intervals. Figure illustrates the model described in Appendix 1. This figure was prepared using R version 4.3.2 with the ggplot2 package (version 3.5.1; Wickham, 2016).

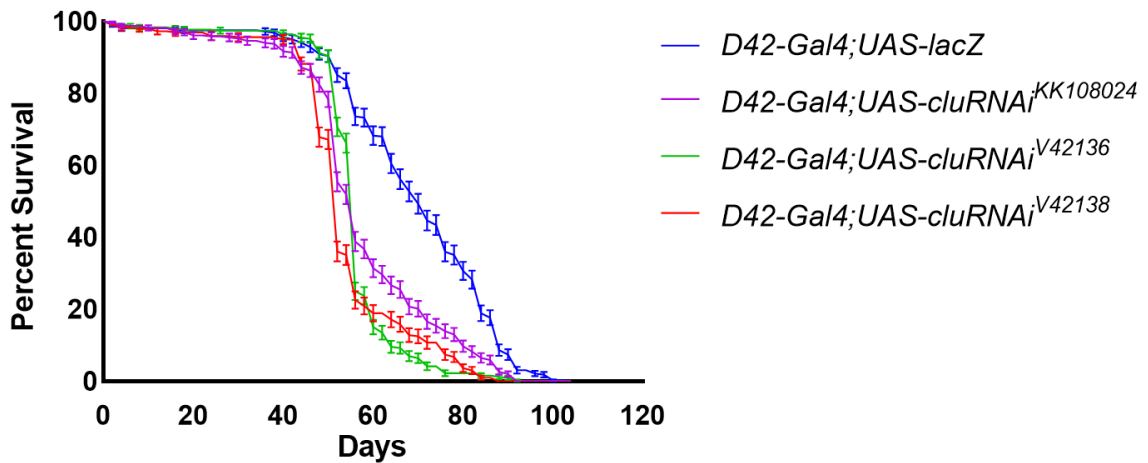


Figure 3.3 Inhibited expression of *clueless* in motor neurons via RNAi reduces lifespan. Expression of *UAS-cluRNAi^{KK108024}*, *UAS-cluRNAi^{V42136}*, and *UAS-cluRNAi^{V42138}* under the control of *D42-Gal4* decreases mean lifespan by 17-22% compared to *UAS-lacZ* controls. *D42-Gal4;UAS-lacZ* controls have a mean survival of 69 days (95% CI: 67-71 days, N=322). *D42-Gal4;UAS-cluRNAi^{KK108024}* individuals have a mean lifespan of 58 days (95% CI: 56-59 days, N=337), while *D42-Gal4;UAS-cluRNAi^{V42136}* individuals have a mean lifespan of 54 days (95% CI: 52-56 days, N=296), and *D42-Gal4;UAS-cluRNAi^{V42138}* individuals have a mean lifespan of 56 days (95% CI: 67-71 days, N=311). Results of lifespan assay are depicted as percent survival with error bars representing standard error of the mean. This figure was prepared using Prism version 10.1.2.

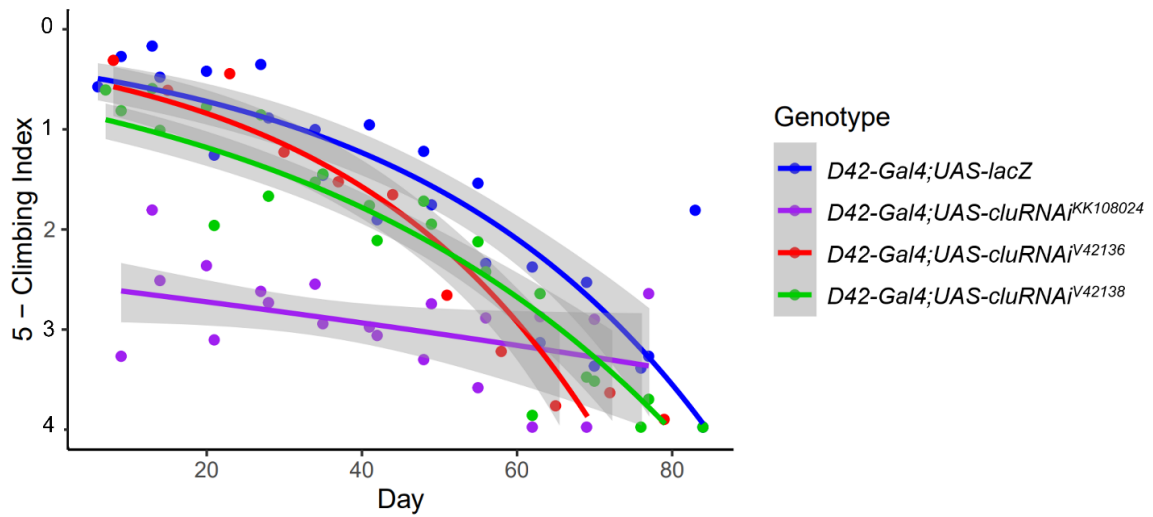


Figure 3.4 Inhibited expression of *clueless* in motor neurons via RNAi reduces climbing ability across lifespan. Climbing ability declines less rapidly on the expression of *UAS-cluRNAi*^{KK108024} and *UAS-cluRNAi*^{V42138} under the control of *D42-Gal4*, however impaired initial climbing ability compared to *UAS-lacZ* controls results in climbing indices that do not overlap within 95% confidence intervals across much of the climbing assay. Climbing ability for *D42-Gal4;UAS-cluRNAi*^{KK108024} individuals is particularly impaired initially, though these show very little decline in climbing ability with age: estimated to be only 0.3% per day. Climbing ability for *D42-Gal4;UAS-lacZ* controls declines at an estimated rate of 2.6% per day, and *D42-Gal4;UAS-cluRNAi*^{V42138} individuals decline at an estimated rate of 2% per day. Climbing ability declines slightly more rapidly on the expression of *UAS-cluRNAi*^{V42136}, though initial climbing ability is similar to *UAS-lacZ* controls, resulting in climbing indices that do not overlap within 95% confidence intervals across much of the climbing assay. Climbing ability for *UAS-cluRNAi*^{V42136} individuals declines at an estimated rate of 3.1% per day. Climbing indices were calculated as per Todd and Staveley (Todd and Staveley, 2004), with curves calculated according to the model $5\text{-Climbing Index} = Ce^{Kt}$ and weighted according to number of individuals measured at each time point. Shaded regions indicate 95% confidence intervals. Figure illustrates the model described in Appendix 2. This figure was prepared using R version 4.3.2 with the ggplot2 package (version 3.5.1; Wickham, 2016).

affect initial climbing ability, though climbing ability declines more rapidly than controls across lifespan and climbing indices do not overlap within 95% confidence intervals across much of the climbing assay. Expression of *UAS-cluRNAi*^{V42138} causes impaired initial climbing ability, and climbing indices do not overlap within 95% confidence intervals across much of the climbing assay.

3.3 Heterozygous *clueless* Mutants Expressing Ectopic *clueless* in Dopaminergic Neurons Have Reduced Climbing Ability But Not Mean Lifespan

clu^{d08713} heterozygotes expressing *UAS-clu* or *UAS-CLUH* under the control of *TH-Gal4* have a slight decrease in mean lifespan compared to wild-type *clu*⁺; *UAS-lacZ* controls, however 95% confidence intervals overlap around the means (Figure 3.5).

clu^{d08713} heterozygotes expressing *UAS-clu* under the control of *TH-Gal4* have reduced climbing ability across lifespan compared to *clu*⁺; *UAS-lacZ* controls (Figure 3.6).

Individuals have an initially impaired climbing ability, and climbing indices do not overlap within 95% confidence intervals across much of the climbing assay. *clu*^{d08713} heterozygotes expressing *UAS-CLUH* do not have significantly different climbing ability across lifespan compared to *clu*⁺; *UAS-lacZ* controls, with climbing indices overlapping within 95% confidence intervals across much of the climbing assay.

3.4 Heterozygous *clueless* Mutants Expressing Ectopic *clueless* in Motor Neurons Have Reduced Mean Lifespan, and Heterozygous *clueless* Mutants Expressing Either Ectopic *clueless* or *CLUH* in Motor Neurons Have Reduced Climbing Ability

clu^{d08713} heterozygotes expressing *UAS-clu* under the control of *D42-Gal4* have decreased mean lifespan compared to wild-type *clu*⁺; *UAS-lacZ* controls, and 95% confidence intervals do not overlap around the means (Figure 3.7). *clu*^{d08713} heterozygotes

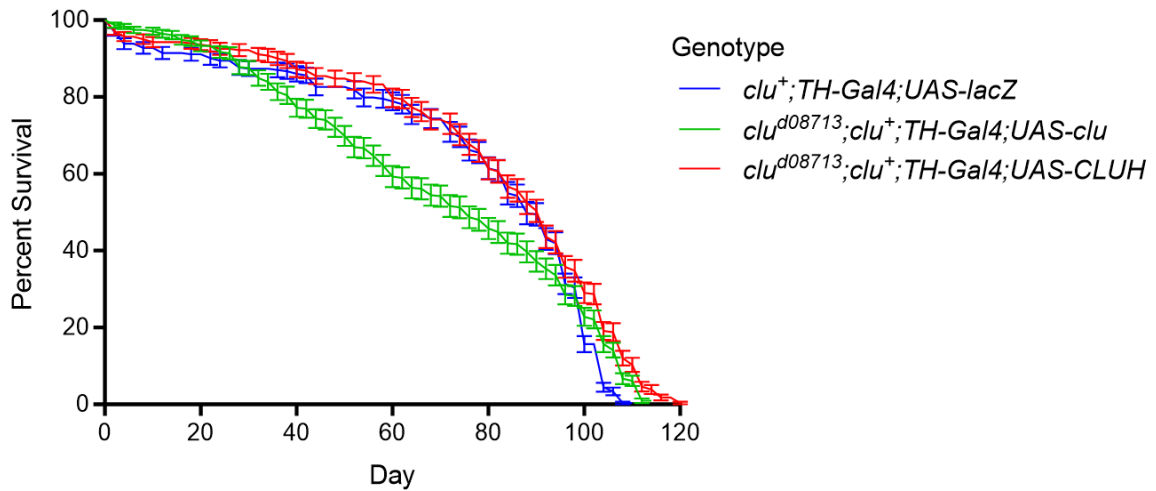


Figure 3.5 Lifespan is not affected in heterozygous *clueless* mutants expressing ectopic *clueless* or *CLUH* in dopaminergic neurons. Mean lifespans differ by 9% or less and 95% confidence intervals overlap around the means where *UAS-clu* and *UAS-CLUH* are expressed under the control of *TH-Gal4* in heterozygous *clu*^{d08713} mutants compared to *clu*⁺; *TH-Gal4*; *UAS-lacZ* controls. *clu*⁺; *TH-Gal4*; *UAS-lacZ* controls have a mean survival of 78 days (95% CI: 74-81 days, N=293), while *clu*^{d08713}; *clu*⁺; *TH-Gal4*; *UAS-clu* individuals with ectopic *clueless* expression in dopaminergic neurons have a mean survival of 71 days (95% CI: 68-75 days, N=312), and *clu*^{d08713}; *clu*⁺; *TH-Gal4*; *UAS-CLUH* individuals with ectopic *CLUH* expression in dopaminergic neurons have a mean survival of 82 days (95% CI: 78-85 days, N=282). Results of lifespan assay are depicted as percent survival with error bars representing standard error of the mean. This figure was prepared using Prism version 10.1.2.

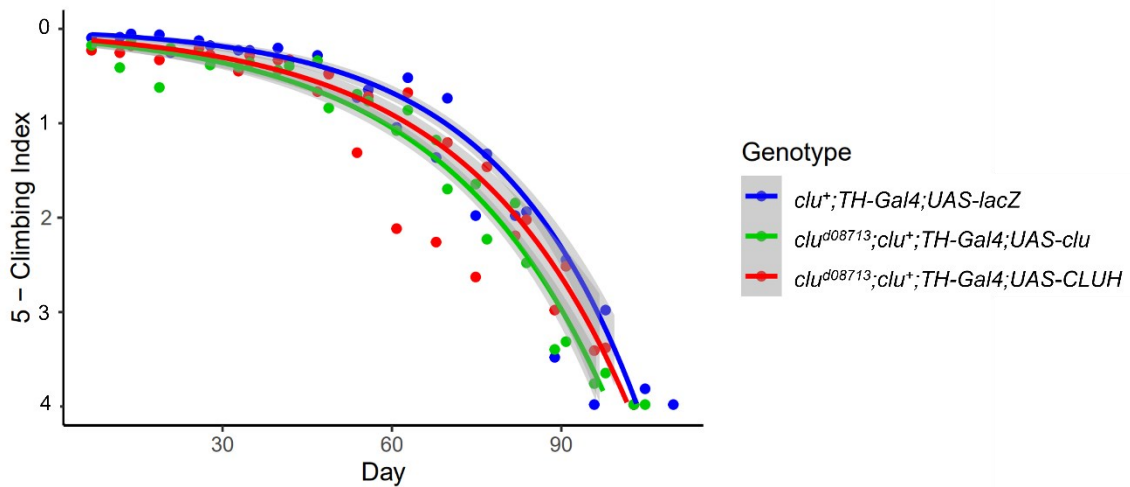


Figure 3.6 Climbing ability across lifespan is reduced in heterozygous *clueless* mutants expressing ectopic *clueless* but not *CLUH* in dopaminergic neurons.

Climbing ability is initially impaired but declines less rapidly where *UAS-clu* is expressed under the control of *TH-Gal4* in heterozygous *clu^{d08713}* mutants compared to *clu⁺;TH-Gal4;UAS-lacZ* controls, resulting in climbing indices that do not overlap within 95% confidence intervals across much of the climbing assay. Climbing ability for *clu⁺;TH-Gal4;UAS-lacZ* controls declines at an estimated rate of 4% per day, while climbing ability for *clu^{d08713};clu⁺;TH-Gal4;UAS-clu* individuals declines at an estimated rate of 3.4% per day. Climbing ability is not significantly affected in *clu^{d08713};clu⁺;TH-Gal4;UAS-CLUH* individuals, with climbing indices overlapping within 95% confidence intervals across much of the climbing assay. Climbing ability for *clu^{d08713};clu⁺;TH-Gal4;UAS-CLUH* individuals declines at an estimated rate of 3.5% per day. Climbing indices were calculated as per Todd and Staveley (Todd and Staveley, 2004), with curves calculated according to the model $5\text{-Climbing Index} = Ce^{Kt}$ and weighted according to number of individuals measured at each time point. Shaded regions indicate 95% confidence intervals. Figure illustrates the model described in Appendix 3. This figure was prepared using R version 4.3.2 with the ggplot2 package (version 3.5.1; Wickham, 2016).

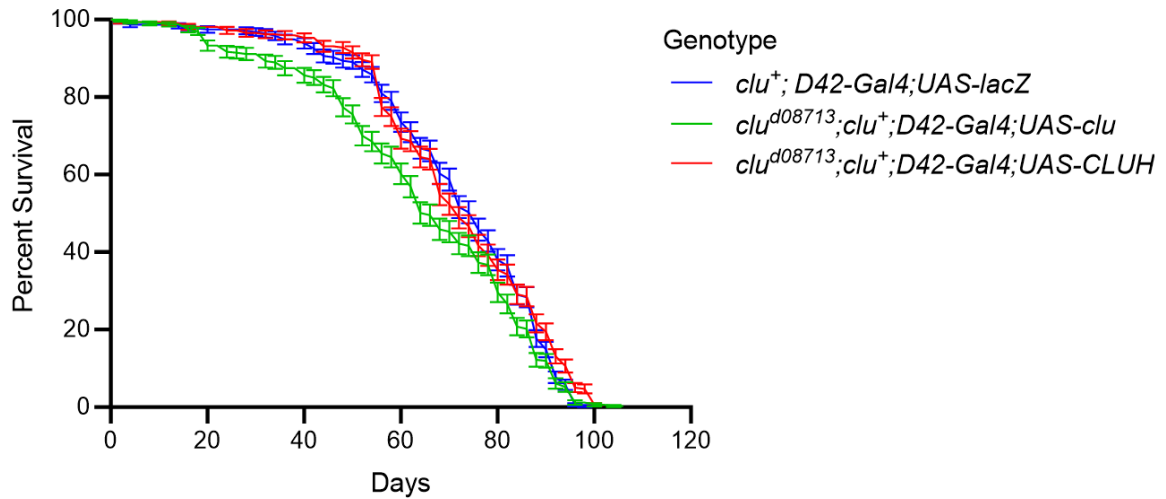


Figure 3.7 Heterozygous *clueless* mutants expressing ectopic *clueless* but not *CLUH* in motor neurons have reduced lifespan. Heterozygous clu^{d08713} mutants expressing *UAS-clu* under the control of *D42-Gal4* have 10% decreased mean lifespan compared to $clu^+; D42-Gal4; UAS-lacZ$ controls. $clu^+; D42-Gal4; UAS-lacZ$ controls have a mean survival of 72 days (95% CI: 70-74 days, N=310), while $clu^{d08713}; clu^+; D42-Gal4; UAS-clu$ individuals with ectopic *clueless* expression in motor neurons have a mean survival of 65 days (95% CI: 63-68 days, N=327). $clu^{d08713}; clu^+; D42-Gal4; UAS-CLUH$ individuals with ectopic *CLUH* expression in motor neurons have a mean survival of 72 days (95% CI: 70-74 days, N=319), showing that lifespan is not impaired compared to controls. Results of lifespan assay are depicted as percent survival with error bars representing standard error of the mean. This figure was prepared using Prism version 10.1.2.

expressing *UAS-CLUH* under the control of *D42-Gal4* do not have affected lifespan compared to *clu⁺;UAS-lacZ* controls. *clu^{d08713}* heterozygotes expressing either *UAS-clu* or *UAS-CLUH* under the control of *D42-Gal4* have reduced climbing ability across lifespan compared to *clu⁺;UAS-lacZ* controls (Figure 3.8). Climbing ability is impaired in young individuals, and climbing indices do not overlap within 95% confidence intervals across much of the climbing assay.

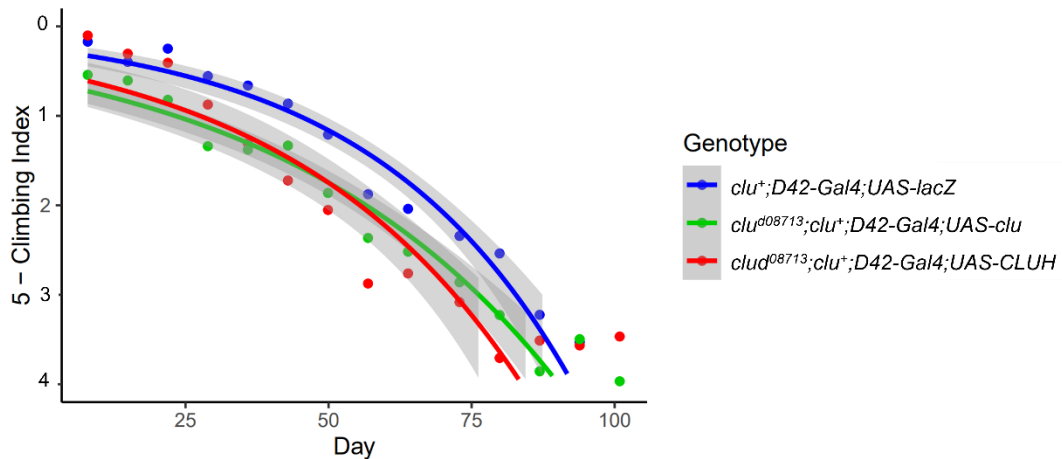


Figure 3.8 Climbing ability across lifespan is reduced in heterozygous *clueless* mutants expressing ectopic *clueless* of *CLUH* in motor neurons. Climbing ability is initially impaired but declines less rapidly where *UAS-clu* is expressed under the control of *D42-Gal4* in heterozygous *clu*^{d08713} mutants compared to *clu*⁺;D42-Gal4;UAS-lacZ controls, resulting in climbing indices that do not overlap within 95% confidence intervals across much of the climbing assay. Climbing ability for *clu*⁺;D42-Gal4;UAS-lacZ controls declines at an estimated rate of 2.8% per day, while climbing ability for *clu*^{d08713};clu⁺;D42-Gal4;UAS-clu individuals declines at an estimated rate 2% per day, and climbing ability for *clu*^{d08713};clu⁺;D42-Gal4;UAS-CLUH individuals declines at an estimated rate of 2.4% per day. Climbing indices were calculated as per Todd and Staveley (Todd and Staveley, 2004), with curves calculated according to the model $5\text{-Climbing Index} = Ce^{Kt}$ and weighted according to number of individuals measured at each time point. Shaded regions indicate 95% confidence intervals. Figure illustrates the model described in Appendix 4. This figure was prepared using R version 4.3.2 with the ggplot2 package (version 3.5.1; Wickham, 2016).

Chapter 4: Discussion

4.1 Inhibited *clueless* Expression in Dopaminergic Neurons Does Not Cause Age-Related Disease

Inhibited expression of *clueless* in *D. melanogaster* DA neurons did not significantly affect mean lifespan or cause a more rapidly progressive loss in climbing ability with age (Figures 3.1, and 3.2). These results may indicate that the role of Clueless in regulating mitochondrial homeostasis in response to age-related stress in DA neurons is not important, that compensatory mitochondrial control mechanisms such as the ubiquitin-proteasome system are upregulated on lifelong *clueless* inhibition in these cells, or that *clueless* expression in these cells was not altered to such a degree as to have an effect on these processes (discussed in Section 4.6). These data show that inhibited expression of *clueless* in *D. melanogaster* DA neurons does not cause age-related neurodegenerative disease comparable to PD.

4.2 Inhibited *clueless* Expression in Motor Neurons Causes Age-Related Disease

Inhibited expression of Clueless in *D. melanogaster* motor neurons decreases mean lifespan, and can cause a more rapidly progressive loss in climbing ability with age (Figures 3.3, and 3.4). Suppression of *clueless* on expression of *UAS-cluRNAi^{V42136}* under the control of *D42-Gal4* causes a more rapid loss of climbing ability with age compared to control, demonstrating a role of Clueless in age-related retention of locomotor function (Figure 3.4). Age-related disease on the inhibited expression of *clueless* exclusively in the motor neurons is likely caused by the progressive loss of these cells with age. These data show that inhibited expression of *D. melanogaster clueless* in motor neurons causes age-related neurodegenerative disease comparable to ALS.

4.3 Inhibition of *clueless* Expression in Motor Neurons Replicates Features of ALS

The suppression of *clueless* in motor neurons in *D42-Gal4;UAS-cluRNAi^{V42136}* *D. melanogaster* replicates key features of ALS: impaired lifespan and premature loss in locomotor function beginning in adulthood (Figures 3.7 and 3.8). As *clueless* is exclusively suppressed in motor neurons in these individuals, these phenotypes likely occur due to the progressive loss of motor neurons with age. Climbing ability of *D42-Gal4;UAS-cluRNAi^{V42136}* individuals across lifespan declines at only a slightly greater rate than that of controls (Figure 3.8). This slightly increased rate of decline in climbing ability results in climbing indices that do not overlap within 95% confidence intervals controls beginning approximately midway through the climbing assay, consistent with midlife ALS onset in humans (Masrori and Van Damme, 2020). *Clueless* and its homologues are RNA-binding proteins thought to regulate mitochondrial homeostasis through control of mitochondrial mRNAs, and influence mitochondrial trafficking and mitophagy (Figure 1.4). The pathways most consistently linked to ALS are RNA metabolism, autophagy, and axonal and cytoskeletal transport; and ALS is associated with mitochondrial dysfunction (Masrori and Van Damme, 2020; Carri *et al.*, 2017). Indications of mitochondrial dysfunction including abnormal mitochondrial morphology as well as impaired mitochondrial transport and mitophagy are linked with ALS, occurring early in the progression of the disease in murine ALS models (Palomo and Manfredi, 2015). Organelle transport defects are common in ALS, and impaired mitochondrial transport broadly impacts mitochondrial function and mitochondrial homeostasis (Dorn, 2019). Impaired autophagy and especially mitophagy contribute to mitochondrial dysfunction in ALS (Kim *et al.*, 2013; Harper *et al.*, 2018). Modelling ALS

using the *D42-Gal4;UAS-cluRNAi^{V42136}* *D. melanogaster* model, then, could be used to investigate the role of mitochondrial dysfunction in the pathology of this disease.

4.4 Ectopic Expression of *clueless* and *CLUH* in Dopaminergic and Motor Neurons of Heterozygous *clu^{d08713}* Mutants

Heterozygous *clueless* mutants that express ectopic *clueless* or *CLUH* in dopaminergic neurons do not have impaired mean lifespan or a more rapidly progressive loss in climbing ability with age (Figures 3.5 and 3.6), and so do not have age-related disease phenotypes as compared to control. Heterozygous *clueless* mutants that express ectopic human *CLUH* in motor neurons do not have age-related disease phenotypes as compared to controls, and heterozygous *clueless* mutants that express ectopic *clueless* do not show a more rapidly progressive reduction in climbing ability with age (Figures 3.7 and 3.8). *clu^{d08713}* is an amorphic allele wherein homozygotes lack detectable Clueless proteins, and adults have locomotor defects and lifespans of only three to seven days (Cox and Spradling, 2009). Mitochondria in ovaries of 4-day old adult *clu^{d08713}* homozygotes have swollen ultrastructure with extensive inner membrane vacuolization. Mitochondria in ovaries of four-day old adult *clu^{d08713}* heterozygotes, however, are morphologically normal. Clueless protein is present in heterozygotes but levels are reduced compared to wild-type. Levels of the mitochondrial proteins pyruvate dehydrogenase and complex V-alpha were reduced in *clu^{d08713}* homozygotes but not heterozygotes (measured at less than seven days following eclosion), compared to wild-type levels. Ubiquitous expression of *UAS-clu* under the control of *da-Gal4* in *clu^{d08713}* homozygotes restores lifespan to that of wild-type (Sen and Cox, 2016). Lack of age-related disease in comparison to *clu⁺;UAS-lacZ* controls where *UAS-clu* and *UAS-CLUH*

are expressed in dopaminergic and motor neurons is consistent with these data, suggesting that altered Clueless levels do not impair lifespan as long as a threshold level is maintained. Interestingly, heterozygous *clueless* mutants that express ectopic *UAS-clu* in motor neurons do have a slight but significant 10% reduction in lifespan as compared to *clu⁺;UAS-lacZ;D42-Gal4* controls (Figure 3.7). This suggests that motor neurons may be particularly sensitive to altered *clueless* expression, but verification through direct measures of *clueless* expression is required before conclusions can be made. Follow-up studies should examine lifespan and climbing ability across lifespan in *clu^{d08713}* heterozygotes not expressing *UAS*-associated *clueless* and *CLUH* transgenes, and the effects of *UAS-clu* and *UAS-CLUH* expression in *clu^{d08713}* heterozygotes compared to *clu^{d08713}* heterozygous controls.

4.5 Early-Life Impairment of Locomotor Function

Inhibited expression of *clueless* under the control of *TH-Gal4* causes initial impairment in climbing ability (Figure 3.2). This indicates an role of Clueless in these neurons in early life. *clueless* inhibition in motor neurons on expression of *UAS-cluRNAi^{V42138}* and *UAS-cluRNAi^{KK108024}* under the control of *D42-Gal4* causes initial impairments in climbing ability (Figure 3.4). Where *clueless* is inhibited specifically in DA or motor neurons, initial climbing impairment suggests either that dysregulation of Clueless impairs development of these neurons, or that dysregulation of Clueless causes neurodegeneration that occurs at earlier than seven days of age. *clu^{d08713}* heterozygotes expressing *UAS-clu* under the control of either *TH-Gal4* or *D42-Gal4* also have impaired initial climbing ability (Figures 3.6 and 3.8), suggesting that impaired locomotor function in young individuals is a common consequence of altered *clueless* expression in DA and

motor neurons. Initial climbing impairments on RNAi-mediated *clueless* suppression in motor neurons are different in *D42-Gal4;UAS-cluRNAi^{KK108024}* versus *D42-Gal4;UAS-cluRNAi^{V42138}* individuals, where expression of *UAS-cluRNAi^{KK108024}* has a much more drastic effect on initial climbing ability (Figure 3.8). Further investigation is required, but it is possible that this RNAi is more efficacious in suppressing the expression of *clueless*, leading to lower Clueless levels *in vivo*.

Locomotor defects in *clueless* mutant *D. melanogaster* have been previously documented in recently eclosed adults (Cox and Spradling, 2009; Sen *et al.*, 2015). This may result from acute pressure on mitochondria occurring upon the switch to oxidative phosphorylation at eclosion, or could alternatively result from a mitochondria-independent role of Clueless and its homologues in development (Schatton and Rugarli, 2018). Developmental viability is unaffected in *D. melanogaster clu^{d08713}* homozygotes, though mitochondria are mislocalized in larval neuroblasts (Sen *et al.*, 2013). Larval mobility is impaired where *clueless* is inhibited either pan-neuronally or in muscles (Sen *et al.*, 2013; Z. Wang *et al.*, 2016). Larval mobility is similarly impacted on inhibition of *clueless* and inhibition of *dgrasp*, which mediates the export of the integrin subunit α PS2 from the endoplasmic reticulum, in *D. melanogaster* muscles (Wang *et al.*, 2015). These data suggest that a mitochondria-independent role of Clueless in development may cause locomotor defects in early life on *clueless* inhibition. The cause of early-life locomotor dysfunction on altered *clueless* expression could be investigated with larval locomotion assays (Nichols *et al.*, 2012): if larval locomotion is unimpaired, where locomotion in young adult individuals is impaired, this would suggest a protective role of *clueless* against the acute pressure on mitochondria that occurs on the switch to primary reliance

on oxidative phosphorylation at eclosion (Schatton and Rugarli, 2018). Impaired larval location, however, would provide evidence for a potentially mitochondria-independent role of *clueless* in development.

Clueless binds to the developmental determinants atypical protein kinase C and bazooka in *D. melanogaster* larvae, which act to determine polarity in asymmetric cell division (Goh *et al.*, 2013). Clueless does not bind to Lethal giant larva, another protein involved in this process, but Clueless suppression in a *lethal giant larva* mutant background rescues phenotypes of defective asymmetric division and tumorigenesis in *D. melanogaster* larvae. Polarity is determined by the equilibrium of complexes formed by these determinants, so altered protein binding on altered *clueless* expression could disrupt the equilibrium and cause developmental abnormalities. *clueless* is highly expressed in larval neuroblasts, though viability of mutants is unaffected and mutants have no difference in neuroblast number compared to wild-type (Sen *et al.*, 2013; Goh *et al.*, 2013). Clueless may have a role in localization of the integrin subunit α PS2 following exit from the endoplasmic reticulum, as α PS2 fails to localize in *clueless* mutants (Wang *et al.*, 2015). As integrin subunits do not mislocalize in *Marf* and *parkin* mutants, and treatment of *clueless* mutants with the chemical chaperones 4-phenylbutyric acid and tauroursodeoxycholic acid rescue abnormal α PS2 localization but not mitochondrial morphology defects, this role of Clueless may be independent of its role in mitochondrial function. Therefore, Clueless and its homologues may have mitochondria-independent functions including in neurodevelopment.

Experiments to assess climbing ability in *D. melanogaster* on altered *clueless* expression were designed for the purpose of fitting the model described by Todd and

Staveley (2004). This methodology is sensitive to differences in climbing ability across lifespan, and a good fit of the model requires frequent measurements with age for each genotype. These measurements do not necessarily need to occur at the same time points, for example one experimental genotype may have been measured first at 10 days and every week thereafter, and another group first measured at 11 days and every week thereafter. To most accurately examine and compare the differences in climbing ability at a certain time point, such as in early life, experimental individuals should be measured on the same day. Follow-up experiments are required to verify the effects of altered *clueless* expression on early-life climbing ability.

4.6 Transgene Expression

Expression of the transgenic constructs used (Tables 2.2 and 2.3) was not directly assessed. Quantification of expression level through real-time PCR or western blotting is required to verify interpretation of these results, and should be included in follow-up studies. Expression of most of the constructs used has been characterized by other groups (Yeh *et al.*, 1995; Friggi-Grelin *et al.*, 2003; Cox and Spradling 2009; Sen and Cox, 2015; Brand and Perrimon, 1993). Notably, expression of human *CLUH* via *UAS-CLUH* in *D. melanogaster* rescues phenotypes associated with *clueless* suppression; including the mitochondrial clustering phenotypes and locomotor ability in *clu*^{d08713} homozygotes, indicating a conserved functional role (Sen and Cox, 2015). Expression of the *UAS-cluelessRNAi* transgenes have not been all experimentally evaluated. One research group found that co-expression of *UAS-cluRNAi*^{V42136} and *UAS-cluRNAi*^{V42138} results in no detectable levels of Clueless protein in western blotting when staining for anti-Clueless antibodies (Z. Wang *et al.*, 2016). This indicates that at least one of these transgenes is

acting to suppress *clueless* translation in cells. The reproducibility of observed phenotypic lifespan effect on expression of sequence-verified *UAS-cluelessRNAi* transgenes (Figure 3.3) generated through different methods (Table 2.3) under the control of *D42-Gal4* supports the inference that these transgenes are acting as expected to suppress *clueless* expression in the presence of Gal4 (Dietzl *et al.*, 2007). Expression of *UAS-cluRNAi^{KK108024}*, *UAS-cluRNAi^{V42136}*, and *UAS-cluRNAi^{V42138}* in motor neurons, however, has very different effects on climbing ability across lifespan (Figure 3.4). This may be a result of varying efficacy of *clueless* suppression, but without a direct measurement of *clueless* expression this cannot be determined. If future studies find differences in Clueless levels on expression of these *UAS-cluelessRNAi* transgenes, then this may indicate a particular sensitivity of motor neurons to altered *clueless* expression and suggest a role of Clueless in protection against age-related motor neuron degeneration such as occurs in ALS. The climbing assay used here is sensitive to subtle phenotypes of age-related neurodegeneration, and when accompanied by accurate expression data may prove useful in elucidating subtle differences in gene expression which may influence the progress of complex heterogenous neurodegenerative diseases (Todd and Staveley, 2004).

4.7 Clueless and Mitochondrial Function

This study did not include direct measures of the impact of altered *clueless* expression on mitochondrial function. Impacts of altered *clueless* expression on mitochondria in age-related disease could be assessed through microscopy techniques. Morphological damage to mitochondria in *clu^{d08713}* homozygotes that can be visualized through electron microscopy includes vacuolization of the inner membranes and loss of cristae structure. If RNAi-mediated inhibition of *clueless* expression in neuronal

subpopulations such as motor neurons results in accumulation of damaged mitochondria with age, then visualization of mitochondria in aged flies should show an increase in morphologically abnormal mitochondria compared to age-matched controls. Alternative behavioural assays may also be used to infer the role of mitochondrial function in age-related disease (Mituzaitte *et al.*, 2021; see Appendix 5). The interaction of *clueless* with mitochondria-associated proteins will also be informative of a role of *clueless* in maintaining mitochondrial homeostasis across lifespan. Overexpression of the mitochondrial fission protein DRP1 upregulates fission and mitophagy, and *Drp1* overexpression ameliorates phenotypes in *clu*^{d08713} homozygotes (Yang *et al.*, 2022). If co-expression of a *UAS-Drp1* in motor neurons with a *UAS-cluelessRNAi* rescues impaired lifespan, this would suggest that dysregulation of mitochondrial dynamics and mitophagy contributes to the disease phenotype reported here. Similar experiments should examine the effects of modulating the interaction of Clueless with ALS-associated VCP and PD-associated PINK1 and Parkin on lifespan and climbing ability across lifespan.

4.8 Further Characterization of Clueless Function

The effects of enhanced expression of *clueless* in dopaminergic and motor neurons on lifespan and climbing ability across lifespan may be informative as to the role of *clueless* in ageing and disease. In *D. melanogaster*, Clueless particles form in response to insulin treatment, and do not form where insulin signalling is disrupted in *InR* insulin receptor mutants (Sheard *et al.*, 2020). In mammalian cells, the mitochondrial clustering phenotype on *CLUH* inhibition is rescued on treatment with the target of rapamycin (TOR) inhibitor rapamycin (Pla-Martín *et al.*, 2020). These granules stain positive for mammalian target of rapamycin (mTOR), a signalling molecule in the nutrient-sensing

TOR pathway (Tian *et al.*, 2017). CLUH could negatively regulate TOR signalling by causing mTOR to be sequestered within granules. *clueless* suppression causes upregulation of proteins involved in stress response (Sen and Cox, 2022). Upregulation of nutrient-sensing stress-response signals results in upregulation of stress-response mechanisms including mitophagy and extends lifespan multiple species, including *D. melanogaster* and mice (Pla-Martín *et al.*, 2020; Sheard *et al.*, 2020; Kenyon, 2010). It may be informative to investigate the effects of *clueless* inhibition where these pathways are upregulated, such as where insulin receptor is suppressed, on *D. melanogaster* lifespan.

4.9 Sex Considerations

Only critical-class male *D. melanogaster* were collected and assayed in order to avoid lifespan effects related to female fertility. *D. melanogaster* reach sexual maturity within eight to twelve hours following eclosion. Reproductive behaviour shortens lifespan of both male and female *D. melanogaster* (Partridge and Gems, 2007; Linford *et al.*, 2013). Female *D. melanogaster*, however, can store sperm for up to two weeks after mating (Hales *et al.*, 2015). To avoid biasing results with impacts of female fecundity on organism health and longevity, collection of critical-class females needs to be carried out frequently and carefully. Sex in *D. melanogaster* is determined by X-chromosome dosage rather than the presence of a Y chromosome as in mammals, and findings of biomedical research in *D. melanogaster* will ultimately need to be confirmed in mammals (Hales *et al.*, 2015; Partridge and Gems, 2007; Jennings, 2011). Virgin females have longer lifespans than males, and so use of female *D. melanogaster* is potentially advantageous for the study of adult-onset age-related neurodegenerative disease (Staats *et al.*, 2018).

Factors affecting lifespan in *D. melanogaster* may have sex-dependent effects, for example the effects of ecdysone receptor sensitivity (Tricoire *et al.*, 2009). Both female and male *D. melanogaster* lifespans are increased in ecdysone receptor heterozygous mutants, but female lifespans are decreased on mild ubiquitous ecdysone receptor suppression via expression of a UAS-associated ecdysone receptor RNAi (Simon *et al.*, 2003; Tricoire *et al.*, 2009). Therefore, conclusions about the impact of experimental treatments assessed in males cannot be assumed to impact females in the same way, and future study of the role of *clueless* in *D. melanogaster* will benefit from the inclusion of females.

4.10 Conclusion

A potential role of Clueless in stress-responsive regulation of mitochondrial homeostasis is illustrated in Figure 1.4. *clueless* interacts with the PD- and ALS-associated genes *PINK1* and *Parkin* (Sen *et al.*, 2015). I report here that inhibited expression of *clueless* in *D. melanogaster* DA and motor neurons causes locomotor dysfunction in young individuals, and altered *clueless* expression in motor neurons causes age-related neurodegenerative disease. RNAi-mediated *clueless* suppression in motor neurons in *D42-Gal4;UAS-cluRNAi^{V42136}* *D. melanogaster* replicates key features of ALS, and this model may be useful in investigating the role of altered mitochondrial homeostasis in the pathology of this disease. As the roles of *D. melanogaster* Clueless and mammalian CLUH are highly conserved, a detailed understanding generated through further evaluation of the effects of altered expression of *clueless* on ageing and neurodegeneration could provide insight into the role of CLUH in protection against age-related neurodegenerative disease in humans.

Literature Cited

- Abdul Wahid, S.F., Law, Z.K., Ismail, N.A., Lai, N.M. 2019. Cell-based therapies for amyotrophic lateral sclerosis/motor neuron disease. *Cochrane Database of Systematic Reviews*. 2019 (12): CD011742. doi: 10.1002/14651858.CD011742.pub3.
- Abeliovich, A., Gitler, A.D. 2016 Defects in trafficking bridge Parkinson's disease pathology and genetics. *Nature*. 539: 207-217. doi: 10.1038/nature20414.
- Adams, M. D., Celniker, S.E., Holt, R.A., Evans, C.A., Gocayne, J.D. *et al.*, & Venter, J.C. 2000. The genome sequence of *Drosophila melanogaster*. *Science*. 287 (4561): 2185-2195. doi: 10.1126/science.287.5461.2185.
- Alfadda, A.A., Sallam, R.M. 2012. Reactive oxygen species in health and disease. *Journal of Biomedicine and Biotechnology*. 2012: 936486. doi: 10.1155/2012/936486.
- Aryal, B., Lee, Y., 2019. Disease model organism for Parkinson disease: *Drosophila melanogaster*. *BMJ Reports*. 52 (4): 250-258. doi: 10.5483/BMBRep.2019.52.4.204.
- Aunan, J.R., Watson, M.M., Hagland, H.R., Søreide, K. 2016. Molecular and biological hallmarks of ageing. *The British Journal of Surgery*. 103 (2): e29-e46. doi: 10.1002/bjs.10053.
- Azuma, Y., Tokuda, T., Shimamura, M., Kyotani, A., Sasayama, H., Yoshida, T., Mizuta, I., Mizuno, T., Nakagawa, M., Fukikake, N., Ueyama, M., Nagai, Y., Yamaguchi, M. 2014. Identification of *ter94*, *Drosophila VCP*, as a strong modulator of motor

- neuron degeneration induced by knockdown of *Caz*, *Drosophila FUS*. *Human Molecular Genetics*. 23 (13): 3467-3480. doi: 10.1093/hmg/ddu055.
- Bastian, F.B., Roux, J., Niknejad, A., Comte, A., Costa, S.S.F. 2021. The Bgee suite: integrated curated expression atlas and comparative transcriptomics in animals. *Nucleic Acids Research*. 49 (D1): D831–D847. doi: 10.1093/nar/gkaa793.
- Bhandari, P., Song, M., Chen, Y., Burrelle, Y., Dorn II, G.W. 2014. Mitochondrial contagion induced by Parkin deficiency in *Drosophila* hearts and its containment by suppressing mitofusins. *Circulation Research*. 114 (2): 257-265. doi: 10.1161/CIRCRESAHA.114.302734.
- Biscof, J., Maeda, R.K., Hediger, K. 2007. An optimized transgenesis system for *Drosophila* using germ-line-specific ϕ C31 integrases. *Proceedings of the National Academy of Science*. 104 (9): :3312-3317. doi: 10.1073/pnas.0611511104.
- Bolus, H., Crocker, K., Boekhoff-Falk, G., Chtarbanova, S. 2020. Modeling neurodegenerative disorders in *Drosophila melanogaster*. *International Journal of Molecular Sciences*. 21 (9): 3055. doi: 10.3390/ijms21093055.
- Bowden, H.A., Dormann, D. 2016. Altered mRNP granule dynamics in FTL D pathogenesis. *Journal of Neurochemistry*. 138 (Suppl 1): 112-133. doi: 10.1111/jnc.13601.
- Brand, A.H., Perrimon, N. 1993. Targeted gene expression as a means of altering cell fates and generating dominant phenotypes. *Development*. 118 (2): 401-415. doi: 10.1242/dev.118.2.401.
- Buchan, J.R., Parker, R. 2009. Eukaryotic stress granules: the ins and outs of translation. *Molecular Cell*. 36 (6): 932-941. doi: 10.1016/j.molcel.2009.11.020.

- Buchan, J.R., Kolaitis, R., Taylor, J.P., Parker, R. 2013. Eukaryotic stress granules are cleared by autophagy and Cdc48/VCP function. *Cell*. 153 (7): 1461-1474. doi: 10.1016/j.cell.2013.05.037.
- Cacciatore, I., Baldassarre, L., Fornasari, E., Mollica, A., Pinnen, F. 2012. Recent advances in the treatment of neurodegenerative diseases based on GSH delivery systems. *Oxidative Medicine and Cellular Longevity*. 2012: 240146. doi: 10.1155/2012/240146.
- Carri, M.T., D'Ambrosi, N., Cozzolino, M. 2017. Pathways to mitochondrial dysfunction in ALS pathogenesis. *Biochemical and Biophysical Research Communications*. 483 (4): 1187-1193. doi: 10.1016/j.bbrc.2016.07.055.
- Chan, D.C. 2007. Mitochondrial dynamics in disease. *New England Journal of Medicine*. 356 (17): 1707-1709. doi: 10.1056/NEJMp078040.
- Chen, H., Chan, D.C. 2009. Mitochondrial dynamics—fusion, fission, movement, and mitophagy—in neurodegenerative diseases. *Human Molecular Genetics*. 18 (2): R169–R176. doi: 10.1093/hmg/ddp326.
- Chen, C., Chein, S. 2010. Prenatal sonographic features of Miller-Dieker syndrome. *Journal of Medical Ultrasound*. 18 (4): 147-152. doi: 10.1111/ahg.12407.
- Chen, Y., Yang, M., Deng, J., Chen, X., Ye, Y., Zhu, L., Liu, J., Ye, H., Shen, Y., Li, Y., Rao, E.J., Fushimi, K., Zhou, X., Bigio, E.H., Mesulam, M., Xu, Q., Wu, J.Y. 2011. Expression of human FUS protein in *Drosophila* leads to progressive neurodegeneration. *Protein and Cell*. 2 (6): 477-486. doi: 10.1007/s13238-011-1065-7.

- Clark, I.E., Dodson, M.W., Jiang, C., Cao, J.H., Huh, J.R., Seol, J.H., Yoo, S.J., Hay, B.A., Guo, M. 2006. *Drosophila pink1* is required for mitochondrial function and interacts genetically with *parkin*. *Nature*. 441 (7097): 1162-1166. doi: 10.1038/nature04779.
- Cornelissen, T., Vilain, S., Vints, K., Goukko, N., Verstreken, P., Vandenberghe, W. 2018. Deficiency of parkin and PINK1 impairs age-dependent mitophagy in *Drosophila*. *eLife*. 7: e35878. doi: 10.7554/eLife.35878.
- Corti, O., Lesage, S., Brice, A. 2011. What genetics tells us about the causes and mechanisms of Parkinson's disease. *Physiological Reviews*. 91 (4): 1161-1218. doi: 10.1152/physrev.00022.2010.
- Cox, R.T., Spradling, A.C. 2009. Clueless, a conserved *Drosophila* gene required for mitochondrial subcellular localization, interacts genetically with parkin. *Disease Models & Mechanisms*. 2: 490-499. doi: 10.1242/dmm.002378.
- Coyle, J.T., Puttfarcken, P. 1993. Oxidative stress, glutamate, and neurodegenerative disorders. *Science*. 262 (5134) :689-695. doi: 10.1126/science.7901908
- Dietzl, G., Chen, D., Schnorrer, F., Su, K., Barinova, Y., Fellner, M., Gasser, B., Kinsey, K., Oettel, S., Scheiblauer, S., Couto, A., Marra, V., Keleman, K., Dickson, B.J. 2007. A genome-wide transgenic RNAi library for conditional gene inactivation in *Drosophila*. *Nature*. 448: 151- 156. doi: 10.1038/nature05954.
- Dorn, G.W., Kitsis, R.N. 2014. The mitochondrial dynamism-mitophagy-cell death interactome. *Circulation Research*. 116 (1): 167-182. doi: 10.1161/CIRCRESAHA.116.303554.

- Dorn, G.W. 2019. Evolving concepts of mitochondrial dynamics. *Annual Review of Physiology*. 81: 1-17. doi: 10.1146/annurev-physiol-020518-114358.
- El Zawily, A.M.E., Schwarzländer, M., Finkemeier, I., Johnston, I.G., Benamar, A., Cao, Y., Gissot, C., Meyer, A.J., Wilson K., Datla, R., Macherel, D., Jones, N.S., Logan, D.C. 2014. *FRIENDLY* regulates mitochondrial distribution, fusion, and quality control in Arabidopsis. *Plant Physiology*. 166 (2): 808-828. doi: 10.1104/pp.114.243824.
- Elia, A.J., Parkes, T.L., Kirby, K., St George-Hyslop, P., Boulianne, G.L., Phillips, J.P., Hilliker, A.J. 1999. Expression of human FALS SOD in motoneurons of *Drosophila*. *Free Radical Biology and Medicine*. 26 (9-10): 1332-1338. doi: 10.1016/s0891-5849(98)00333-5.
- Eliyahu, E., Pnueli, L., Melamed, D., Scherrer, T., Gerber, A.P., Pines, O., Rapaport, D., Arava, Y. 2010. Tom20 mediates localization of mRNAs to mitochondria in a translation-dependent manner. *Molecular and Cellular Biology*. 30 (1): 284-294. doi: 10.1128/MCB.00651-09.
- Erickson, S.L., Lykke-Andersen, J. 2011. Cytoplasmic mRNP granules at a glance. *Journal of Cell Science*. 124 (Pt 3): 293-297. doi: 10.1242/jcs.072140.
- Feany, M.B., Bender, W.W. 2000. A *Drosophila* model of Parkinson's disease. *Nature*. 404: 394-398. doi: 10.1038/35006074.
- Ferguson, M., Mockett, R.J., Shen, Y., Orr, W.C., Sohal, R.J. 2005. Age-associated decline in mitochondrial respiration and electron transport in *Drosophila melanogaster*. *The Biochemical Journal*. 390 (Pt 2): 501-511. doi: 10.1042/BJ20042130.

- Fields, S.D., Conrad, N.M., Clarke, M. 1998. The *S. cerevisiae* *CLU1* and *D. discoideum* *cluA* genes are functional homologues that influence mitochondrial morphology and distribution. *Journal of Cell Science*. 111 (12): 1717-1727. doi: 10.1242/jcs.111.12.1717.
- Foster, L.A., Salajegheh, M.K. 2019. Motor neuron disease: pathophysiology, diagnosis, and management. *The American Journal of Medicine*. 132 (1): 32-37. doi: 10.1016/j.amjmed.2018.07.012.
- Friggi-Grelin, F., Coulom, H., Meller, M., Gomez, D., Hirsch, J., Birman, S. 2003. Targeted gene expression in *Drosophila* dopaminergic cells using regulatory sequences from tyrosine hydroxylase. *Journal of Neurobiology*. 54 (4): 618-627. doi: 10.1002/neu.10185.
- Fu, H. Hardy, J., Duff, K. 2018. Selective vulnerability in neurodegenerative diseases. *Nature Neuroscience*. 21: 1350-1358. doi: 10.1038/s41593-018-0221-2.
- Funayama, M., Nishioka, K., Li, Y., Hattori, N. 2023. Molecular genetics of Parkinson's disease: contributions and global trends. *Journal of Human Genetics*. 68 (3): 125-130. doi: 10.1038/s10038-022-01058-5.
- Gao, J., Schatton, D., Martinelli, P., Hansen, H., Pla-Martin, D., Barth, E., Becker, C., Altmueller, J., Frommolt, P., Sardiello, M., Rugarli, E.I. 2014. CLUH regulates mitochondrial biogenesis by binding mRNAs of nuclear-encoded mitochondrial proteins. *Journal of Cell Biology*. 207 (2): 213-223. doi: 10.1083/jcb.201403129.
- Garza-Lombó, C., Pappa, A., Panayiotidis, M.I. Franco, R. 2020. Redox homeostasis, oxidative stress and mitophagy. *Mitochondrion*. 51: 105-117. doi: 10.1016/j.mito.2020.01.002.

- Ge, P., Dawson, V.L., Dawson, T.M. 2020. PINK1 and Parkin mitochondrial quality control: a source of regional vulnerability in Parkinson's disease. *Molecular Neurodegeneration*. 15: 20. doi: 10.1186/s13024-020-00367-7.
- Gerhrke, S., Wu, Z., Klinkenberg, M., Sun, Y., Auburger, G., Guo, S., Lu, B. 2015. PINK1 and Parkin control localized translation of respiratory chain component mRNAs on mitochondria outer membrane. *Cell Metabolism*. 21 (1): 95-108. doi: 10.1016/j.cmet.2014.12.007.
- Giacomello, M., Pyakurel, A., Glytsou, C., Scorrano, L. 2020. The cell biology of mitochondrial membrane dynamics. *Nature Reviews Molecular Cell Biology*. 21 (4): 204-224. doi: 10.1038/s41580-020-0210-7.
- Goh, L.H., Zhou, X., Lee, M.C., Lin, S., Wang, H., Luo, Y., Yang, X. 2013. Clueless regulates aPKC activity and promotes self-renewal cell fate in *Drosophila lgl* mutant larval brains. *Developmental Biology*. 381 (2): 353-364. doi: 10.1016/j.ydbio.2013.06.031.
- Green, D.R., Galluzzi, L., Kroemer, G. 2011. Mitochondria and the autophagy-inflammation-cell death axis in organismal aging. *Science*. 333 (6046): 1109–1112. doi: 10.1126/science.1201940.
- Greene, J.C., Whitworth, A.J., Kuo, I., Andrews, L.A., Feany, M.B., Pallanck, L.J. 2003. Mitochondrial pathology and apoptotic muscle degeneration in *Drosophila parkin* mutants. *Proceedings of the National Academy of Sciences of the United States of America*. 100 (7): 4078-4083. doi: 10.1073/pnas.0737556100.

- Hales, K.G., Korey, C.A., Larracuente, A.M., Roberts, D.M. 2015. Genetics on the fly: a primer on the *Drosophila* model system. *Genetics*. 201(3): 815-842. doi: 10.1534/genetics.115.183392.
- Han, S.K., Lee, D., Lee, H., Kim D., Son, H.G., Yang, J., Lee, S.V., Kim, S. 2016. OASIS 2: online application for survival analysis 2 with features for the analysis of maximal lifespan and healthspan in aging research. *Oncotarget*. 7 (35): 56147-56152. doi: 10.18632/oncotarget.11269.
- Harper, J.W., Ordureau, A., Heo, J. 2018. Building and decoding ubiquitin chains for mitophagy. *Nature Reviews. Molecular Cell Biology*. 19 (2): 93-108. doi: 10.1038/nrm.2017.129.
- Hartenstein, V., Cruz, L., Lovick, J., K., Guo, M. 2016. Developmental analysis of the dopamine-containing neurons of the *Drosophila* brain. *Journal of Comparative Neurology*. 525 (2): 363-379. doi: 10.1002/cne.24069.
- Haywood, A.F.M., Staveley, B.E. 2004. *parkin* counteracts symptoms in a *Drosophila* model of Parkinson's disease. *BMC Neuroscience*. 5: 14. doi: 10.1186/1471-2202-5-14.
- Hegna, H.A. 2012. *Drosophila (Drosophila) mojavensis* [Image]. *PhyloPic*. Retrieved from: <https://www.phylopic.org/images/0cd6cc9f-683c-470e-a4a6-3b68beb826fa/drosophila-drosophila-mojavensis>.
- Hémono, M., Haller, A., Chicher, J., Duchêne, A., Ngondo, R.P. 2022. The interactome of CLUH reveals its association to SPAG5 and its co-translational proximity to mitochondrial proteins. *BMC Biology*. 20 (1): 13. doi: 10.1186/s12915-021-01213-y.

- Horan, M.P., Pichaud, N., Ballard, J.W.O. 2012. Review: quantifying mitochondrial dysfunction in complex diseases of aging. *The Journals of Gerontology: Series A*. 67 (10): 1022-1035. doi: 10.1093/gerona/qlr263.
- Huang, M., Bargues-Carot, A., Riaz, Z., Wickham, H., Zenitsky, G., Jin, H., Anantharam, V., Kanthasamy, A., Kanthasamy, A.G. 2022. Impact of environmental risk factors on mitochondrial dysfunction, neuroinflammation, protein misfolding, and oxidative stress in the etiopathogenesis of Parkinson's disease. *International Journal of Molecular Sciences*. 23 (18): 10808. doi: 10.3390/ijms231810808.
- Hung, C.H., Cheng, S.S., Cheung, Y., Wuwongse, S., Zhang, N.Q., Ho, Y., Lee, S.M., Chang, R.C. 2018. A reciprocal relationship between reactive oxygen species and mitochondrial dynamics in neurodegeneration. *Redox Biology*. 14: 7-19. doi: 10.1016/j.redox.2017.08.010.
- Hurley, E.P., Staveley, B.E. 2020. *TER94*, the *Drosophila* homolog of the ALS-related *VCP* gene, influences lifespan and leads to a decline in motor function. *Research Square*. 60498. Pre-print. doi: 10.21203/rs.3.rs-60498/v1.
- Iliadi, K.G., Gluscencova, O.B., Boulianne, G.L. 2016. Psychomotor behavior: a practical approach in *Drosophila*. *Frontiers in Psychiatry*. 7: 153. doi: 10.3389/fpsyt.2016.00153.
- Imai, Y. 2020. PINK1-Parkin signaling in Parkinson's disease: Lessons from *Drosophila*. *Neuroscience Research*. 159: 40-46. doi: 10.1016/j.neures.2020.01.016.
- Ingre, C., Roos, P.M., Piehl, F., Kamel, F., Fang, F. 2015. Risk factors for amyotrophic lateral sclerosis. *Clinical Epidemiology*. 7: 181-193. doi: 10.2147/CLEP.S37505.

- Ivanov, P., Kedersha, N., Anderson, P. 2019. Stress granules and processing bodies in translational control. *Cold Spring Harbor Perspectives in Biology*. 11 (5): a032813. doi: 10.1101/cshperspect.a032813.
- Jennings, B.H. 2011. *Drosophila* – a versatile model in biology & medicine. *Materials Today*. 14(5): 190-195. doi: 10.1016/S1369-7021(11)70113-4.
- Karess, R.E., Rubin, G.M. 1984. Analysis of P transposable element functions in *Drosophila*. *Cell*. 38 (1): 135-146. doi: 10.1016/0092-8674(84)90534-8.
- Karczewski K.J., Francioli, L.C., Tiao, G., Cummings, B.B., Alföldi, J., *et al.*, & MacArthur, D.G. 2020. The mutational constraint spectrum quantified from variation in 141,456 humans. *Nature*. 581 (7809): 434-443. Accessed February 2023. doi: 10.1038/s41586-020-2308-7.
- Kenyon, C.J. 2005. The plasticity of aging: insights from long-lived mutants. *Cell*. 120 (4): 449-460. doi: 10.1016/j.cell.2005.02.002.
- Kenyon, C.J. 2010. The genetics of ageing. *Nature*. 464 (7288): 504-512. doi: 10.1038/nature08980.
- Kim, N.C., Tresse, E., Kolaitis, R.M., Molliex, A., Thomas, R.E., Alami, N.H., Wang, B., Joshi, A., Smith, R.B., Ritson, G.P., Winborn, B.J., Moore, J., Lee, J., Yao, T., Pallanck, L., Kundu, M., Taylor, J.P. 2013. VCP is essential for mitochondrial quality control by PINK1/ Parkin and this function is impaired by VCP mutations. *Neuron*. 78 (1): 65-80. doi: 10.1016/j.neuron.2013.02.029.
- Kimonis, V.E., Fulchiero, E., Vesa, J., Watts, G. 2008. VCP disease associated with myopathy, Paget disease of bone and frontotemporal dementia: review of a unique

- disorder. *Biochimica et Biophysica Acta*. 1782 (12): 744-748. doi: 10.1016/j.bbadis.2008.09.003.
- Landrum, M.J., Lee, J.M., Benson, M., Brown, G.R., Chao, C., Chitipiralla, S., Gu, B., Hart, J., Hoffman, D., Jang, W., Karapetyan, K., Katz, K., Liu, C., Maddipatla, Z., Malheiro, A., McDaniel, K., Ovetsky, M., Riley, G., Zhou, G., Holmes, J.B., Kattman, B.L., Maglott, D.R. 2018. ClinVar: improving access to variant interpretations and supporting evidence. *Nucleic Acids Research*. 46 (D1): D1062-D1067. Accessed February 2023. doi: 10.1093/nar/gkx1153.
- Lee, J.J., Sanchez-Martinez, A., Zarate, A.M., Benincá, C., Mayor, U., Clague, M.J., Whitworth, A.J. 2018. Basal mitophagy is widespread in *Drosophila* but minimally affected by loss of Pink1 or parkin. *Journal of Cell Biology*. 217 (5): 1613-1622. doi: 10.1083/jcb.201801044.
- Lee, J.J., Andrezza, A., Whitworth, A.J. 2020. The STING pathway does not contribute to behavioural or mitochondrial phenotypes in *Drosophila Pink1/parkin* or mtDNA mutator models. *Scientific Reports*. 10: 2693. doi: 10.1038/s41598-020-59647-3.
- Lees, A.J., Hardy, J., Revesz, T. 2009. Parkinson's disease. *The Lancet*. 373 (9680): 2055-2066. doi: 10.1016/S0140-6736(09)60492-X.
- Lenz, S., Karsten, P., Schulz, J.B., Voigt, A. 2013. *Drosophila* as a screening tool to study human neurodegenerative diseases. *Journal of Neurochemistry*. 127 (4): 453-460. doi: 10.1111/jnc.12446.

- Lesnik, C., Galani-Armon, A., Arava, Y. 2015. Localized translation near the mitochondrial outer membrane: An update. *RNA Biology*. 12 (8): 801-809. doi: 10.1080/15476286.2015.1058686.
- Linford, N.J., Bilgir, C., Ro, J., Pletcher, S.D. 2013. Measurement of Lifespan in *Drosophila melanogaster*. *Journal of Visualized Experiments*. 71: 50068. doi: 10.3791/50068.
- Liu, J., Lillo, C., Jonnson, P.A., Velde, C.V., Ward, C.M., Miller, T.M., Subramaniam, J.R., Rothstein, J.D., Marklund, S., Andersen, P.M., Brännström, B., Gredal, O., Wong, P.C., Williams, D.S., Cleveland, D.W. 2004. Toxicity of familial ALS-linked SOD1 mutants from selective recruitment to spinal mitochondria. *Neuron*. 43 (1): 5-17. doi: 10.1016/j.neuron.2004.06.016.
- Liu, Z., Wang, X., Yu, Y., Li, X., Wang, T., Jiang, H., Ren, Q., Jiao, Y., Sawa, A., Moran, T., Ross, C.A., Montell, C., Smith, W.W. 2008. A *Drosophila* model for LRRK2-linked parkinsonism. *Proceedings of the National Academy of Science of the United States of America*. 105 (7) :2693-2698. doi: 10.1073/pnas.0708452105.
- Livnat-Levanon, N., Glickman, M.H. 2011. Ubiquitin-proteasome system and mitochondria – reciprocity. *Biochimica et Biophysica Acta*. 1809 (2) :80-87. doi: 10.1016/j.bbagrm.2010.07.005.
- Lloyd, T.E., Taylor, J.P. 2010. Flightless flies: *Drosophila* models of neuromuscular disease. *Annals of the New York Academy of Science*. 1184: e1-20. doi: 10.1111/j.1749-6632.2010.05432.x.

- Logan, D.C., Scott, I., Tobin, A.K. 2003. The genetic control of plant mitochondrial morphology and dynamics. *The Plant Journal*. 36 (4): 500-509. doi: 10.1046/j.1365-313x.2003.01894.x.
- Ma, K., Chen, G., Li, W., Kepp, O., Zhu, Y., Chen, Q. 2020. Mitophagy, mitochondrial homeostasis, and cell fate. *Frontiers in Cell and Developmental Biology*. 8: 467. doi: 10.3389/fcell.2020.00467.
- Markaki, M., Tavernarakis, N. 2020. Mitochondrial turnover and homeostasis in ageing and neurodegeneration. *FEBS Letters*. 594 (15): 2370-2379. doi: 10.1002/1873-3468.13802.
- Masrori, P., Van Damme, P. 2020. Amyotrophic lateral sclerosis: a clinical review. *European Journal of Neurology*. 27 (10): 1918-1929. doi: 10.1111/ene.14393.
- McGurk, L., Berson, A., Bonini, N.M. 2015. *Drosophila* as an *in vivo* model for human neurodegenerative disease. *Genetics*. 201 (2): 377-402. doi: 10.1534/genetics.115.179457.
- Mituzaitė, J., Petersen, R., Claridge-Chang, A., Baines, R.A. 2021. Characterization of seizure induction methods in *Drosophila*. *eNeuro*. 8 (4): ENEURO.0079-21.2021. doi: 10.1523/ENEURO.0079-21.2021.
- Mochida, G.H. 2009. Genetics and biology of microcephaly and lissencephaly. *Seminars in Pediatric Neurology*. 16 (3): 120-126. doi: 10.1016/j.spen.2009.07.001.
- Nakagawa, S., Cuthill, I.C. 2007. Effect size, confidence interval and statistical significance: a practical guide for biologists. *Biological Reviews*. 82 (4): 591-605. doi: 10.1111/j.1469-185X.2007.00027.x.

- Nguyen, D.K.H., Thombre, R., Wang, J. 2019. Autophagy as a common pathway in amyotrophic lateral sclerosis. *Neuroscience Letters*. 697: 34-48. doi: 10.1016/j.neulet.2018.04.006.
- Nichols, C.D., Becnel, J., Pandey, U.B. 2012. Methods to assay *Drosophila* behavior. *Journal of Visualized Experiments*. 61: 3795. doi: 10.3791/3795.
- Nyathi, Y., Wilkinson, B.M., Pool, M.R. 2013. Co-translational targeting and translocation of proteins to the endoplasmic reticulum. *Biochimica et Biophysica Acta*. 1833 (11): 2392- 2402. doi: 10.1016/j.bbamcr.2013.02.021.
- Palikaras, K., Lionaki, E. Tavernarakis, N. 2015. Balancing mitochondrial biogenesis and mitophagy to maintain energy metabolism homeostasis. *Cell Death and Differentiation*. 22 (9): 1399-1401. doi: 10.1038/cdd.2015.86.
- Palomo, G.M., Manfredi, G. 2015. Exploring new pathways of neurodegeneration in ALS: the role of mitochondria quality control. *Brain Research*. 1607: 36-46. doi: 10.1016/j.brainres.2014.09.065.
- Park, J., Lee, S.B., Lee, S, Kim, Y., Song, S., Kim, S., Bae, E., Kim, J., Shong, M., Kim, J., Chung, J. 2006. Mitochondrial dysfunction in *Drosophila PINK1* mutants is complemented by *parkin*. *Nature*. 441 (7097): 1157-1161. doi: 10.1038/nature04788.
- Parks, A.L., Cook, K.R., Belvin, M., Dompe, N.A., Fawcett, R., et al. 2004. Systematic generation of high-resolution deletion coverage of the *Drosophila melanogaster* genome. *Nature Genetics*. 36 (3): 288-292. doi: 10.1038/ng1312.
- Partridge, L., Gems, D. 2007. Benchmarks for ageing studies. *Nature*. 450: 165-167. doi: 10.1038/450165a..

- Patten, D.A., Germain, M., Kelly, M.A., Slack, R.S. 2010. Reactive oxygen species: stuck in the middle of neurodegeneration. *Journal of Alzheimer's Disease*. 20 (S2): S357-S367. doi: 10.3233/JAD-2010-100498.
- Pla-Martín, D., Schatton, D., Wiederstein, J.L., Marx, M., Khiati, S., Krüger, M., Rugarli, E.I. 2020. CLUH granules coordinate translation of mitochondrial proteins with mTORC1 signaling and mitophagy. *The EMBO Journal*. 39 (9): e102731. doi: 10.15252/embj.2019102731.
- Poole, A.C., Thomas, R.E., Andrews, L.A., McBride, H.M., Whitworth, A.J., Pallanck, L.J. 2008. The PINK1/Parkin pathway regulates mitochondrial morphology. *Proceedings of the National Academy of Sciences of the United States of America*. 105 (5): 1638-1643. doi: 10.1073/pnas.0709336105.
- Popov, L. 2020. Mitochondrial biogenesis: an update. *Journal of Cellular and Molecular Medicine*. 24 (9): 4892-4899. doi: 10.1111/jcmm.15194.
- Pringsheim, T., Jette, N., Frolkis, A., Steeves, T.D.L. 2014. The prevalence of Parkinson's disease: a systematic review and meta-analysis. *Movement Disorders*. 29 (13): 1583-1590. doi: 10.1002/mds.25945.
- Quinn, P.M.J., Moreira, P.I., Ambrósio, A.F., Alves, C.H. 2020. PINK1/PARKIN signalling in neurodegeneration and neuroinflammation. *Acta Neuropathologica Communications*. 8: 189. doi: 10.1186/s40478-020-01062-w.
- Ravanelli, S., den Brave, F., Hoppe, T. 2020. Mitochondrial quality control governed by ubiquitin. *Frontiers in Cell and Developmental Biology*. 8: 270. doi: 10.3389/fcell.2020.00270.

- Reynolds, E.R. 2018. Shortened lifespan and other age-related defects in bang sensitive mutants of *Drosophila melanogaster*. *G3 (Bethesda)*. 8 (12): 3953-3960. doi: 10.1534/g3.118.200610.
- Ritson, G.P., Custer, S.K., Freibaum, B.D., Guinto, J.B., Geffel, D., Moore, J., Tang, W., Winton, M.J., Neumann, M., Trojanowski, J.Q., Lee, V.M., Forman, M.S., Taylor, J.P. 2010. TDP-43 mediates degeneration in a novel *Drosophila* model of disease caused by mutations in *VCP/p97*. *Journal of Neuroscience*. 30 (22): 7729-7739. doi: 10.1523/JNEUROSCI.5894-09.2010.
- Rodolfo, C., Campello, S., Cecconi, F. 2018. Mitophagy in neurodegenerative diseases. *Neurochemistry International*. 117: 156-166. doi: 10.1016/j.neuint.2017.08.004.
- Rubin, G.M., Spradling, A.C. 1982. Genetic transformation of *Drosophila* with transposable element vectors. *Science*. 218 (4570): 348-353. doi: 10.1126/science.6289436.
- Ruegseggar, G.N., Crea, A.L., Cortes, T.M., Dasari, S., Sreekumaran Nair, K. 2018. Altered mitochondrial function in insulin-deficient and insulin-resistant states. 128 (9): 3671- 3681. doi: 10.1172/JCI120843.
- Schatton, D., Pla-Martin, D., Marx, M., Hansen, H., Mourier, A., Nemazanyy, I., Pessia, A., Zentis, P., Corona, T., Kondylis, V., Barth, E., Schauss, A.C., Velagapudi, V., Rugarli, E.I. 2017. CLUH regulates mitochondrial metabolism by controlling translation and decay of target mRNAs. *Journal of Cell Biology*. 216 (3): 675-693. doi: 10.1083/jcb.201607019.

- Schatton, D., Rugarli, E.I. 2018. A concert of RNA-binding proteins coordinates mitochondrial function. *Critical Reviews in Biochemistry and Molecular Biology*. 53 (6): 652-666. doi: 10.1080/10409238.2018.1553927.
- Sen, A., Damm, V.T., Cox, R.T. 2013. *Drosophila clueless* is highly expressed in larval neuroblasts, affects mitochondrial localization and suppresses mitochondrial oxidative damage. *PLoS One*. 8 (1): e54283. doi: 10.1371/journal.pone.0054283.
- Sen, A., Kalvakuri, S., Bodmer, R., Cox, R.T. 2015. Clueless, a protein required for mitochondrial function, interacts with the PINK1-Parkin complex in *Drosophila*. *Disease Models & Mechanisms*. 8: 577-589. doi: 10.1242/dmm.019208.
- Sen, A., Cox, R.T., 2016. Clueless is a conserved ribonucleoprotein that binds the ribosome at the mitochondrial outer membrane. *Biology Open*. 5: 195-203. doi: 10.1242/bio.015313.
- Sen, A., Cox, R.T. 2017. Fly models of human diseases: *Drosophila* as a model for understanding human mitochondrial mutations and disease. *Current Topics in Developmental Biology*. 121: 1-27. doi: 10.1016/bs.ctdb.2016.07.001.
- Sen, A., Cox, R.T. 2022. Loss of *Drosophila* Clueless differentially affects the mitochondrial proteome compared to loss of Sod2 and Pink1. *Frontiers in Physiology*. 13: 1004099. doi: 10.3389/fphys.2022.1004099.
- Sheard, K. M., Thibault-Sennet, S.A., Sen, A., Shewmaker, F., Cox, R.T. 2020. Clueless forms dynamic, insulin-responsive bliss particles sensitive to stress. *Developmental Biology*. 459 (2): 149-160. doi: 10.1016/j.ydbio.2019.12.004.

- Simon, A.F., Shih, S., Mack, A., Benzer, S. 2003. Steroid control of longevity in *Drosophila melanogaster*. *Science*. 299 (5611): 1407-1410. doi: 10.1126/science.1080539.
- Slade, F.A., Staveley, B.E. 2015. *Arm-Gal4* inheritance influences development and lifespan in *Drosophila melanogaster*. *Genetics and Molecular Research*. 14 (4): 12788-12796. doi: 10.4238/2015.October.19.22.
- Staats, S., Lüersen, K., Wagney, A.E., Rimbach, G. 2018. *Drosophila melanogaster* as a versatile model organism in food and nutrition research. *Journal of Agricultural and Food Chemistry*. 66 (15): 3737-3753. doi: 10.1021/acs.jafc.7b05900.
- Sunderhaus, E.R., Kretzschmar, D. 2016. Mass histology to quantify neurodegeneration in *Drosophila*. *Journal of Visualized Experiments*. 118: e54809. doi: 10.3791/54809.
- Tafuri, F., Ronchi, D., Magri, F., Comi, G.P., Corti, S., 2015. SOD1 misplacing and mitochondrial dysfunction in amyotrophic lateral sclerosis pathogenesis. *Frontiers in Cellular Neuroscience*. 9: 336. doi: 10.3389/fncel.2015.00336.
- Thibault, S.T., Singer, M.A., Miyazaki, W.Y., Milash, B., Dompe, N.A., *et al.* 2004. A complementary transposon tool kit for *Drosophila melanogaster* using P and piggyBac. *Nature Genetics*. 36 (3): 283-287. doi: 10.1038/ng1314.
- Tian, X., Seluanov, A., Gorbunova, V. 2017. Molecular mechanisms determining lifespan in short- and long-lived species. *Trends in Endocrinology and Metabolism*. 29 (10): 722-734. doi: 10.1016/j.tem.2017.07.004.
- Tian, S., Curnutte, H.A., Trcek, T. 2020. RNA granules: a view from the RNA perspective. *Molecules*. 25 (14): 3130. doi: 10.3390/molecules25143130.

- Todd, A.M., Staveley, B.E. 2004. Novel assay and analysis for measuring climbing ability in *Drosophila*. *Drosophila Information Service*. 87: 101-108.
- Todd, A.M., Staveley, B.E. 2008. *Pink1* suppresses α -synuclein-induced phenotypes in a *Drosophila* model of Parkinsons disease. *Genome*. 51 (12): 1040-1046. doi: 10.1139/G08-085.
- Todd, A.D., Staveley, B.E. 2012. Expression of *Pink1* with α -synuclein in the dopaminergic neurons of *Drosophila* leads to increases in both lifespan and healthspan. *Genetics and Molecular Research*. 11 (2): 1497-1502. doi: 10.4238/2012.May.21.6.
- Tricoire, H., Battisti, V., Trannoy, S., Lasbleiz, C., Pret, A., Monnier, V. 2009. The steroid hormone receptor EcR finely modulates *Drosophila* lifespan during adulthood in a sex-specific manner. *Mechanisms of Ageing and Development*. 130 (8): 547-552. doi: 10.1016/j.mad.2009.05.004.
- Vardi-Okin, D., Arava, Y. 2019. Characterization of factors involved in localized translation near mitochondria by ribosome-proximity labeling. *Frontiers in Cell and Developmental Biology*. 7: 305. doi: 10.3389/fcell.2019.00305.
- Vincow, E.S., Merrihew, G., Thomas, R.E., Shulman, N.J., Beyer, R.P., MacCos, M.J., Pallanck, L.J. 2013. The PINK1–Parkin pathway promotes both mitophagy and selective respiratory chain turnover in vivo. *Proceedings of the National Academy of Sciences of the United States of America*. 110 (16): 6400-6405. doi: 10.1073/pnas.1221132110.
- Wang, Z., Rabouille, C., Geisbrecht, E.R. 2015. Loss of a Clueless-dGRASP complex results in ER stress and blocks Integrin exit from the perinuclear endoplasmic

- reticulum in *Drosophila* larval muscle. *Biology Open*. 4: 636-648. doi: 10.1242/bio.201511551.
- Wang, B., Abraham, N., Gao, G., Yang, Q. 2016. Dysregulation of autophagy and mitochondrial function in Parkinson's disease. *Translational Neurodegeneration*. 5: 19. doi: 10.1186/s40035-016-0065-1.
- Wang, Z., Clark, C., Geisbrecht, E.R. 2016. *Drosophila* clueless is involved in Parkin-dependent mitophagy by promoting VCP-mediated Marf degradation. *Human Molecular Genetics*. 25 (10): 1946-1964. doi: 10.1093/hmg/ddw067.
- Wasserstein, R.L., Lazar, N.A. 2016. The ASA statement on *p*-values: context, process, and purpose. *The American Statistician*. 70 (2): 129-133. doi: 10.1080/00031305.2016.1154108.
- Wasserstein, R.L., Schirm, A.L., Lazar, N.A. 2019. Moving to a world beyond "*p* < 0.05". *The American Statistician*. 73 (S1): 1-19. doi: 10.1080/00031305.2019.1583913.
- Wickham, H. 2016. *ggplot2: Elegant graphics for data analysis*, 2 ed. Springer. doi: 10.1007/978-3-319-24277-4.
- Winterbourn, C.C. 2008. Reconciling the chemistry and biology of reactive oxygen species. *Nature Chemical Biology*. 4 (5): 278-286. doi: 10.1038/nchembio.85.
- Xu, Z., Poidevin, M., Li, X., Li, Y., Shu, L., Nelson, D.L., Li, H., Hales, C.M., Gearing, M., Wingo, T.S., Jin, P. 2013. Expanded GGGGCC repeat RNA associated with amyotrophic lateral sclerosis and frontotemporal dementia causes neurodegeneration. *Proceedings of the National Academy of Science of the United States of America*. 110 (19): 7778-7783. doi: 10.1073/pnas.1219643110.

- Yamamoto, S., Seto, E.S. 2014. Dopamine dynamics and signaling in *Drosophila*: an overview of genes, drugs and behavioral paradigms. *Experimental Animals*. 63(2): 107-119. doi: 10.1538/expanim.63.107.
- Yang, Y., Ouyang, Y., Yang, L., Beal, M.F., McQuibban, A., Vogel, H., Lu, B. 2008. Pink1 regulates mitochondrial dynamics through interaction with the fission/fusion machinery. *Proceeding of the National Academy of Sciences*. 105 (19): 7070-7075. doi: 10.1073/pnas.0711845105.
- Yang, H., Sibilla, C., Liu, R., Yun, J., Hay, B.A., Blackstone, C., Chan, D.C., Harvey, R.J., Guo, M. 2022. Clueless/CLUH regulates mitochondrial fission by promoting recruitment of Drp1 to mitochondria. *Nature Communications*. 13 (1): 1582. doi: 10.1038/s41467-022-29071-4.
- Yeh, E., Gustafson, K., Boulianne, G.L. 1995. Green fluorescent protein as a vital marker and reporter of gene expression in *Drosophila*. *Proceedings of the National Academy of Sciences of the United States of America*. 92 (15): 7036-7040. doi: 10.1073/pnas.92.15.7036.
- Yeo, B.K., Yu, S. 2016. Valosin-containing protein (VCP): structure, functions, and implications in neurodegenerative diseases. *Animal Cells and Systems*. 20 (6): 303-309. doi: 10.1080/19768354.2016.1259181.
- Zarei, S., Carr, K., Reiley, L., Diaz, K., Guerra, O., Altamirano, P.F., Pagani, W., Lodin, D., Orozco, G., Chinea, A. 2015. A comprehensive review of amyotrophic lateral sclerosis. *Surgical Neurology International*. 6: 171. doi: 10.4103/2152-7806.169561.

- Zemirli, N., Morel, E., Molino, D. 2018. Mitochondrial dynamics in basal and stressful conditions. *International Journal of Molecular Sciences*. 19 (2): 564. doi: 10.3390/ijms19020564.
- Zhou, X., Escala, W., Papapetropoulos, S., Zhai, R.G. 2010. β -N-methylamino-L-alanine induces neurological deficits and shortened life span in *Drosophila*. *Toxins*. 2 (11): 2663-2679. doi: 10.3390/toxins2112663.
- Zhu, Q., Hulen, D., Liu, T., Clarke, M. 1997. The cluA- mutant of Dictyostelium identifies a novel class of proteins required for dispersion of mitochondria. *Proceedings of the National Academy of Sciences of the United States of America*. 94 (14): 7308-7313. doi: 10.1073/pnas.94.14.7308.
- Zhu, T., Chen, J., Wang, Q., Shao, W., Qi., B. 2018. Modulation of mitochondrial dynamics in neurodegenerative diseases: an insight into prion diseases. *Frontiers in Aging Neuroscience*. 10: 336. doi: 10.3389/fnagi.2018.00336.
- Zhu, K.Y., Palli, S.R. 2020. Mechanisms, applications, and challenges of insect RNA Interference. *Annual Reviews in Entomology*. 65: 293-311. doi: 10.1146/annurev-ento-011019-025224.

Appendix 1. Parameter estimates for modeled climbing ability across lifespan where expression of *clueless* in *Drosophila melanogaster* dopaminergic neurons is inhibited.

Parameter estimates are for the model $5\text{-Climbing Index} = Ce^{Kt}$ weighted according to number of individuals measured at each time point generated based upon climbing indices calculated for *TH-Gal4;UAS-cluRNAi^{KK108024}*, *TH-Gal4;UAS-cluRNAi^{V42136}*, and *TH-Gal4;UAS-cluRNAi^{V42138}* individuals, given as contrasts to *TH-Gal4;UAS-lacZ* controls. Parameter estimates for *TH-Gal4;UAS-lacZ* controls are C= -2.562844 (or, estimated 8.7 cm climbed at day 0) and K= 0.038014(or, estimated 3.8% decline in climbing ability per day). Parameter estimates for *TH-Gal4;UAS-cluRNAi^{KK108024}* individuals are C= -1.03039 (or, estimated 9.5 cm climbed at day 0) and K= 0.021408 (or, estimated 2.1 % decline in climbing ability per day). Parameter estimates for *TH-Gal4;UAS-cluRNAi^{V42136}* individuals are C= -1.30491 (or, estimated 9.4 cm climbed at day 0) and K= 0.026197 (or, estimated 2.6% decline in climbing ability per day). Parameter estimates for *TH-Gal4;UAS-cluRNAi^{V42138}* individuals are C= -1.410895 (or, estimated 9.3 cm climbed at day 0) and K= 0.026092 (or, estimated 2.6% decline in climbing ability per day).

	Estimate	Standard Error	t value	Pr(> t)
Intercept (<i>TH-Gal4;UAS-lacZ</i>)	-2.56284	0.31095	-8.242	4.02E-11
Day (<i>TH-Gal4;UAS-lacZ</i>)	0.038014	0.00351	10.82	3.92E-15
<i>TH-Gal4;UAS-cluRNAi^{KK108024}</i>	1.532454	0.34523	4.439	4.50E-05
<i>TH-Gal4;UAS-cluRNAi^{V42136}</i>	1.257934	0.3446	3.65	0.00059
<i>TH-Gal4;UAS-cluRNAi^{V42138}</i>	1.151949	0.35165	3.276	0.00184
Day: <i>TH-Gal4;UAS-cluRNAi^{KK108024}</i>	-0.01661	0.00403	-4.126	0.00013
Day: <i>TH-Gal4;UAS-cluRNAi^{V42136}</i>	-0.01182	0.00396	-2.985	0.00426
Day: <i>TH-Gal4;UAS-cluRNAi^{V42138}</i>	-0.01192	0.00404	-2.952	0.00466

Appendix 2. Parameter estimates for modeled climbing ability across lifespan where expression of *clueless* in *Drosophila melanogaster* motor neurons is inhibited.

Parameter estimates are for the model 5-Climbing Index= Ce^{Kt} weighted according to number of individuals measured at each time point generated based upon climbing indices calculated for *D42-Gal4;UAS-cluRNAi^{KK108024}*, *D42-Gal4;UAS-cluRNAi^{V42136}*, and *D42-Gal4;UAS-cluRNAi^{V42138}* individuals, given as contrasts to *D42-Gal4;UAS-lacZ* controls. Parameter estimates for *D42-Gal4;UAS-lacZ* controls are C= -0.81552 (or, estimated 9.6 cm climbed at day 0) and K= 0.02611 (or, estimated 2.6% decline in climbing ability per day). Parameter estimates for *D42-Gal4;UAS-cluRNAi^{KK108024}* individuals are C= 0.937585 (or, estimated 9.5 cm climbed at day 0) and K= 0.003671 (or, estimated 3.6% decline in climbing ability per day). Parameter estimates for *D42-Gal4;UAS-cluRNAi^{V42136}* individuals are C= -0.757976 (or, estimated 9.6 cm climbed at day 0) and K= 0.030641 (or, estimated 3.1% decline in climbing ability per day). Parameter estimates for *D42-Gal4;UAS-cluRNAi^{V42138}* individuals are C= -0.215493 (or, estimated 9.9 cm climbed at day 0) and K= 0.020138 (or, estimated 2% decline in climbing ability per day).

	Estimate	Standard Error	t value	Pr(> t)
Intercept (<i>D42-Gal4;UAS-lacZ</i>)	-0.81552	0.16829	-4.85	7.31E-06
Day (<i>D42-Gal4;UAS-lacZ</i>)	0.02611	0.00273	9.575	2.35E-14
<i>D42-Gal4;UAS-cluRNAi^{KK108024}</i>	1.75311	0.18503	9.475	3.59E-14
<i>D42-Gal4;UAS-cluRNAi^{V42136}</i>	0.05755	0.28046	0.205	0.83802
<i>D42-Gal4;UAS-cluRNAi^{V42138}</i>	0.60003	0.21453	2.797	0.00666
Day: <i>D42-Gal4;UAS-cluRNAi^{KK108024}</i>	-0.02244	0.00338	-6.64	5.75E-09
Day: <i>D42-Gal4;UAS-cluRNAi^{V42136}</i>	0.00454	0.00462	0.981	0.32997
Day: <i>D42-Gal4;UAS-cluRNAi^{V42138}</i>	-0.00597	0.00375	-1.59	0.11642

Appendix 3. Parameter estimates for modeled climbing ability across lifespan where *clueless* or *CLUH* are ectopically expressed in *Drosophila melanogaster* dopaminergic neurons in heterozygous *clu^{d08713}* mutants. Parameter estimates are for the model $5\text{-Climbing Index} = Ce^{Kt}$ weighted according to number of individuals measured at each time point generated based upon climbing indices calculated for *clu^{d08713};clu⁺;TH-Gal4;UAS-clu*, and *clu^{d08713};clu⁺;TH-Gal4;UAS-CLUH* individuals, given as contrasts to *clu⁺;TH-Gal4;UAS-lacZ* controls. Parameter estimates for *clu⁺;TH-Gal4;UAS-lacZ* controls are C= -2.780738 (or, estimated 8.6 cm climbed at day 0) and K= 0.040247 (or, estimated 4% decline in climbing ability per day). Parameter estimates for *clu^{d08713};clu⁺;TH-Gal4;UAS-clu* individuals are C= -1.999169 (or, estimated 9 cm climbed at day 0) and K= 0.034328 (or, estimated 3.4% decline in climbing ability per day). Parameter estimates for *clu^{d08713};clu⁺;TH-Gal4;UAS-CLUH* individuals are C= -2.175934 (or, estimated 8.9 cm climbed at day 0) and K= 0.034941 (or, estimated 3.5% decline in climbing ability per day).

	Estimate	Standard Error	t value	Pr(> t)
Intercept (<i>clu⁺;TH-Gal4;UAS-lacZ</i>)	-2.78074	0.22599	-12.31	< 2e-16
Day (<i>clu⁺;TH-Gal4;UAS-lacZ</i>)	0.040247	0.00274	14.712	< 2e-16
<i>clu^{d08713};clu⁺;TH-Gal4;UAS-clu</i>	0.781569	0.26898	2.906	0.0047
<i>clu^{d08713};clu⁺;TH-Gal4;UAS-CLUH</i>	0.604804	0.29586	2.044	0.0442
Day: <i>clu^{d08713};clu⁺;TH-Gal4;UAS-clu</i>	-0.00592	0.00324	-1.825	0.0717
Day: <i>clu^{d08713};clu⁺;TH-Gal4;UAS-CLUH</i>	-0.00531	0.00369	-1.438	0.1542

Appendix 4. Parameter estimates for modeled climbing ability across lifespan where *clueless* or *CLUH* are ectopically expressed in *Drosophila melanogaster* motor neurons in heterozygous *clu*^{d08713} mutants. Parameter estimates are for the model 5-Climbing Index=Ce^{Kt} weighted according to number of individuals measured at each time point generated based upon climbing indices calculated for *clu*^{d08713};*clu*⁺;*D42-Gal4*;*UAS-clu*, and *clu*^{d08713};*clu*⁺;*D42-Gal4*;*UAS-CLUH* individuals, given as contrasts to *clu*⁺;*D42-Gal4*;*UAS-lacZ* controls. Parameter estimates for *clu*⁺;*D42-Gal4*;*UAS-lacZ* controls are C= -1.245631 (or, estimated 9.4 cm climbed at day 0) and K= 0.028435 (or, estimated 2.8% decline in climbing ability per day). Parameter estimates for *clu*^{d08713};*clu*⁺;*D42-Gal4*;*UAS-clu* individuals are C= -0.440233 (or, estimated 9.8 cm climbed at day 0) and K= 0.020301 (or, estimated 2% decline in climbing ability per day). Parameter estimates for *clu*^{d08713};*clu*⁺;*TH-Gal4*;*UAS-CLUH* individuals are C= -0.634774 (or, estimated 9.7 cm climbed at day 0) and K= 0.024188 (or, estimated 2.4% decline in climbing ability per day).

	Estimate	Standard Error	t value	Pr(> t)
Intercept (<i>clu</i> ⁺ ; <i>D42-Gal4</i> ; <i>UAS-lacZ</i>)	-1.24563	0.232873	-5.35	5.57e-06
Day (<i>clu</i> ⁺ ; <i>D42-Gal4</i> ; <i>UAS-lacZ</i>)	0.028435	0.003339	8.516	4.75e-10
<i>clu</i> ^{d08713} ; <i>clu</i> ⁺ ; <i>D42-Gal4</i> ; <i>UAS-clu</i>	0.805398	0.274576	2.933	0.00588
<i>clu</i> ^{d08713} ; <i>clu</i> ⁺ ; <i>D42-Gal4</i> ; <i>UAS-CLUH</i>	0.610857	0.277758	2.199	0.03456
Day: <i>clu</i> ^{d08713} ; <i>clu</i> ⁺ ; <i>D42-Gal4</i> ; <i>UAS-clu</i>	-0.00813	0.004046	-2.01	0.05216
Day: <i>clu</i> ^{d08713} ; <i>clu</i> ⁺ ; <i>D42-Gal4</i> ; <i>UAS-CLUH</i>	-0.00425	0.00405	-1.05	0.30153

Appendix 5. Bang Sensitivity Assay

A5.1 Introduction

Seizures are a feature of mitochondrial disease (Sen and Cox, 2017). Mutations in *Drosophila melanogaster* mitochondrial genes, including in the nuclear-encoded mitochondrial ribosome protein S12, cause increased susceptibility to mechanosensory-induced seized seizures, known as “bang sensitivity”. Bang-sensitivity is a distinct response where, upon stimulation, individuals 1) briefly seize, including repeat proboscis extension and wing buzzing, 2) lay paralyzed for five seconds or more, 3) briefly seize again, and finally 4) recover posture (Reynolds, 2018). Recovery time following induced seizures is genotype-specific, increases with age, and is not predicted by adult or larval locomotor ability (Reynolds, 2018; Mituzaitė *et al.*, 2021). A seizure-susceptibility assay may be useful in elucidating the effect of altered expression of mitochondrial genes on mitochondrial function across *D. melanogaster*. Here, I worked towards the development of such an assay.

A5.2 Methods

Approximately 100 individuals of each experimental *D. melanogaster* genotype were collected. Experimental *D. melanogaster* were transferred to fresh media every three to four days throughout the duration of the assay, including between 30 minutes and one day prior to measurement of climbing ability. Bang sensitivity was assessed within the first two weeks following eclosion and every week thereafter until fewer than 10 total individuals of each genotype remained. Any individuals that were injured or lost on handling were excluded from analyses. Bang sensitivity was assessed during daylight hours only, and experimental *D. melanogaster* were allowed at least 20 minutes to

acclimate to room temperature of $\sim 22^{\circ}\text{C}$ prior to measurement. Experimental *D. melanogaster* were then transferred into empty plastic vials and placed on a laboratory vortexer set to maximum speed for 10 seconds. Following exposure to mechanical stimulation, the number of individuals that had not yet to recovered posture was counted every five seconds until 60 seconds had passed. Experimental *D. melanogaster* were measured in groups of up to 15 individuals, until all individuals of each genotype were scored.

Mean recovery time was calculated for each genotype at each time point measured. Curve fitting was done according to the model $\text{Recovery Time} = Ce^{Kt}$, where C is the y-intercept, e is the mathematical constant e , K is the slope of the fitted curve, and t is age in days. Diagnostic plots were visually analyzed to confirm that the assumptions of the nonlinear regression were satisfied. Residual versus fitted, normal Q-Q, scale location, and residual versus leverage plots were used to assess for normality, heteroscedasticity, and for the presence of outliers. Recovery time across lifespan of experimental genotypes were compared to climbing ability of controls assayed concurrently. Fitted curves were compared within 95% confidence intervals to determine differences in climbing ability across lifespan. The estimated slope parameter representing change in climbing ability across lifespan was compared. All curve fitting and parameter estimates were performed using R version 4.2.2.

A5.3 Results and Discussion

Average recovery time increased with age for all genotypes assessed (Figures A5.3.1, A5.3.3, and A5.3.5). However, data was not a good fit to the model (Figures A5.3.2, A5.3.4, and A5.3.6). Mortality across the assay was greater than expected

considering evaluated effects of expression the transgenic constructs on lifespan (Figures 3.3, 3.5, and 3.7). A low number of experimental individuals at later time points led to low-confidence measurements of bang-sensitivity in aged *D. melanogaster*, where the effects of altering expression of mitochondrial proteins linked to age-related disease might be expected to have differing impacts. I assessed bang sensitivity weekly in the same experimental individuals across over their lifespan. Reynolds *et al.* (2018) report that daily seizure induction does not exacerbate the bang-sensitivity phenotype. It is possible, however, that repeat seizure induction through mechanical stimulation causes accumulating health defects in *D. melanogaster* which may affect mortality. In follow-up studies, I will assess experimental individuals collected from the same cohort only once, at pre-determined timepoints across lifespan. For example, I may assess bang-sensitivity in 50 control and individuals expressing *UAS-chuelessRNAi* in motor neurons at days 20, 40, 60, and 80.

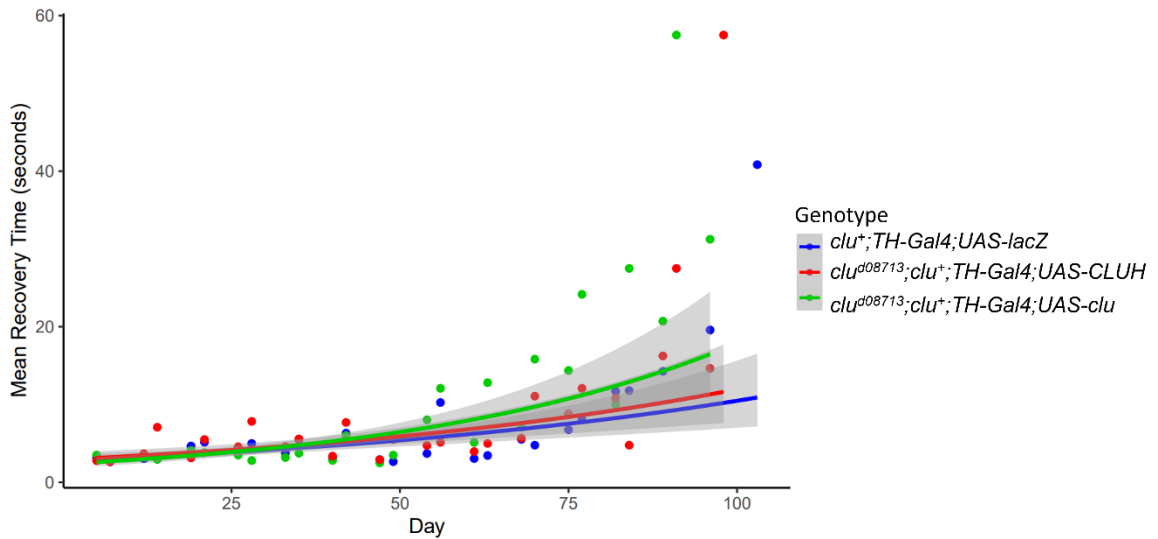


Figure A5.3.1 Bang-sensitivity across lifespan in heterozygous *clueless* mutants expressing ectopic *clueless* but not *CLUH* in dopaminergic neurons. Mean recovery from seizures induced by mechanical stimulation increases with age in *clu*⁺; *TH-Gal4*; *UAS-lacZ*, *clu*^{d08713}; *clu*⁺; *TH-Gal4*; *UAS-clu*, and *clu*^{d08713}; *clu*⁺; *TH-Gal4*; *TH-Gal4*; *UAS-CLUH* individuals. Fit of the model evaluated in Figure A5.3.2. This figure was prepared using R version 4.3.2 with the ggplot2 package (version 3.5.1; Wickham, 2016).

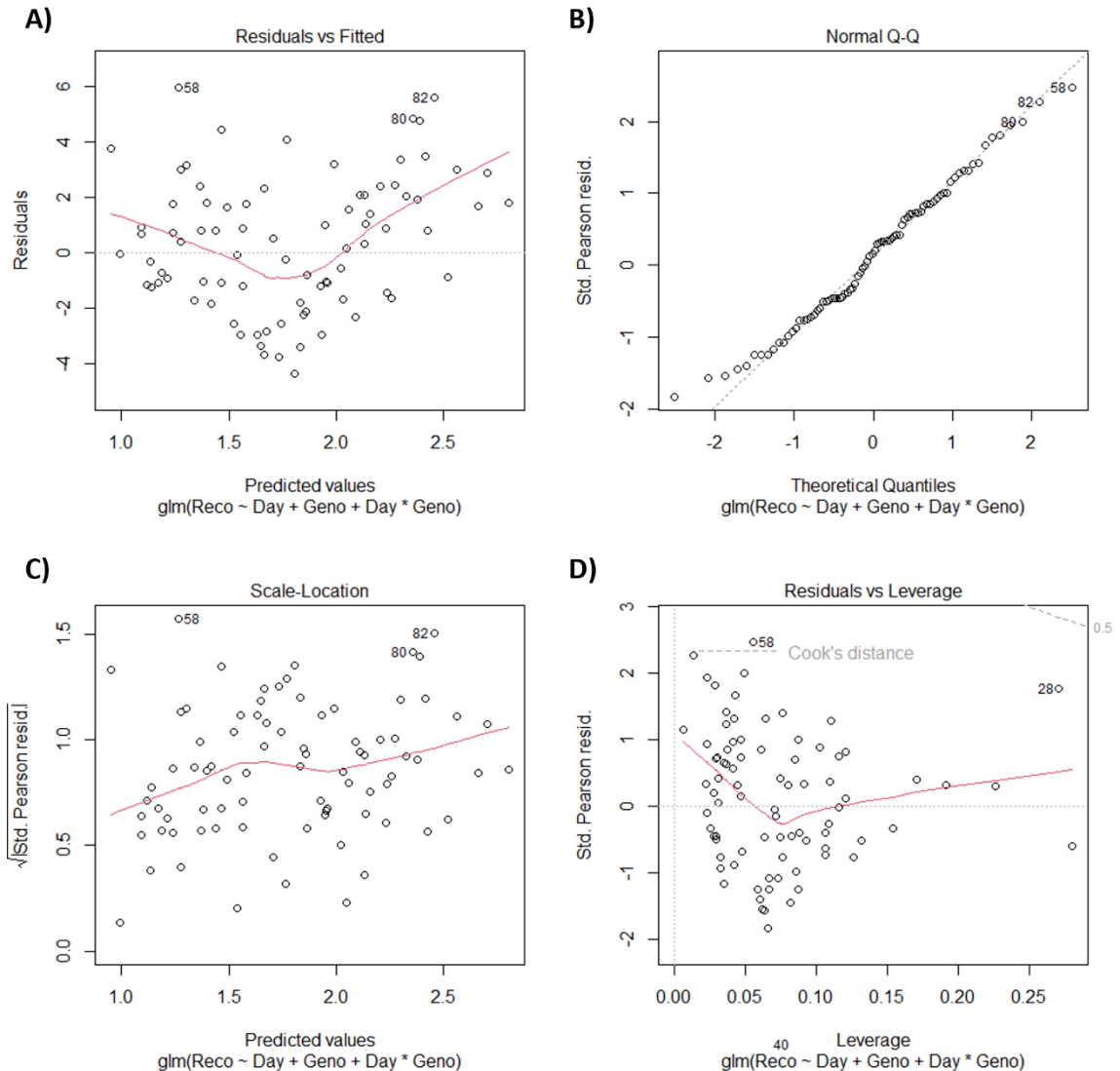


Figure A5.3.2 Diagnostic plots to assess the fit of the model to describe bang-sensitivity across lifespan in heterozygous *clueless* mutants expressing ectopic *clueless* but not *CLUH* in dopaminergic neurons A) The residuals versus the fitted values for the model. Non-linear shape indicates non-normal distribution. B) The standardized residuals versus theoretical quantities for the model. Most points are along the diagonal line, so the distribution appears to be normal. C) Square root of the standardized residuals versus fitted values for the model. As residuals appear to be randomly spread, the distribution appears to be within acceptable limits of heteroscedasticity. D) Standardized residuals versus leverage for the model. All points are within Cook's distance lines, indicating that there are no outliers among the data. This figure was prepared using R version 4.3.2.

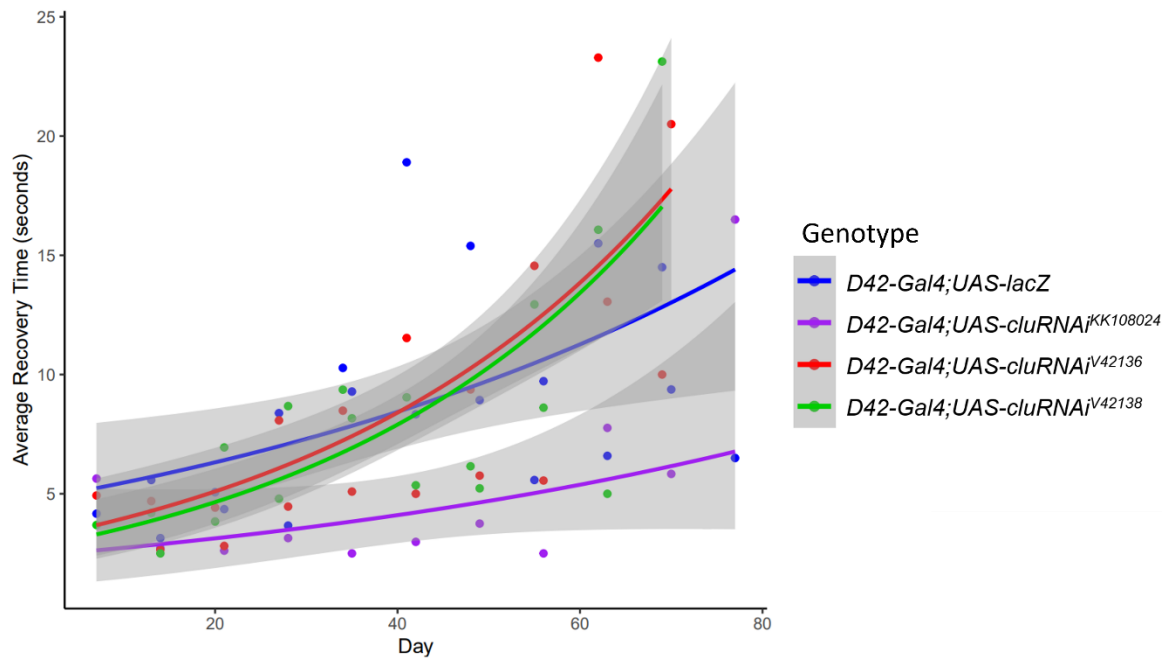


Figure A5.3.3 Bang-sensitivity across lifespan on inhibited expression of *clueless* in motor neurons via RNAi. Mean recovery from seizures induced by mechanical stimulation increases with age in *D42-Gal4;UAS-lacZ*, *D42-Gal4;UAS-cluRNAi^{KK108024}*, *UAS-cluRNAi^{V42136}*, *D42-Gal4;UAS-cluRNAi^{V42138}* individuals. Fit of the model evaluated in Figure A5.3.4. This figure was prepared using R version 4.3.2 with the ggplot2 package (version 3.5.1; Wickham, 2016).

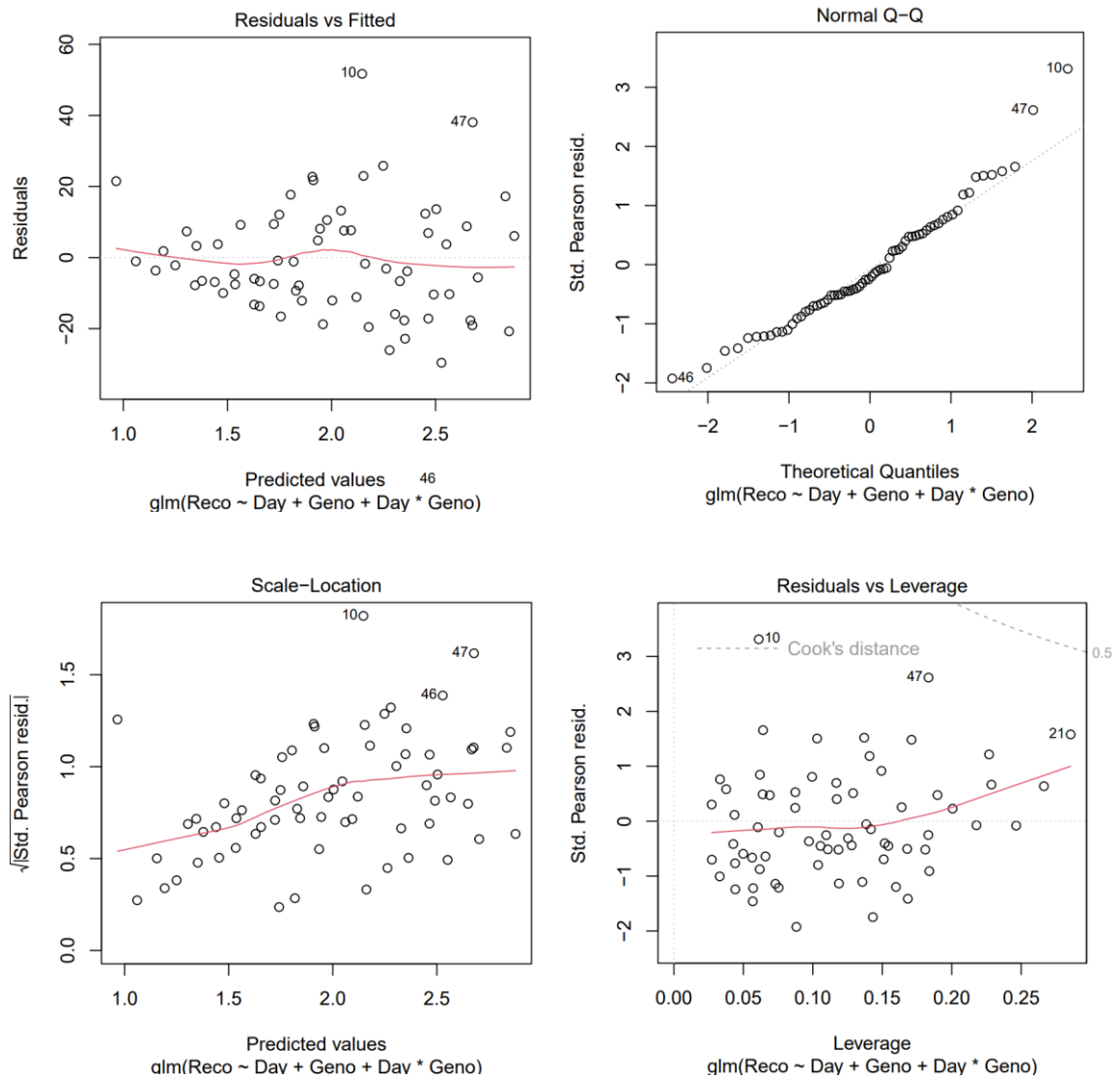


Figure A5.3.4 Diagnostic plots to assess the fit of the model to describe bang-sensitivity across lifespan on inhibited expression of *clueless* in motor neurons. A) The residuals versus the fitted values for the model. Data tapers as one end, indicating a non-normal distribution. B) The standardized residuals versus theoretical quantities for the model. Most points are along the diagonal line, so the distribution appears to be normal. C) Square root of the standardized residuals versus fitted values for the model. Residuals do not appear to be randomly spread, so the distribution is not within acceptable limits of heteroscedasticity. D) Standardized residuals versus leverage for the model. All points are within Cook's distance lines, indicating that there are no outliers among the data. This figure was prepared using R version 4.3.2.

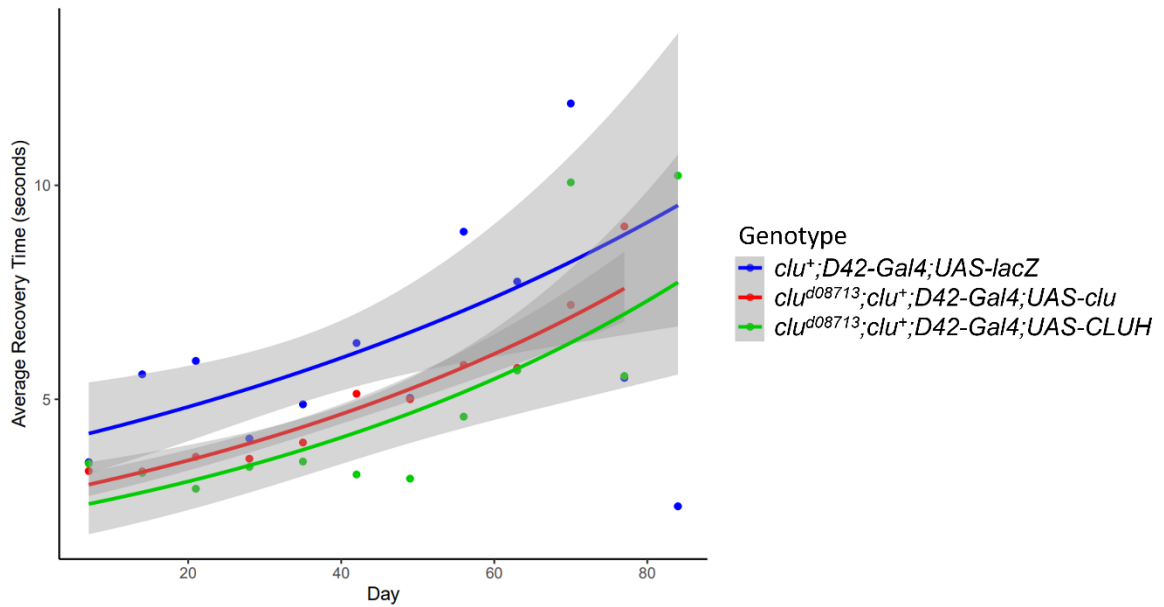


Figure A5.3.5 Bang-sensitivity across lifespan in heterozygous *clueless* mutants expressing ectopic *clueless* but not *CLUH* in motor neurons. Mean recovery from seizures induced by mechanical stimulation increases with age in *clu*⁺;D42-Gal4;UAS-lacZ, *clu*^{d08713};clu⁺;D42-Gal4;UAS-clu, and *clu*^{d08713};clu⁺;D42-Gal4;TH-Gal4;UAS-CLUH individuals. Fit of the model evaluated in Figure A5.3.6. This figure was prepared using R version 4.3.2 with the ggplot2 package (version 3.5.1; Wickham, 2016).

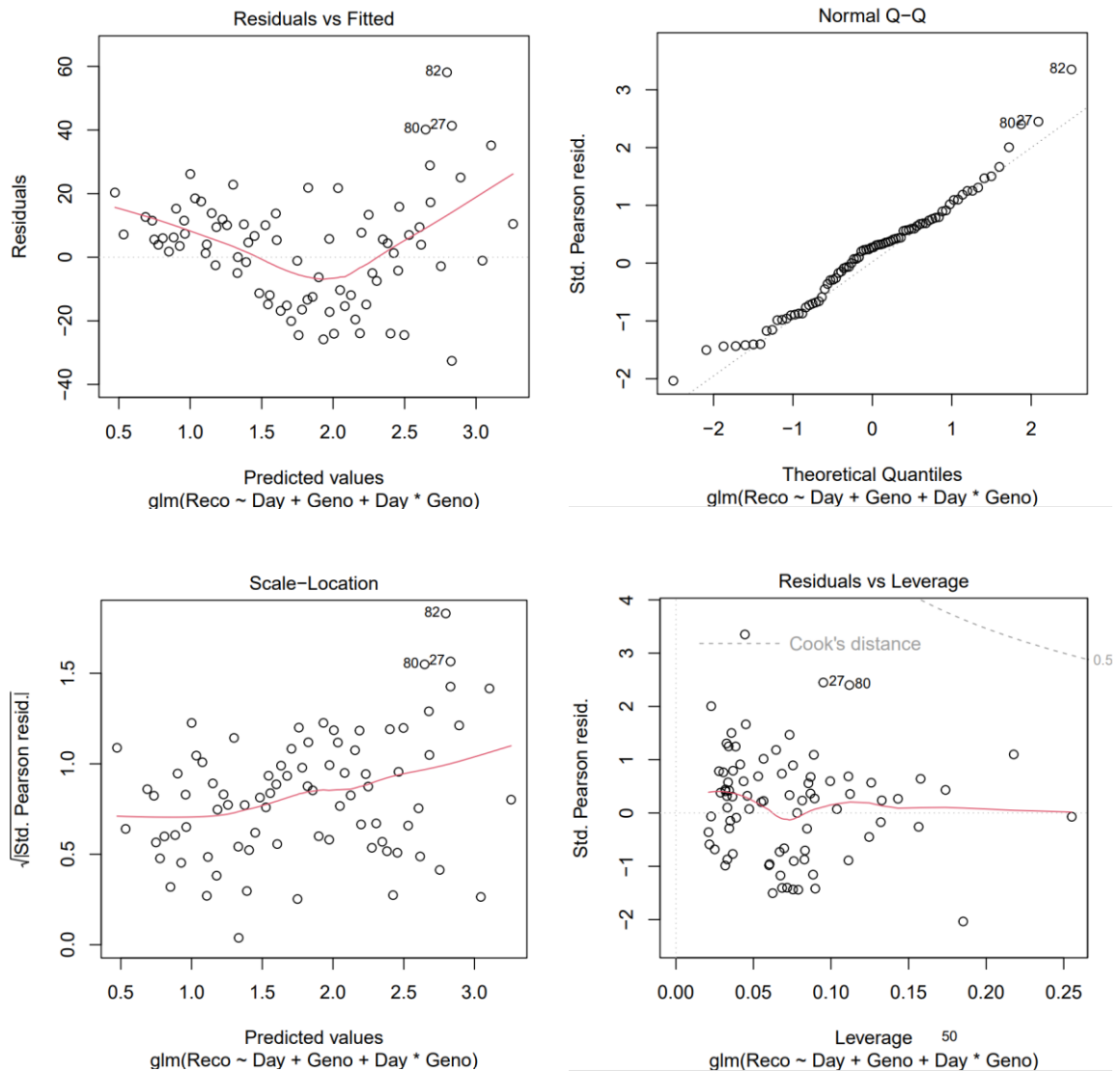


Figure A5.3.6 Diagnostic plots to assess the fit of the model to describe bang-sensitivity across lifespan in heterozygous *clueless* mutants expressing ectopic *clueless* but not *CLUH* in motor neurons. A) The residuals versus the fitted values for the model. Non-linear shape indicates non-normal distribution. B) The standardized residuals versus theoretical quantities for the model. Most points are along the diagonal line, so the distribution appears to be normal. C) Square root of the standardized residuals versus fitted values for the model. As residuals appear to be randomly spread, the distribution appears to be within acceptable limits of heteroscedasticity. D) Standardized residuals versus leverage for the model. All points are within Cook's distance lines, indicating that there are no outliers among the data. This figure was prepared using R version 4.3.2.